Master's thesis

NTNU
Norwegian University of Science and Technology
Faculty of Social and Educational Sciences
Department of Psychology

Mikkel N. Haug

Seeing Odors and Smelling Light

Multimodal Processing in Higher Order Brain Regions

Master's thesis in Psychology
Supervisor: Dr. Jonas H. Kymre
Co-supervisor: Dr. Xi Chu and Prof. Bente G. Berg
May 2024

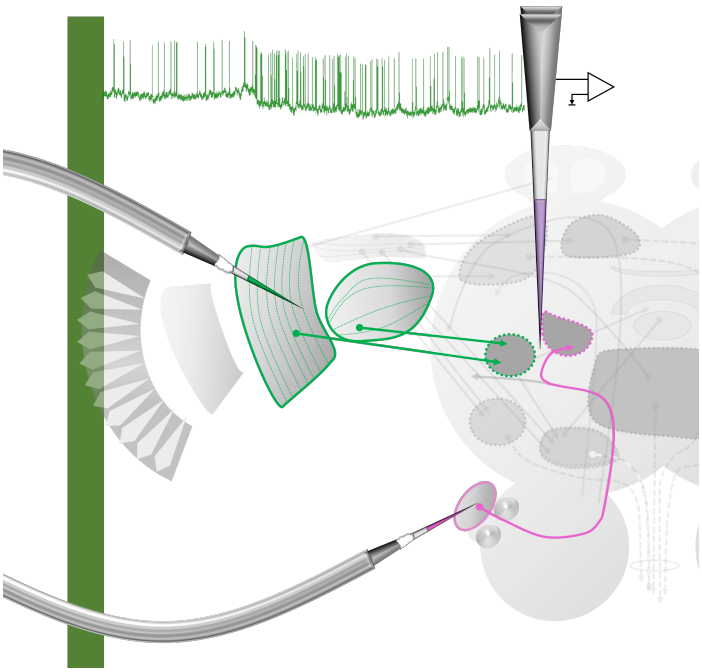

NTNU
Norwegian University of
Science and Technology

Mikkel N. Haug

Seeing Odors and Smelling Light

Multimodal Processing in Higher Order Brain Regions

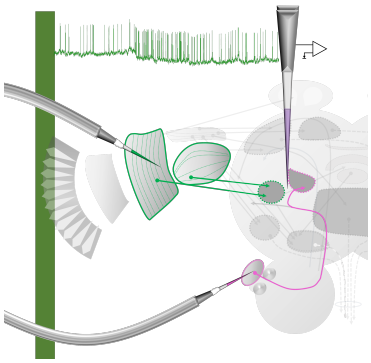

Master's thesis in Psychology
Supervisor: Dr. Jonas H. Kymre
Co-supervisor: Dr. Xi Chu and Prof. Bente G. Berg
May 2024

Norwegian University of Science and Technology
Faculty of Social and Educational Sciences
Department of Psychology

NTNU
Norwegian University of
Science and Technology

Preface and Acknowledgments

The experimental work and writing of this thesis were conducted at the Chemosensory Laboratory, Department of Psychology, Norwegian University of Science and Technology (NTNU). As a first-year student, I swiftly became immersed in the captivating world of sensory input processing. From my very first semester, I attended neurophysiology lectures held by Professor Bente G. Berg, which were truly inspiring. Later, I was offered a position in her laboratory, marking the beginning of my journey. Under the mentorship of Dr. Xi Chu, I eagerly absorbed her profound knowledge, and started my own experiments with exploratory freedom and her remarkable guidance. Our shared interest led us to push boundaries and develop our novel air pressure mass staining technique. With this basis, I found inspiration in Dr. Jonas H. Kymre, a postdoctoral researcher in the lab at the time, who explored the concept of multimodality. Enthusiastically agreeing to supervise my Master's, he invited me to discover what lies beyond the known. Early mornings, late nights, intriguing conversations, and the highs and lows of research characterized my journey. I want to convey my appreciation to my supervisors, all members of the lab, collaborators, and visitors for fostering a warm and supportive environment, which has opened further avenues for exploration as I embark on the next chapter of my scientific journey. However far my journey may extend, I will never forget where it started, all thanks to Professor Bente G. Berg.

Pursuing my interest to such an extent would not have been possible without the support of my family and friends. I extend my gratitude for the unwavering presence of my partner, patiently listening to the numerous hours of my "scientific voice". Additionally, there is one person who has consistently supported me and taken a keen interest in every aspect of my journey. Therefore, this thesis serves as a tribute to my grandmother's unfulfilled aspiration to pursue science, ensuring that her legacy lives on through my academic journey.

Mikkel N. Haug

Abstract

Sensory information processing is vital for navigation across all organisms, from the smallest single-celled entities to multicellular human beings. While the study of single sensory modalities has greatly advanced our knowledge, it is also essential to explore sensory processing trough the concept of multimodality. Here, we investigated how olfactory and visual inputs are processed in higher order brain regions of the male moth *Helicoverpa armigera*. By employing single neuron intracellular recordings in the pheromone processing superior intermediate protocerebrum, located adjacent to the visual neuropil anterior optic tubercle, I expected to discover individual neurons with multimodal characteristics. To confirm the relevance of this potential recording site, we developed a new air pressure mass staining technique providing precise information about areas relevant to visual-olfactory multimodal processing. The subsequent intracellular recordings, involving stimulation with olfactory, visual, and multimodal stimuli, were followed by staining and confocal imaging to assess the neurons' morphological characteristics. The results included four groups of neurons, of which 40 % displayed multimodal responses. The remaining portion were classified as olfactory (24%), visual (18%), or nonresponsive (18%) protocerebral interneurons. A main portion of the multimodal neurons, i.e. 70%, had branches overlapping with the candidate region, superior intermediate protocerebrum. In this thesis, I present how olfactory input influences information processing in visual projection neurons, as well as how neurons with responses to various odor components display increased activity when visual stimulation is present. Through observations of seemingly pre- and post-synaptic visual neurons, I discuss similarities in central processing convergence between the visual- and olfactory system, despite their fundamentally different peripheral input. Furthermore, I discuss some of the principles typifying multimodal higher order processing. Through my research, I have emphasized the importance of not underestimating the capabilities of a small brain.

Abbreviations

ΔLP – Delta Region in Lateral Protocerebrum

AOTU – Anterior Optic Tubercle

AL – Antennal Lobe

ALTs – Antennal Lobe Tracts

CA – Calyces

CNs – Centrifugal Neruons

Cu - Cumulus

dALT – dorsal Antennal Lobe Tract

dmALT – dorsomedial Antennal Lobe Tract

dma – dorsomedial anterior unit

dmp – dorsomedial posterior unit

GNG – Gnathal Ganglion

IPS – Inferior Posterior Slope

LAL – Lateral Accessory Lobe

LH – Lateral Horn

LO - Lobula

LOX – Lobula Complex

LNs – Local Interneurons

lALT – lateral Antennal Lobe Tract

MB – Mushroom Bodies

ME - Medulla

mALT – medial Antennal Lobe Tract

mlALT – mediolateral Antennal Lobe Tract

MGC – Macroglomerular Complex

OL – Optic Lobe

ORs – Olfactory Receptors

PCNs – Protocerebral Interneurons

PLP – Posteriorlateral Protocerebrum

PNs – Projection Neurons

SEZ – Subesuphangeal Zone

SCL – Superior Clamp

SIP – Superior Intermediate Protocerebrum

SLP – Superior Lateral Protocerebrum

SMP – Superior Medial Protocerebrum

tALT – transverse Antennal Lobe Tract

VLP – Ventrolateral Protocerebrum

VNC – Ventral Nerve Cord

Table of Contents

Introduction

Throughout evolutionary history, all organisms, from single-celled bacteria to multicellular mammals, have relied on their senses to navigate the intricacies of their surroundings. As humans, for example, we can be aware of the shape, color, and scent of a blossoming flower, and use these distinct types of sensory information as central cornerstones of our perception and interaction with the environment. Yet, these sensory inputs go way beyond the sensation itself; they extend into the depth of our cognition, shape our thoughts, guide our behavior, and lay the foundation for our decision making. While the study of single sensory modalities (e.g. Buck & Axel, 1991; Goodale & Milner, 1992) has greatly advanced our knowledge of perception, it is now essential to delve into the interplay of different senses trough the concept of multimodality (Shimojo & Shams, 2001; Thiagarajan & Sachse, 2022).

Scientific descriptions on navigating organisms frequently center on the adaptive behaviors elicited by disparate sensory inputs (e.g. Budick et al., 2007; Chow & Frye, 2008; Fadamiro et al., 1998; Frye et al., 2003; Goyret et al., 2007; Guo & Guo, 2005; Reinhard et al., 2006; Rowe, 2002; van Swinderen & Greenspan, 2003). However, a fundamental inquiry persists regarding how the distinct sensory modalities influence each other. This issue forms the core for understanding the dynamics of change that underlie adaptive behaviors.

Despite its theoretical significance, the exploration of multimodality, construed as the processing of multiple sensory inputs is not well understood in the single neuron. The lack of knowledge is largely attributable to methodological constraints and the intricacies of the human brain's anatomy, which very often preclude invasive examination of direct neuronal communication. Consequently, to circumvent such limitations, researchers often turn to model organisms possessing closely related sensory organs and offering relatively more controllable input conditions. Thus, adapting this approach to the concept of multimodality could therefore provide great insight into the processing of multiple senses in single neurons.

Vision stands as one of the paramount senses among multiple organisms, pivotal for their survival and ecological success. Organisms rely on the perception of light not only to discern objects and their surroundings, but also to obtain rich, intricate details inaccessible to other senses. Examples of this include monarch butterflies (*Danaus plexippus*) using the position of the sun and the light intensity as well as polarization of the sky for navigation (el Jundi et al., 2014). Other examples include the fruit fly (*Drosophila melanogaster*) and its ability to encode circadian rhythm using light levels (Homberg, 2020), and the male sphinx moth (*Manduca sexta)* detecting moving objects in the visual field to avoid collision when tracing a female (Verspui & Gray, 2009). Moreover, vision provides a unique perspective, enabling organisms to detect and respond to stimuli from afar, thereby enhancing their ability to assess and adapt to dynamic environmental conditions. In essence, vision affords organisms a panoramic view of their world, granting insight and versatility crucial for their survival strategies and environmental interaction.

Vision is often accompanied by other sensory input, such as audition or somatosensation. However, relatively little attention has been given the chemical senses, providing detailed information of the environment through non-visual cues. Some organisms rely more heavily on their chemical senses than the visual input, such as octopuses (Maselli et al., 2020), dogs (Andrews et al., 2022), and moles (Catania, 2019). In multiple organisms, humans included, the dynamics between the chemical senses could be understood as taste giving basic, necessary information, while olfaction provides detailed information of the complex composition of the chemical stimuli (Sharma et al., 2019). Taste also requires direct contact with what is being tasted (e.g. Gravina et al., 2013), whereas olfactory cues often consist of airborne (in non-aquatic organisms) molecules distant from the object of origin (Sharma et al., 2019).

Both vision and olfaction have been extensively investigated in various scientific disciplines, but most of the research has focused on each system separately. Still, the interplay of the two senses remains relatively understudied. For exploring the neural mechanisms underlying multimodal processing of vision and olfaction, it is essential to identify an organism with relatively well-understood single sensory modalities. This organism should also facilitate invasive exploration to elucidate characterization of individual neuronal physiology and morphology, which serves as the foundation for multimodal processing. Furthermore, the organism should be susceptible to controllable sensory cues to ensure precise experimental control.

The moth, *Helicoverpa armigera* (Lepidoptera, *Noctuidae*, *Heliothinae*), is suitable model organism for studying processing of visual-olfactory input. Given its status as a nocturnal insect, *H. armigera* experiences relative limited visual input, relying primarily on olfaction for environmental navigation. That said, visual cues are in fact of considerable importance for the nocturnal moth. For example, it has been pointed out that visual input is conveyed as feedback signals when a male moth is tracing an odor source (Baker & Hansson, 2016).

The olfactory system of the moth is relatively well-studied (e.g. Chu et al., 2020; Homberg et al., 1988; Ian et al., 2017; Kuebler et al., 2012; Kvello et al., 2009; Kymre et al., 2021b; Kymre et al., 2021a; Kymre et al., 2022; Løfaldli et al., 2012; Namiki, 2014), providing advanced knowledge about one of its most important sensory inputs. The species, *H. armigera*, relies heavily on pheromones for reproduction and plant odors for locating sources of nutrition. The pheromone system in the male moth has been investigated to a great extent, providing specific information about the intricate detection system and higher-order coding principles affecting behavior.

Utilizing this well-established system would imply studying components related to stereotypical innate behavior, including the hardwired pheromone pathway, which offers insight into primal communication cues. Additionally, it allows for studying a low-dimensional model, providing a simplified yet comprehensive understanding of complex behaviors. Furthermore, the system facilitates parallel processing of multiple pheromone signals simultaneously, enabling a deeper exploration of the intricate coding mechanisms underlying behavioral responses.

The *H. armigera* male moth offers the advantage of narrowing down the relevant number of olfactory cues to a manageable selection by focusing solely on pheromones, given its reliance on olfaction for environmental perception (Chu et al., 2020). Additionally, its nocturnal behavior simplifies the design of relevant visual stimuli for basic visual perception, further enhancing the feasibility of studying multimodal processing.

The Olfactory System of the Male *H. armigera*

Peripheral Olfactory Processing

The organization of the olfactory system in the insect is widely known due to extensive research during many years. In fact, the moth itself has a very well-developed system for detection of odors, even in the presence of high background noise (Røstelien, 2019, p. 50). Insects, as *H. armigera*, uses the antenna for detection of odors. The antennae house a wide range of olfactory receptors (ORs) located on olfactory sensory neurons (OSNs), pivotal for detection of relevant olfactory cues (Fleischer et al., 2018).

The OSNs produce electrical signals when odors contact the ORs, and projects the signals through axons forming the antennal nerve. These axons are directly connected to what is known as the antennal lobe (AL), the primary olfactory center, corresponding to the mammalian olfactory lobe. Within the AL, incoming olfactory signals are organized into

around 80 glomeruli (Zhao et al., 2016), with each glomerulus receiving projections from OSNs of the same functional type, i.e. expressing the same ORs (Vosshall et al., 1999).

Olfactory Processing in the Antennal Lobe

The majority of the glomeruli in the AL organizes information concerning plant odors (Zhao et al., 2016), relevant for behavior connected to for instance pollination and nutrition (Røstelien, 2019, p. 50). It is also known that one distinct glomerulus within the AL codes information regarding CO_2 (KC et al., 2020; Kent et al., 1986; Zhao et al., 2013). Some of the glomeruli are reported to process information regarding humidity and temperature, such as in the honeybee (Nishino et al., 2009) and fly (Gallio et al., 2011). Kymre et al. (2021a) discussed how this also might be the case for the *H. armigera*, based on the similarities in morphological traits of signaling pathways between the moth, fruit fly, honeybee, and cockroach.

Within the AL there is a male-specific group of glomeruli, called the macroglomerular complex (MGC), exclusively dedicated to organization of sex pheromones (Homberg et al., 1989). The male *H. armigera* utilizes three types of pheromones (i) primary pheromone (Z11-16:Al), (ii) secondary pheromone (Z9-16:Al), (iii) behavioral antagonist (Z9-14:Al), all secreted by the female moth. The primary and secondary pheromone, in a ratio of 98:2 respectively, function as an attractant for the male (Kehat & Dunkelblum, 1990; Liu et al., 2013; Xu et al., 2016). When a larger amount of the secondary component is present, it will inhibit the attractivity of the primary pheromone. This allows for discrimination between conspecifics and the sympatric and closely related moth, *Helicoverpa assulta*, which share the same pheromones, but in opposite ratios (5:95, Xu et al., 2016). The third component, the behavioral antagonist, suppresses the male sexual attraction when presented at high concentration (Kehat & Dunkelblum, 1990). However, as recent research has demonstrated, it seems to have a comparable function to the secondary pheromone since this compound

facilitates attraction at low concentrations (Wu et al., 2015). The pheromone processing MGC in *H. armigera* consists of three compartments named cumulus (Cu), dorsomedial posterior (dmp) unit, and dorsomedial anterior (dma) unit (Zhao et al., 2016). Each of the three pheromones components is represented in its respective glomerulus within the MGC. The OSNs responding to the primary pheromone projects to the Cu. The dma houses innervations from the OSNs responding to the secondary pheromone, and the dmp receives input about the behavioral antagonist (Wu et al., 2015).

In addition to housing the terminals of the OSNs, the AL also contains many local interneurons (LNs, Kymre et al., 2021a), which provide lateral communication between the different glomeruli within the AL (Fusca & Kloppenburg, 2021; Tabuchi et al., 2015; Warren & Kloppenburg, 2014), and projection neurons (PNs) connecting the AL to the protocerebrum (Kymre et al., 2022). The AL also receives feedback from the protocerebrum via a least seven types of centrifugal neurons (CNs, Kymre et al., 2021a). The LNs possess dendrites functioning as both pre- and post-synaptic terminals, with ability of both receiving and releasing neurotransmitters (Horne et al., 2018; Tabuchi et al., 2015). This allows a singular LN to provide bidirectional interglomerular signaling. Subsequent to the processing of odor input, the AL conveys the information into the protocerebrum through PNs projecting in six antennal lobe tracts (ALTs), organized into three main (medial, mALT; lateral, lALT; mediolateral, mlALT) and three minor (transverse, tALT; dorsomedial, dmALT; dorsal, dALT) tracts.

Olfactory Representation in the Protocerebrum

From the AL the pheromone signals, along with signals pertaining to plant odors, are projected through the three main tracts of the olfactory system, i.e. the mALT, lALT, and mlALT. The three minor tracts, tALT, dmALT, and dALT, function mainly as pathways for plant odors, CO_2, and potentially temperature and humidity (Kymre et al., 2022). Among all

the PNs physiologically and morphologically identified in the *H. armigera* so far, no pheromone-responding PNs have been observed in these three minor tracts.

According to Kymre et al. (2021b), PNs with dendrites in the Cu, processing the primary pheromone, innervate the calyces (CA) of the mushroom bodies (MB), ventrolateral protocerebrum (VLP), superior lateral protocerebrum (SLP), and superior intermediate protocerebrum (SIP) collectively via the three main tracts. The CA is a higher order center involved in memory processing in insects (Galizia, 2014) and receive input from several sensory modalities like olfaction, vision (Buehlmann, 2020), and taste (Yagi et al., 2016). For the VLP, it has been suggested that this neuropil has a central role in combinatorial coding of female-produced signals for optimal recognition of the specific species (Kymre et al., 2021b). The superior neuropils in the protocerebrum (specifically, SLP and SIP), are known as the primary processing areas for pheromones related to sexual attraction (Chu et al., 2020; Ian et al., 2016; Kymre et al., 2021b). Specifically, primary-pheromone responding PNs in the medial tract innervate the anterior SLP heavily along with some terminals extending into the SIP, while primary-pheromone PNs in the lateral tract solely target the SIP. In both morphological and physiological terms, the lALT PNs provide a fast and direct pathway, compared to the slower mALT PNs (Kymre et al., 2022).

With regard to the PNs innervating the dma (secondary pheromone) and dmp (behavioral antagonist), these also project through the mALT, targeting the CA. However, the innervation of MGC projection neurons into the CA is relatively minor compared to the innervation of plant odors. This applies particularly to PNs originating in the Cu (Homberg et al., 1988; Kymre et al., 2021b; Namiki et al., 2013; Zhao et al., 2014). The mALT projections from the dma and dmp also separate from the Cu-projections in that they mainly project to anterior parts of the lateral horn (LH) and VLP (Kymre et al., 2021b). MGC PN output onto the LH is associated with the behavioral antagonist and secondary pheromone (Kymre et al.,

2021b), both of which serve to inhibit mate-seeking behaviors in male moths when present in high concentrations (Kehat and Dunkelblom, 1990). In general, the LH does not only receive input about pheromones, but from all glomerular groups (Homberg et al., 1988; Kymre et al., 2022), of which the majority process plant odors.

When it comes to the mlALT, PNs innervating all three MGC components project to the VLP, whereas one unique PN with dendrites restricted to the Cu targets both the VLP, SLP, and SIP (Kymre et al., 2021b). For a complete visualization of the described pheromone projections, see figure 1 adapted from Kymre et al. (2021b).

In addition to projections targeting the SLP and SIP, the superior neuropils also encompass another region called the superior medial protocerebrum (SMP, Ito et al., 2014). This region has been demonstrated to receive pheromone information from what is known as the delta region of the lateral protocerebrum (ΔLP) in the closely related moth *Bombyx mori* (Namiki et al., 2014; Seki et al., 2005). The ΔLP region overlaps with anterior parts of the SLP, dorsal parts of the superior clamp (SCL), SIP, and some of the VLP (Lee et al., 2019). From this site, there are neurons projecting either through the SMP and then to the lateral accessory lobe (LAL), or directly from the ΔLP region to the LAL. The LAL then integrates this input and prepare a pre-motoric descending signal (Namiki & Kanzaki, 2016). We do not, however, have complete understanding of the olfactory processing occurring within the superior neuropils.

The Visual System in Insects

Currently, information on visual neural pathways in *H. armigera* has not yet been published. However, there are a few articles describing central visual neurons in other moth species (Collett, 1972; Namiki et al., 2018; Wicklein & Strausfeld, 2000). Altogether, an across-species perspective in which one looks at central visual pathways in insects more generally, could enrich the understanding relevant to the current investigation. It should be

Figure 1

Overview of macroglomerular complex projections across the three main olfactory tracts

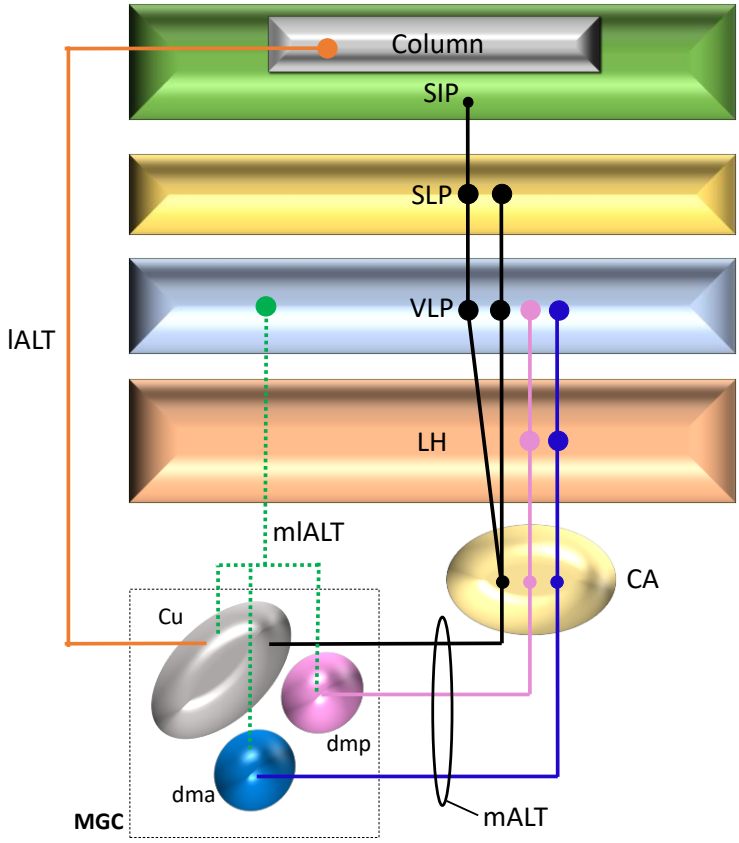

Note. The macroglomerular complex (MGC) consist of three glomeruli: cumulus (Cu), dorsomedial posterior unit (dmp), and dorsomedial anterior unit (dma). The medial antennal lobe tract (mALT, black, pink, and blue lines) neurons from the dma and dmp projects to the calyces (CA), lateral horn (LH), and terminate in the ventrolateral protocerebrum (VLP). In the very same tract, neurons from the Cu, also projects to the CA, but splits from here in that some neurons projects to the VLP and terminate in the superior lateral protocerebrum (SLP), and that other neurons projects to the VLP, SLP, and terminate by sparsely innervating the superior intermediate protocerebrum (SIP). Neurons from the Cu also projects through the lateral antennal lobe tract (lALT, orange line), to a specific region, the column, within the SIP. The mediolateral antennal lobe tract (mlALT, green dotted line) houses neurons projecting from all the glomeruli of the MGC to the VLP. As. The figure is adapted from Kymre et al. (2021).

noted that to our knowledge, there is no published literature with a complete overview of the entire visual system in insects. Thus, the following is meant to provide a brief overview.

Insects, like *H. armigera*, has two compound eyes, consisting of bilateral outgrowth regions of the protocerebrum, dedicated to vision. These compound eyes house the optic lobes (OL). Additionally, they have two simple eyes, called ocelli, located dorsally on the head, which function as sensors for ambient light intensity (Honkanen et al., 2018). Yet, their specific function in relation to behavior is relatively less known, compared to the OL. For most insects, the OL are compartmentalized, consisting mainly of three distinct neuropils subsequent to the outermost retina: lamina (LA), medulla (ME), and the lobula complex (LOX).

Optic Lobes – Retina, Lamina, Medulla, and Lobula Complex

Like its mammalian analogue, the insect retina consists of photoreceptor cells transducing photons into electrical signals (Honkanen et al., 2017). It houses different types of photoreceptors responding to distinct wavelengths leading to the perception of colors (Song & Lee, 2018). The retina of *H. armigera* has been shown to contain three types of photoreceptors sensitive to wavelength 400nm (ultraviolet), 483nm (blue), and 562nm (green, van der Kooi et al., 2021). Within the LA, different types of cells have been observed. Commonly, the different types of cells have shown a strong high pass filtering of the retinal signals, enhancing high-frequency components and reducing low-frequency components, allowing detection of rapid changes or edges in the visual field (Järvilehto & Zettler, 1971). The ME houses both local interneurons and output neurons. The first mentioned type connects various ME layers, and is being described as a relevant element for processing light intensity (Yukizane et al., 2002). The output neurons connect the neuropil to the LOX (Borst, 2009), a region consisting of two specific neuropils, the lobula (LO) and the lobula plate (LOP), known as the highest order visual neuropils in the optic lobes (Hausen, 1984). The LO

processes visual information about the size of objects (Ryu et al., 2022), which evokes behaviors such as escape, avoidance, and landing (Egelhaaf, 2023). In the LOP, neurons form a system sensitive to motion along either horizontal or vertical directions of moving objects (Scott et al., 2002). All together, these neuropils (ME, LO, LOP) project filtered and processed visual information into different neuropils the protocerebrum.

Visual Processing in the Protocerebrum

As previously mentioned, there is a lack of complete overview of the network connectivity within visual-relevant neuropils of the protocerebrum in any insect species. Therefore, based on previous studies across different species, I summarize what could be perceived as the seven key output regions of the visual projections from the OL (Fig. 2). These neuropiles are the anterior optic tubercle (AOTU), VLP, mushroom bodies (MB), gnathal ganglion (GNG), inferior posterior slope (IPS), posteriorlateral protocerebrum (PLP), and lateral accessory lobes (LAL, e.g. Buehlmann, 2020; Eriksson et al., 2019; Homberg, 2004; Otsuna et al., 2014)

The AOTU receives direct input from ME and LO and has been suggested to serve as a primary output region for visual information from the OL (Otsuna et al., 2014). The protocerebral neuropil also appears to be connected with innate behaviors such as navigation and courtship (Ryu et al., 2022). In the fly *Drosophila melanogaster*, this neuropil has also been shown to house terminals of neurons processing green light (Ryu et al., 2022).

The VLP, PLP, and LAL are direct output regions from the LOX (Eriksson et al., 2019; Homberg, 2004; Lin et al., 2016). Research has shown that VLP encodes information concerning the shape and velocity of moving objects (Klapoetke et al., 2022). The PLP has been demonstrated to be involved in perception of objects moving towards the insect (looming), which allows the insect to escape from predators, avoid collision with objects in the environment, and calculate necessary sequences involved in landing (Egelhaaf, 2023).

FIGURE 2

Overview of Seven Key Output Regions for Visual Projections from the Optic Lobes in Insects

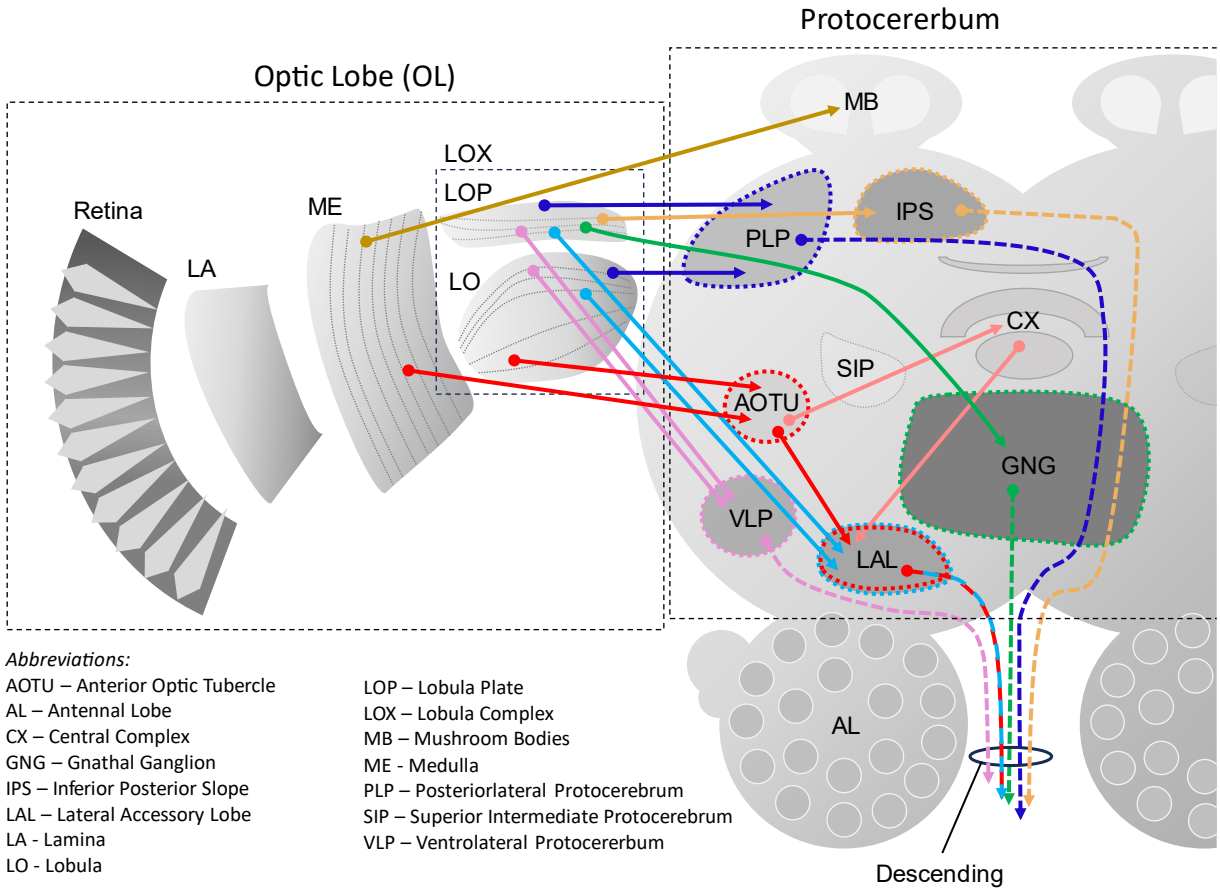

Note. Visual information from ME projects to the MB, AOTU. The LOX consists of the LO - with projections to PLP, VLP), LAL - and the LOP - with projections to the PLP, IPS, GNG, VLP, and LAL. The AOTU is one of the main input regions to the CX. Marked neuropils in the protocerebrum have been colored by the relative depth of their location, seen in dorsal view. The PLP, IPS, VLP, LAL, and GNG house descending neurons, projecting visual information to the ventral nerve cord. Constructed on the basis of Egelhaaf (2023); Otsuna et al. (2014); Ryu et al. (2022).

The function of the LAL could be separated with regard to the neuropil`s anatomical upper and lower part, where the upper receives input from various higher order brain regions in the protocerebrum (e.g. Central Complex and AOTU) and combine different types of information, while the lower part produces the premotor signal (Namiki & Kanzaki, 2016).

The MB receives output from the ME highly relevant for learning and memory, in which the input activates parts of the MB required in accurate steering information in visual navigation (Buehlmann, 2020). However, to our knowledge, there has not been observed any direct connections from the OL and MB calyx in the noctuid moth. Projections from LOP target the GNG and the IPS, with GNG outputs being associated with goal-direction, initiation, and maintenance of movement (Emanuel et al., 2020), while the IPS outputs are rather associated with course control based on optic flow-distance and rotation (Egelhaaf, 2023). Together, they also process information for optomotor responses, particularly in the neck of the insect (Ryu et al., 2022). From these seven OL-output regions, descending signals project to the ventral nerve cord (VNC). A more comprehensive explanation is provided in Figure 2.

A common downstream target for the majority of the OL-output regions is the central complex (CX, el Jundi et al., 2011; Homberg et al., 2011), known for being involved in various functions such as compass computations (Heinze & Homberg, 2007), spatial memory (Neuser et al., 2008), visual learning (Liu et al., 2006), multimodal processing (Homberg, 1994; Ritzmann et al., 2008), and motor control (Strauss, 2002; Triphan et al., 2010).

Olfactory-Visual Multimodal Processing in Lepidoptera

Having presented a brief overview of what is currently known about of olfactory and visual perception and associated pathways in the insect brain, it now becomes crucial to nominate regions relevant for the study of multimodality. Multimodality, or multimodal processing, is here understood as the ability to process more than one sensory modality. The concept of multimodality could be interpreted at various levels, and in the current study, it is to be referred to at the single neuron level. That is, the capacity of one single neuron to process information from at least two modalities. By looking at common output areas from the AL and OL, multiple regions will stand out. At a first glance of the presented

protocerebral regions, one might think VLP or MB would be good candidate regions for such studies. However, they have certain limitations.

Both the olfactory system and visual system has projections targeting the VLP. Yet, this region receives broad input from both pheromones and plant odors, making the determination of odor-specific-cues difficult (Kymre et al., 2022). A more distinct pathway would be preferable in this case if one has an emphasis on studying pheromone processing.

The MB could potentially be a candidate center for studying multimodality, however there are already several studies on the multimodal function of the MB (e.g. Strausfeld & Li, 1999; Strube-Bloss & Rössler, 2018; Yagi et al., 2016). In the case of the current investigation, the MBs would not be suitable for study, compared to other candidates. As already mentioned, the innervation of the MB calyces is also more substantial for AL PNs innervating glomeruli associated with plant odorants, than for pheromones (Homberg et al., 1988; Zhao et al., 2014).

Searching for a candidate center with direct pathways from the AL and OL, which also has substantial innervation from pheromone-responsive PNs, thus leads to another interesting region, namely the SIP. This neuropil is innervated by MGC PNs via all three main ALTs, each with distinct response patterns, biophysical properties, and spatiotemporal features (Kymre et al., 2022). The SIP has also been reported to receive input from ordinary glomeruli, yet studies have shown that the lALT neurons innervating the SIP without having dendrites limited to the cumulus are multiglomerular (Homberg et al., 1988; Ian et al., 2017; RØ et al., 2007), while PN innervations in this region from the mlALT commonly innervate all glomeruli, including the MGC (Kymre et al., 2021a). Altogether, these findings imply that the majority of AL inputs to the SIP are related to the primary pheromone, highlighting the suitability of this region for investigation of higher order pheromone processing. In addition, the adjacent anterior part of the SLP also receives input from PNs with innervations in the

primary-pheromone processing Cu, whereas posterior parts of the SLP are rather associated with the remaining AL glomeruli (Kymre et al., 2022). Indeed, pheromone sensitivity has been reported in protocerebral interneurons (PCNs) with innervations in the superior neuropils across multiple moth species (Lei et al., 2001; Lei et al., 2013; Namiki et al., 2014; Namiki & Kanzaki, 2019).

As illustrated in Figure 2, the OL output regions do not include the SIP. However, the closely situated AOTU was highlighted. Chu et al. (2020) has formerly stated that the close proximity of the AOTU and the SIP is rather intriguing as neurons projecting to these regions from the OL (to AOTU) and AL (to SIP) might share downstream targets. Indeed, it appears to be a common feature of PCNs to have widespread dendritic arbors spanning multiple adjacent neuropils (e.g. Lei et al., 2001; Namiki, 2014). Chu & colleagues (2020) further speculated that the SIP region might contribute with optimization of olfactory information so that it could be integrated with visual information, as the insect fundamentally rely on the visual system in tracing of odors (Baker & Hansson, 2019). This, combined with the limited knowledge about the SIP, described as multimodal in the commonly studied fruit fly (Taisz et al., 2023), makes it an interesting candidate for the investigation of multimodality between pheromones and vision.

Aim of the Thesis

Considering the importance of understanding how organisms use disparate sensory input in adapting behavior for navigational goals, the current study take aim at discovering olfactory, visual, and multimodal processing in a higher order brain region of the male moth, *Helicoverpa armigera*. With wide knowledge about the olfactory and visual system, and environmental cues in insects, we attempt to discover the vision-specific, odor-specific, and multimodal characteristics of single neurons by inserting sharp intracellular recoding electrodes into the region of a remarkably suitable candidate center, the SIP. Recordings will

be followed by iontophoretic staining (for morphological assessment), and extraction of physiological properties. If multimodal neurons are discovered, we intend to describe the single-modal properties as well as the combined, multimodal characteristics. Prior to this, we will develop a new technique for mass staining, allowing precise injection of fluorescent dye solution into highly restricted neuropils in order to assess AL and OL projection patterns and their relation to the SIP.

Materials and Methods

Insects and Experimental Preparatory Procedure

H. armigera pupae were obtained from Andermatt Group AG (Grossdietwil, Switzerland). Upon arrival pupae were sorted by sex and kept in separated climate chambers (IPP260, Memmert GmbH + Co.KG, Schwaback, Germany) with approximately 80% humidity at 23°C, alongside a 6pm – 8am light cycle. Imagos were translocated into cylindric, acrylic containers (20 cm H x 12.5 cm I.D.), lined with soft tissue paper, housing a maximum of 8 same sex moths. A 10% sucrose solution was provided in the containers, and moths were stored for four to six days prior to experiment conduction. In accordance with Norwegian legislation on animal welfare, there are no limitations pertaining to the experimental utilization of Lepidoptera (see https://lovdata.no/dokument/NL/lov/2009-06-19-97).

Male moths were immobilized in plastic tubes and the head capsule was restrained using dental wax (Kerr corporation, Romulus, MI) ensuring the integrity of antennae while protruding from the plastic tube. Observing through a stereomicroscope (Leica DMC 4500), a precise incision was made into the cuticular layer of the head capsule using a razor blade scalpel, thereby facilitating access to the brain. Tracheal extraction preceded the immobilization of the antennae through the application of copper wires. Application of Ringer´s solution (in nM: 150 NACl, 3 CaCl2, KCl, 25 sucrose, and 10 N-tris (dydromethyl)-methyl-2-amino-ethanesulfonic acid, pH 6.9) was done consistently to prevent dehydration of the neural tissue.

Air Pressure Mass Staining Experiments

A novel technique for mass staining was developed in collaboration with Dr. Xi Chu. Conventional approaches involve manually collecting small dye crystals and inserting them vertically into the neural tissue, resulting in a relatively large area of staining. In contrast, our novel air pressure method utilizes a glass microprobe to inject dye solution into highly restricted regions. Specifically, the microprobe was pulled from a glass capillary (0.5mm I.D.)

using a horizontal Flaming/Brown puller (P-97; Sutter instrument, Novato, CA, USA). The tip of the microprobe was first back-filled with (1) 4% solution of biotinylated dextran-conjugated tetramethylrhodamine (3000mw, micro-ruby, Molecular Probes; Invitrogen, Eugene, OR, USA) or (2) 4% Alexa Flour 488 (10000mw, Molecular Probes; Invitrogen, Eugene, OR, USA) in distilled water. Potassium acetate (KAc, 0.2 mM) was then added to fill the entire probe. Dental wax was carefully applied to seal the gap between the microprobe and a flexible silicon tube (1m Length, 5 mm I.D.), which facilitated airflow (Fig. 3). To improve tissue penetration, the tip of the microprobe was manually refined with forceps to create sharp edges without compromising the integrity of the dye solution. To perform the staining, air pressure was applied by gently blowing through the tube following the insertion of the microprobe into the target brain region.

Intracellular Experiments and Stimuli

All single unit recordings were conducted during daytime, i.e. when the noctuid insects were confined in darkness within the climate chamber. Quartz electrodes (7.5 cm Length, 0.50mm I.D.) were pulled using a horizontal laser puller (p-2000; Sutter instrument, Novato, CA, USA). The tip was filled with a 4% solution of biotinylated dextran-conjugated tetramethylrhodamine (3000mw, micro-ruby, Molecular Probes; Invitrogen, Eugene, OR, USA) in KAc, and further backfilled with KAc solution (0.2 mM). A chlorinated, silver wire was used as a reference electrode inserted into the muscle tissue of the proboscis. Preceding the insertion into neural tissue, the resistance of the recording electrode was measured, assuring resistance in the 100-200 MΩ range. The recording electrode was then inserted into the protocerebrum, using a Leica micromanipulator. Recordings were carried out utilizing a setup composed of a HS-2 head-stage preamplifier (Axon instruments, Union, CA, USA), and an Axoprobe-1A amplifier (Axon instruments), together with a Micro1401 mkII data acquisition unit (Cambridge Electronic Design Limited, Cambridge, UK) and a

Figure 3

Equipment used for novel air pressure mass staining technique

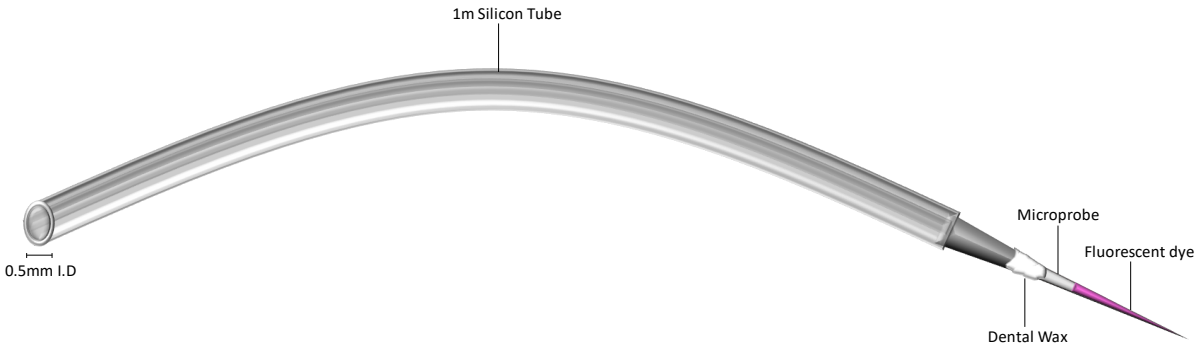

Note. Our novel method utilizes a glass microprobe pulled from a glass capillary. The tip of the microprobe was first back-filled with 4% solution of micro-ruby or 4% Alexa Flour 488 in distilled water, and then with potassium acetate. Dental wax was applied to seal the gap between the microprobe and a flexible silicon tube, which facilitated airflow. By manually blowing into the silicone tube, fluorescent dye was injected into highly restricted regions. *Abbreviations:* I.D, inner diameter.

loudspeaker (Tektronix 511A, Oregon, USA). Software Spike 2, version 6.18 (Cambridge Electronic Design, Cambridge, England), was used to register electrophysiological traces.

Odor Stimulation

Upon establishing contact with a neuron in the region of interest, the insect was presented with the following seven odorants in a semi-randomized sequence: (1) primary pheromone (Z11-16:Al), (2) secondary pheromone (Z9-16:Al), (3) behavioral antagonist (Z9-14:Al), (4) a 95:5 ratio blend of primary and secondary pheromone, (5) insect attractor component (IAC) consisting of a blend of five plant odors (50µl Phenylacetaldehyde, 20µl Salicylaldehyde, 10µl Methyl 2-methoxyy benzoate, 10µl Linalool, and 10µl (R)-(+)-Limonene) (Guo et al., 2021) and (6) YlangYlang. For control (7) hexane was employed owing to its function as a solvent for both pheromones (10^{-6}) and plant odors (10^{-3}), and (8) a mechanosensory stimulation consisting of air only.

Odorants were applied (20µm) on a filter paper prior to placing into a 120mm glass cartridge. Further, they were administered using a solenoid-activated valve (General Valve Group, Fairfield, NJ, USA), which directed a continuous flow of fresh air into the odorant-containing glass cartridge in a series of 20 pulses lasting 80 milliseconds each, with a 520-millisecond interval between pulses for a total of 12 seconds of odor stimulation.

Visual Stimulation

Visual stimulation was provided on a 55 inches LCD color screen (Sony Corporation) with a 1920 x 1018 resolution. The screen was placed in front of the recording set-up, outside a mesh-wired Faraday cage, with a distance of 70cm from the insect. Visual stimulation was created using PowerPoint software (Version 2311, Microsoft Corporation) and consisted of two similar animations in contrasting colors. Stimulus 1 consisted of a moving green bar (#33CC33B3) on a black screen (#000000). The bar was moving from (1) four seconds left to right, (2) four seconds right to left, (3) two seconds top to bottom, and (4) two seconds bottom to top, adding up to a total of 12 seconds corresponding with the time of odor stimulation (Fig. 4, Stimulus 1). Stimulus 2 consisted of a black bar on a green screen, moving in the exact same pattern, with the same color gradient as in stimulus 1 (Fig. 4, Stimulus 2). To ensure that the wavelength of the green color of the stimulus corresponded to wavelength of the green sensitive photoreceptor in the retina of the moth, I sought support from PhD candidate Frederik Hanslin at el Jundi lab, who kindly confirmed that the green stimulus color correctly corresponded to 535nm, with a light intensity of 4.2081E11 photons/cm2/sec (measured 20 cm from the screen).

Multimodal Stimulation

Multimodal stimuli consisted of a combination of odor stimuli and visual stimuli. For vision, stimulus 1 (moving green bar on black screen) was chosen based on the

Figure 4

Overview of visual stimulations

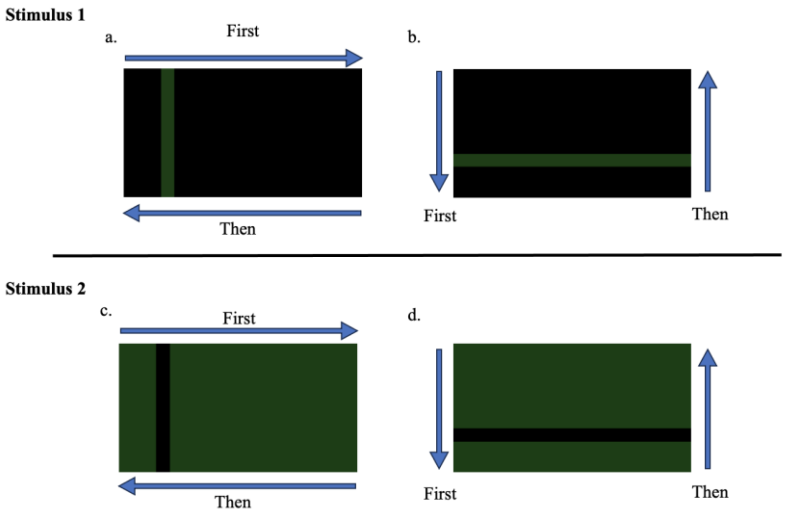

Note. Stimulus 1: green bar on black screen moving firstly (a) left to right, right to left, then (b) top to bottom, and bottom to top. Stimulus 2: black bar on green screen moving firstly (c) left to right, right to left, then (d) top to bottom, and bottom to top.

Figure 5

Overview of multimodal stimulus

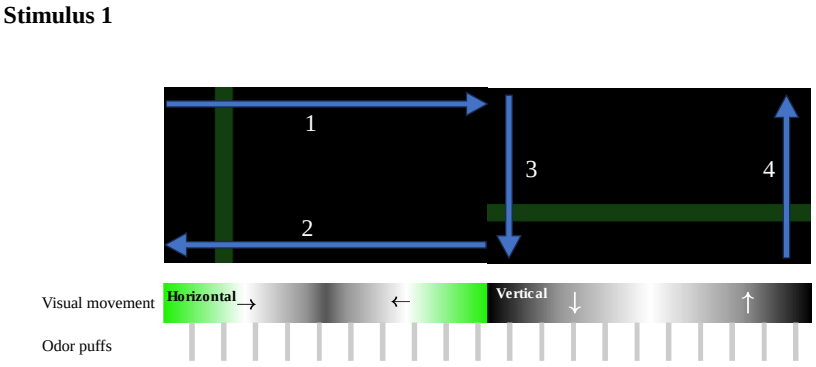

Note. Multimodal stimuli were systematically aligned with the movement trajectory observed in visual stimuli alone. Specifically, all multimodal stimuli were characterized by the presence of a green bar against a black screen, adhering consistently to the sequential order of movement denoted as 1-2-3-4. This visual representation of movement is graphically depicted by the graded bar underneath marked ′visual movement′. Concurrently, during the designated stimulation period for the visual modality, a total of 20 odor puffs, each lasting 80 milliseconds, were administered with an inter-pulse interval of 520 milliseconds.

photoreceptor's sensitivity to this color, and the connected neurons' projections to the AOTU. Each multimodal stimulus comprised one specific odorant paired with the designated visual stimulation, ensuring a synchronized presentation of olfactory and visual cues (Fig. 5). The order of multimodal stimulations followed the same randomized order as presented in the odor-only stimulation.

Iontophoretic Staining

Subsequent to stimulation, neurons that exhibited a response were iontophoretically stained. This procedure entailed the injection of depolarizing current pulses ranging from 3-3.3nA with a duration of 200 milliseconds at a frequency of 1 Hz for 5-7 minutes. Cuticle of insects was then sealed with Vaseline preventing dehydration and stored at 4°C overnight to facilitate dye-transportation. Following this procedure, the brain was dissected out and kept overnight at 4°C in an Eppendorf tube containing 4% paraformaldehyde (Roti-histofix 4%,Carl Roth GmbH, Karlsruhe, Germany), before dehydrating in a series of ethanol solutions (50%, 70%, 90%, 96%, 2x100%). The brain was then made transparent, by being inserted into methyl salicylate (methyl 2-hydroxybenzonate: Merck KGaA, Germany) for 10minutes, before being mounted in aluminum plates containing the very same substance.

Confocal Laser Scanning Microscopy

Investigation of morphological characteristics was conducted by scanning the brain preparation in a LSM800 confocal laser scanning microscope (CLSM, Carl Zeiss Microscopy, GmbH, Jena, Germany). The microscope was equipped with a C-apochromat 10x/0.45 water objective together with a Plan-Neoflunar 20x/0.5 air objective. Obtaining images of injected MicroRuby signals required excitation by a 553 nm HeNe laser, with emitted light captured by a long-pass filter. In the case of Alexa Flour 488, the dye was excited using a 493 nm Argon laser together with a 505-550 nm band pass filter to collect emitting light. The distance

of the optical slices was set to 3.00 – 9.06 µm, with pinhole size of 1 airy unit, and pixel resolution range between 1024x1024 to 1450x1450.

Data Analyses

Morphological Analyses

Utilizing the ZEISS Efficient Navigation (ZEN) software 2.3 blue edition (Carl Zeiss Microscopy), confocal z-stacks were scrutinized to assess the morphological characteristics of stained neurons. Only individual neurons demonstrating adequate staining, exhibiting discernible dendrites, axon, soma, and axon terminals, were deemed eligible for inclusion in the final analyses. Stains lacking clear attribution to a single neuron were excluded from further analyses due to concerns regarding internal validity. This way, we circumvented the attribution of physiological features to a neuron whose identity could not be definitively confirmed. In such cases, the electrophysiological data acquired was likewise omitted. Classification of input- and output- regions was based on the morphological properties of the neuron´s branches. Thus, smooth branches were classified as postsynaptic sites, and varicose processes as presynaptic sites. This aligns with previous reports (e.g. Cardona et al., 2010)

Z-stacks eligible for further analysis was processed with orthogonal projection, creating maximum intensity projections, and exported into Photoshop (version 2024, Adobe Inc.) for color corrections adjustments.

Nomenclature

Morphological descriptions followed the standardized insect brain nomenclature by following the 3D model from Ito et al. (2014). Locations of distinct neuropils were adapted according to species-specific landmarks characteristic of the male moth. In Lepidopteran species, fiber bundles and commissures are not yet clearly identified. Therefore, classification of such structures was based on the standard fruit fly brain, *Drosophila melanogaster*.

Spike Analyses

Spike2 version 10.13 was utilized for spike sorting, i.e. assessing waveform homogeneity to establish that analyzed spikes belonged to a single neuron. The sorted data were exported as text files of peri-stimulus histograms and transferred into MATLAB R2023b for further analyses. Each trial analyzed contained a 15 second stimulation period, including a 1000 ms pre-stimulus window, and a 2000 ms post-stimulus duration. The mean Z-scored instantaneous firing rate (MZIFR) across trials for each neuron was generated by using a customized MATLAB package, with a 1ms bin size.

To determine of visual responsivity, we manually inspected the pattern of MZIFR traces (with a 100ms bin size). In doing so, we only classified clear and obvious changes in spike firing frequencies as visual responses, and may have somewhat underestimated responsivity. Specifically, we characterized responses as *visual field responses* when firing frequency changed during bar movement in a specific part of the insect`s visual field, as *direction selective responses* when firing pattern change was substantial and differential during bar movement in opposite directions, or as *ON/OFF responses* when firing pattern change occurred as the visual stimulus turned on or off.

To ascertain significant odor-evoked responses, we used a two-step analysis. First, we identified every timepoint where the MZIFR within the corresponding bin surpassed an upper (T_U) or lower (T_L) threshold. Here, MZIFR in the pre-stimulus window ($MZIRF_{PS}$) was used to calculate these thresholds. Calculations was carried out utilizing a signification level of α = .05 together with the same formula as prior publications (Chu et al., 2020):

$$T_U\ of\ repetitive\ trials = \overline{MZIFR_{PS}} + 1.96\sigma_{MZIFR_{PS}}$$

$$T_L\ of\ repetitive\ trials = \overline{MZIFR_{PS}} - 1.96\sigma_{MZIFR_{PS}}$$

In the second step, we calculated the sum of those time points surpassing the thresholds, and characterized a response as when the sum was over 10% of the 12 seconds stimulation window.

Classification Strategy of Protocerebral Interneurons

Classification of the protocerebral interneurons (PCNs) was based on the physiological responses of each neuron. Neurons only showing responses to odors were classified as olfactory PCNs, while neurons only displaying either direction selective-, visual field- and/or light ON/OFF responses, were classified as visual PCNs. If a neuron displayed both (i) responses to olfactory stimuli, and (ii) direction selective-, visual field- or light on and/or off responses, it was classified as a multimodal PCN. For those neurons that did not display any response to any olfactory stimulation, or direction selective-, visual field- or light on and/or off responses, a fourth class was made grouping such neurons.

Results

Identification of Relevant Olfaction-Vision Integration Site

In order to identify the relevant site for intracellular recordings, mass stainings were conducted. For injection of dye, our novel air-pressure mass staining was applied. In total, two male moths were utilized to obtain the necessary data for identification. In the first experiment, micro-ruby was injected into the MGC and Alexa488 into the OL (Fig 5A). Results from the first experiments displayed neurons from the MGC projecting to several regions, but most interestingly the SIP (Fig. 5B). Neurons from the OL were observed innervating large parts of the ipsilateral hemisphere (Fig. 5C). Among these regions, clear innervations of the AOTU were observed. Thus, projections from the MGC and OL were observed targeting two regions closely situated in the superior protocerebrum.

In the second experiment, micro-ruby was injected into the restricted region encompassing SIP and AOTU. Results from the second experiment displayed innervations into the OL and the MGC, thus confirming the results observed in the first mass staining experiment. Specifically, results showed innervation into the ipsilateral OL, AOTU, and MGC, as well as projections into the contralateral AOTU, and minor innervations of the contralateral SMP (Fig. 5D). The two mass staining experiments laid the basis for selecting a target region into which the sharp intracellular recording electrodes were inserted.

Protocerebral Interneurons and Corresponding Physiological Characteristics

Based on the identification of a potential integration site from the mass staining experiments, single cell intracellular recordings were conducted targeting the insertion of the electrode into the region encompassing SIP. In total, 30 moths were utilized for experimental purposes, out of which nine protocerebral interneurons (PCNs) were successfully recorded and stained (PCN2 – PCN10), qualifying for quantitative analysis (30% success rate). Additionally, one PCN (PCN1) was gathered by the co-supervisor Dr. Xi Chu, and seven PCNs (PCN11 – PCN17) by the supervisor Dr. Jonas H. Kymre. Four PCNs were classified

Figure 5

Visualization of mass staining for identification of pheromonal and visual pathway

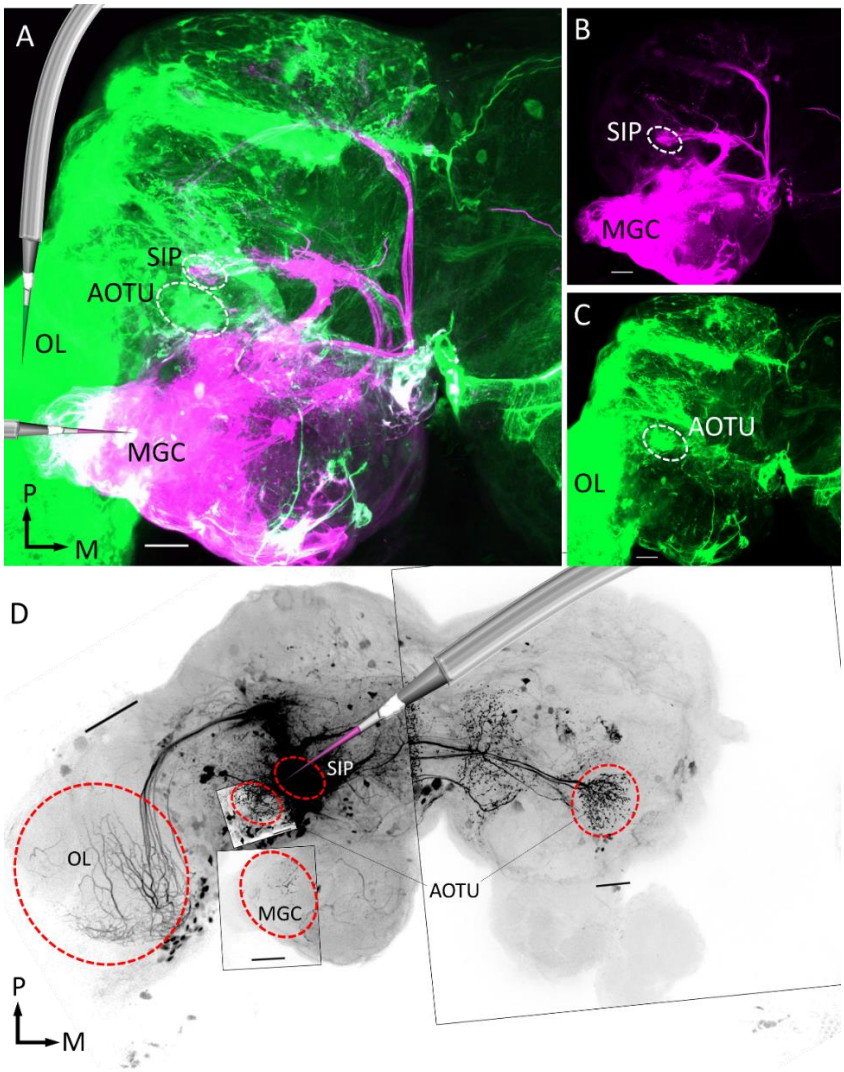

Note. Air-pressure injection mass stainings. (**A**) Maximum intensity projection confocal image of the closely located output regions of the OL and MGC, i.e. the anterior optic tubercle (AOTU) and superior intermediate protocerebrum (SIP), respectively. The OL (green) was stained with Alexa488 and the MGC (magenta) with micro-ruby. (**B**) Single-channel MGC projections, with marked output region SIP. (**C**) Single-channel OL projections, with marked output region AOTU. (**D**) Confocal image of fluorescent dye injection site (SIP/AOTU-region), with projections to OL, MGC, and contralateral AOTU. Scale bars = 100 µm.

as olfactory neurons, three as visual, and seven as multimodal neurons. Three PCNs did not meet our criteria for either of the categories, we thereby termed these as nonresponsive PCNs (Morphological features are summarized in Appendix A).

Olfactory PCNs

In total, four neurons filled the set criteria for classification as olfactory PCNs. Among the olfactory stimulations, six out of eight stimuli induced a significant response lasting more than 10% of the stimulus window duration. Only one neuron displayed inhibitory responses to some of the odors. Olfactory PCNs and corresponding odor stimulations with response duration in percentages are shown in table 1 (also see peak ZIFR in Appendix B). For these neurons, no clear response to the visual stimulation was observed by visual inspection.

PCN3

PCN3's (Fig. 6) soma was positioned within the cell body rind laterally adjacent to the AL(rALl). Originating from this location, neurites resembling dendrites extended toward the subesophageal zone (SEZ) via the great commissure (GC). Axon terminals displayed robust projection patterns predominantly targeting the LO, with supplementary projections evident in the PLP. The PCN responded with the behavioral antagonist, and ylang-ylang. The offset was relatively more delayed for the ylang-ylang compared to the behavioral antagonist. Phasic-tonic responses were observed for the behavioral antagonist, while responses to ylang-ylang were mainly phasic.

Table 1

Overview of Odor Response Duration in percentages for all Categorized Olfactory PCNs

ODOR / NEURON	Primary Pheromone	Behavioral Antagonist	Pheromone Blend	Insect Attractor Component	YlangYlang	Hexane
PCN3	0,88	14,10	7,24	3,75	12,58	1,99
PCN6	10,28	12,23	23,23	8,85	2,29 (1,88)	13,05
PCN10	7,03	2,20	7,38	17,07	2,8	5,33
PCN14	8,49	11,34	4,63	10,97	4,66	2,41

Note. Only odors that had a significant response which lasted more than 10% of the stimulus window duration are colorized in the table. Numbers signifies the response duration as a percentage of the entire stimulation window duration of each stimulus. Green and blue boxes indicate excitatory and inhibitory responses, respectively.

Figure 6

Morphological and Physiological Visualization of PCN3

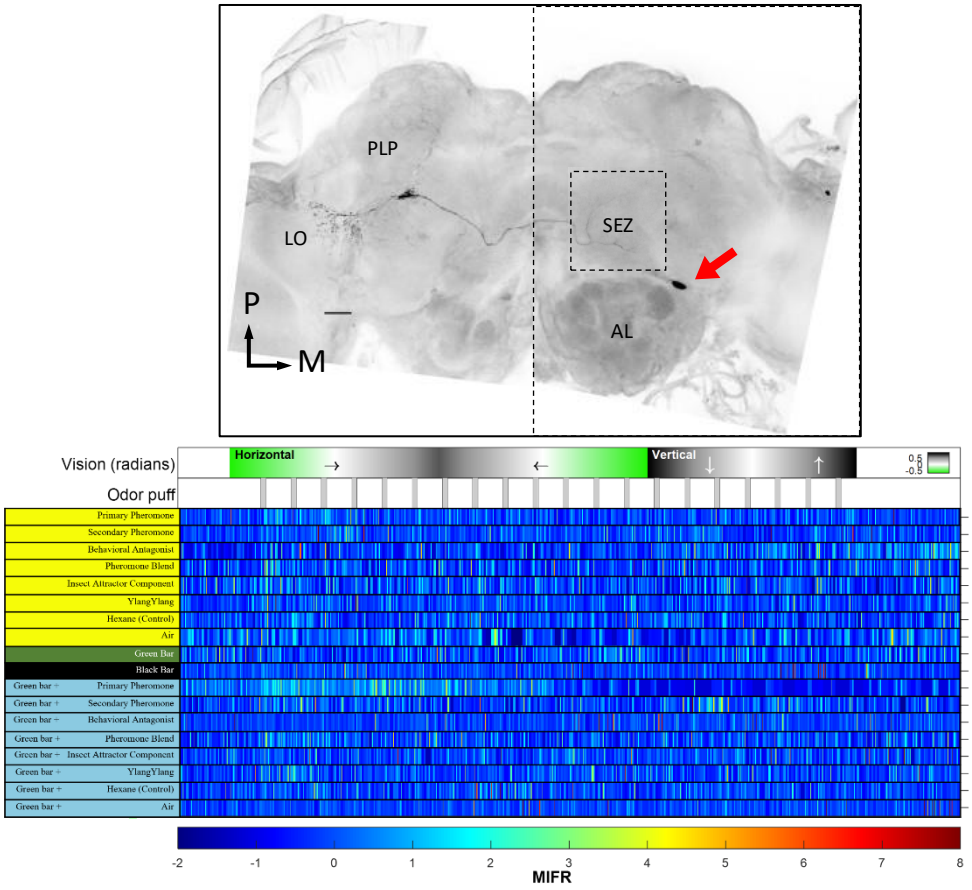

Note. Upper; confocal image of a protocerebral interneuron (ID, PCN3) in dorsal view. The neuron connected the subesophageal zone (SEZ) with the lobula (LO) and posteriorlateral protocerebrum (PLP). Soma location is marked with *red* arrow. Scale bar = 100 µm. *Lower;* responses to odor-only (yellow), vison-only (green and black), and multimodal (blue) stimuli. Responses are represented as mean instantaneous firing rate with 10 milliseconds bin size. Total registration period spans 18 seconds, comprising a one second pre-stimulus window, a 15 seconds stimulation period, and a two seconds post-stimulus window. Location and motion of bar for visual stimulation is illustrated at the top, with the angular measurement of the bar relative to the moth subject expressed in radians (Horizontal: green = left, white = middle, grey = right; Vertical: black = top, white = middle), alongside a relative time frame of 20 odor puffs presented below (80ms puff, 520ms inter-pulse interval). The neuron displayed an excitatory, phasic-tonic response to the behavioral antagonist, and mainly phasic response to ylang-ylang. No other odors evoked a sum of response period greater than our pre-set criteria, i.e., 10% of the stimulus window duration. Responses to visual-only stimulations were not observable. *Abbreviations*: AL, antennal lobe; M, medial; MIFR, mean instantaneous firing rate; P, posterior. Bin size = 10ms.

PCN6

PCN6's soma was identified within the cell body rind dorsal to the SMP (rSMPd, Fig. 7E). From this point, dendritic processes exhibited symmetrical branching, innervating major parts of the superior neuropils (including SLP, and SIP, Fig. 7A, 7D, 7C) and minor branches in the inferior neuropils via the superior PLP commissure (sPLPc). Axon terminals were observed predominantly distributed across the PB (Fig. 7B), with secondary projections observed within the SMP (Fig. 7A) and lateral accessory lobe (LAL, Fig. 7C). The neuron (Fig.7E) had excitatory phasic responses for the behavioral antagonist, particularly in the first half of the stimulation window. The primary pheromone elicited strong and long-lasting inhibitory responses with less potent inhibition in the later part of the stimulation window. The most pronounced inhibition induced by the pheromone blend occurred about 10 ms after the first puff. A second inhibition was observed in the middle of the stimulation window, and rather less potent after this point. Additionally, PCN6 displayed a phasic excitation to the first puff of hexane, but no such response was observed to air.

PCN10

PCN10's soma was located within the cell body rind dorsally positioned to the SIP (rSIPd, Fig. 8D). Emerging from this locus, dendritic neurites displayed extensive branching patterns encompassing the SMP (Fig. 8B), SLP (Fig. 8C) via the superior PLP commissure (sPLPC), and the superior fiber system (SFS), with sparse extensions into the contralateral SMP (Fig. 8A). Axon terminals exhibited bilateral innervation primarily targeting the CA (Fig. 8A). The neuron (Fig. 8E) only responded to insect attractor component, expressing phasic-tonic excitatory responses after the first quarter of the stimulation trails. During the first quarter, inhibitory responses were observed.

Figure 7

Morphological and Physiological Visualization of PCN6

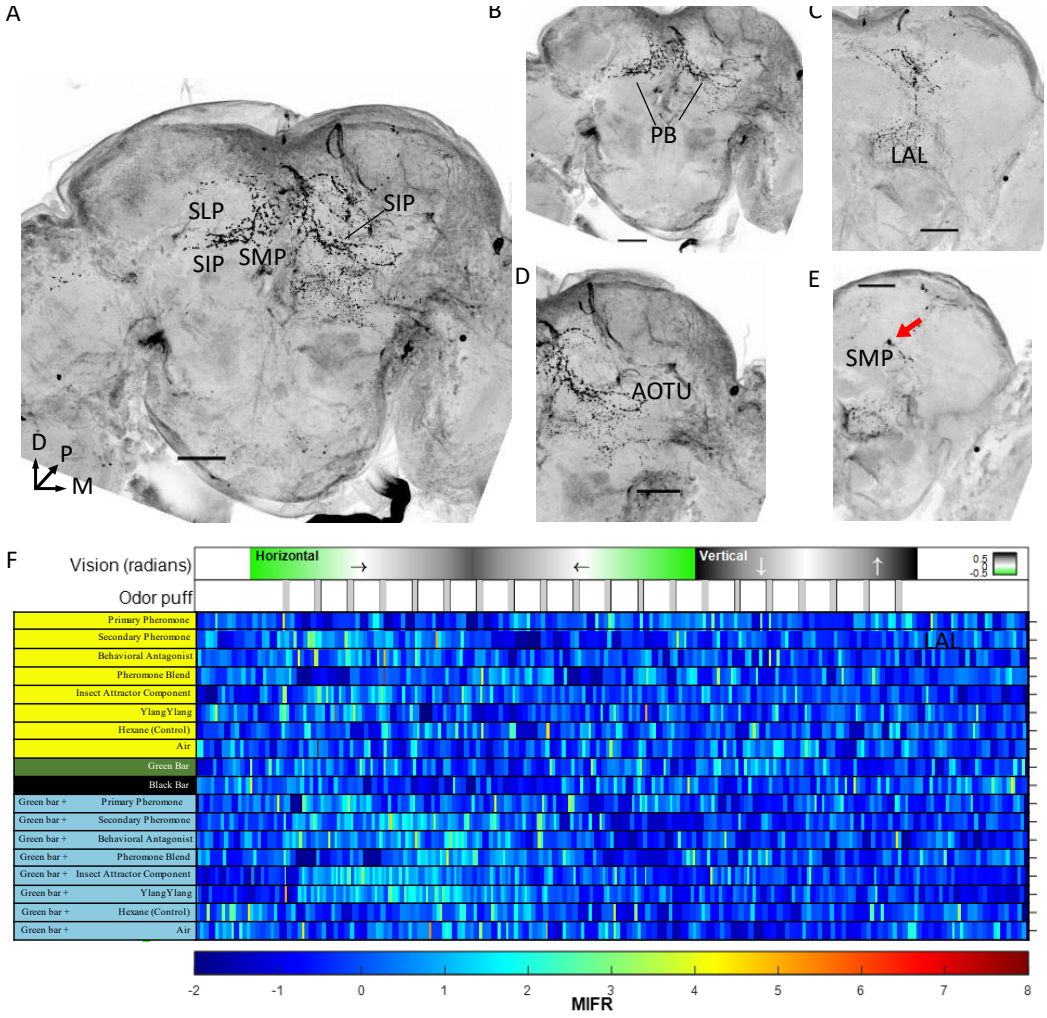

Note. Confocal images of a protocerebral interneuron (ID, PCN6) in frontal-dorsal view. Neuron connecting (**A**) major parts of the superior protocerebrum, minor parts of the inferior protocerebrum (**B**), protocerebral bridge (PB), (**C**) lateral accessory lobe (LAL), and (**D**) anterior optic tubercle (AOTU). Soma location is marked with *red* arrow (**E**). Scale bar = 100 µm. (**F**) responses to odor-only (yellow), vison-only (green and black), and multimodal (blue) stimuli. Responses are illustrated in the same way as described in figure 6. The neuron displayed phasic excitation in response to the behavioral antagonist, long-lasting inhibition to the primary pheromone, and even stronger inhibition to the pheromone blend. Hexane elicited a phasic excitatory response. All other odors did not induce a response lasting longer than our pre-set criteria of 10% of the stimulus window duration. Responses to visual-only stimuli were not observable. *Abbreviations*: AL, antennal lobe; M, medial; MIFR, mean instantaneous firing rate; P, posterior. Bin size = 10ms.

Figure 8

Morphological and Physiological Visualization of PCN10

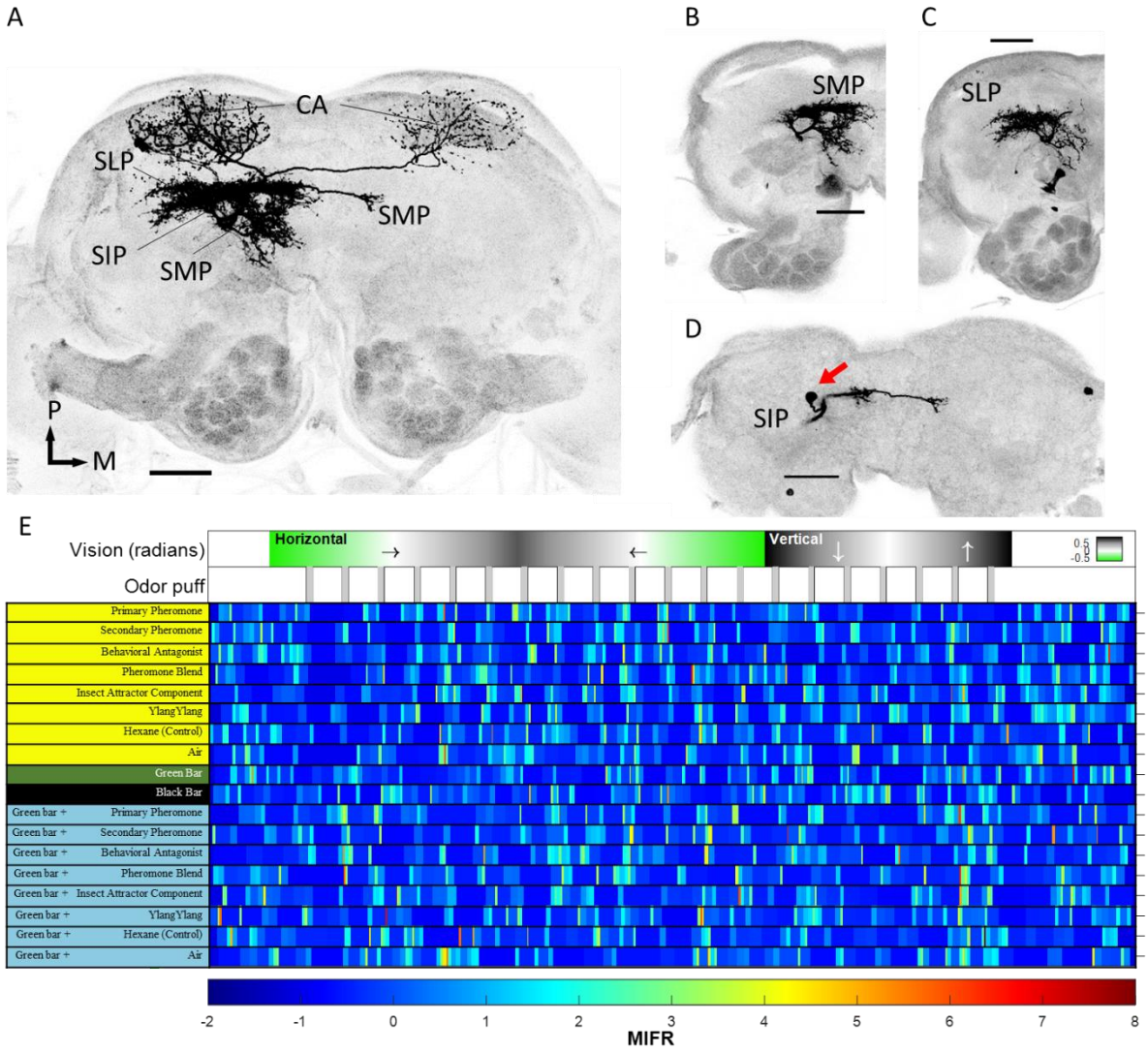

Note. Confocal image of a protocerebral interneuron (ID, PCN10) in dorsal view. (**A**) Neuron connecting bilateral calyces (CA), superior intermediate protocerebrum, (**B**) superior medial protocerebrum (SMP), and (**C**) superior lateral protocerebrum (SLP). (**D**) Soma location is marked with *red* arrow. Scale bar = 100 µm. (**E**) responses to odor-only (yellow), vison-only (green and black), and multimodal (blue) stimuli. Responses are illustrated in the same way as described in figure 6. The neuron only responded with insect attractor component. All other odors did not induce a response lasting longer than our pre-set criteria of 10% of the stimulus window duration. Responses to visual-only stimuli were not observable. *Abbreviations*: M, medial; MIFR; mean instantaneous firing rate; P, posterior. Bin size = 10ms.

PCN14

The neuron's soma (Fig. 9A) resided within the cell body rind medioposterior to the SMP (rSMPmp). From here, dendrites elongated toward the contralateral PLP (Fig. 9B) via the superior PLP commissure (sPLPC) and the superior ellipsoid commissure (SEC). Axon terminals were predominantly sent to the SLP, VLP, and LH, with relatively minor projections into the PLP, and accessory calyces. PCN14 responded (Fig. 9C) with the behavioral antagonist and the insect attractor component. For both odors, the excitatory responses were observed shortly after most of the puffs, indicating inhibition release responses or delayed excitation. The inhibition release had a more phasic pattern for the behavioral antagonist, and tonic pattern for the insect attractor component.

Visual PCNs

A total of three neurons met the criteria for classification as visual PCNs. Among these three PCNs, all reacted to rightward bar movement. PCN12 and PCN13 also displayed upward direction selective responses, while PCN13 was the only visual PCN that had visual field responses, when the bar was moving in both horizontal directions. No left- or downwards direction selective responses, nor light ON/OFF responses were clearly observable for the three visual PCNs. All three neurons had their soma located within the cell body rind posterior to the PLP. PCN11 did not have any response to olfactory stimulation that crossed our threshold of 10% of the stimulus duration, while PCN12 and PCN13 only responded to mechanosensory stimuli in the olfactory stimulation trail. All visual PCNs and observed responses have been summarized in table 2.

PCN11

PCN11 (Fig. 10) had its soma located posteriorly to PLP within the cell body rind (rPLPp). Dendritic extensions displayed sparse innervation of PLP and VLP, with major innervation observed in LAL through the LAL commissure (LALC).

Figure 9

Morphological and Physiological Visualization of PCN14

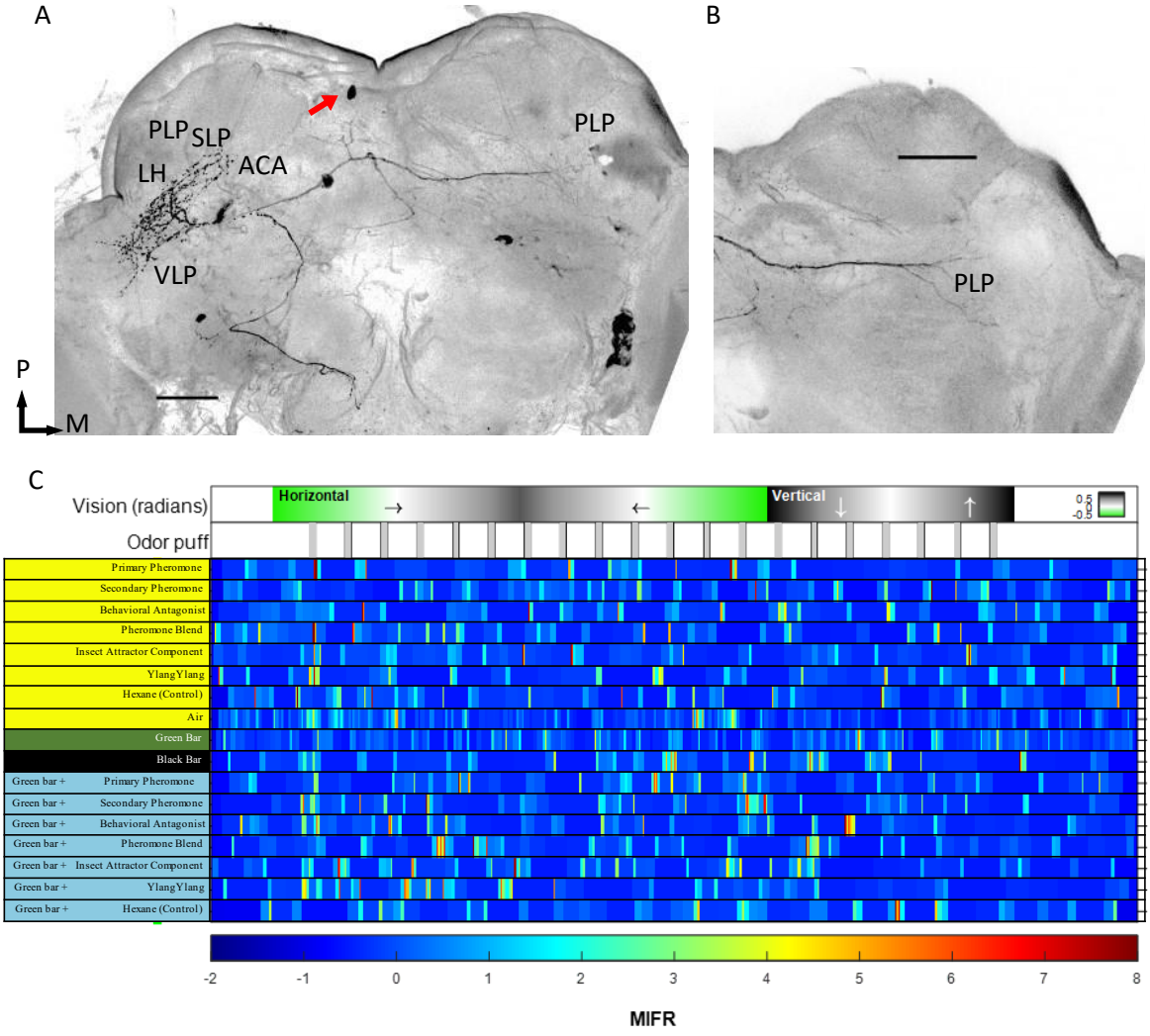

Note. Confocal image of a protocerebral interneuron (ID, PCN14) in dorsal view. (**A**) Neuron connecting lateral protocerebral neuropils with the (**B**) contralateral posterior lateral protocerebrum (PLP). Soma location is marked with *red* arrow (**A**). Scale bar = 100 µm. (**C**) responses to odor-only (yellow), vison-only (green and black), and multimodal (blue) stimuli. Responses are illustrated in the same way as described in figure 6. The neuron only responded with behavioral antagonist and insect attractor component. All other odors did not induce a response lasting longer than our pre-set criteria of 10% of the stimulus window duration. Responses to visual-only stimulation was not observable. *Abbreviations*: ACA, accessory calyces; LH, lateral horn; M, medial; MIFR, mean instantaneous firing rate; P, posterior; SLP, superior lateral protocerebrum; VLP, ventrolateral protocerebrum. Bin size = 10ms.

Table 2

Overview of Visual Responses for all Categorized Visual PCNs

Visual Response / NEURON	Direction Selective RIGHT	Direction Selective LEFT	Direction Selective DOWN	Direction Selective UP	Visual Field	Light ON/OFF
PCN11	✓	-	-	-	-	-
PCN12	✓	-	-	✓	-	-
PCN13	✓	-	-	✓	✓	-

Note. Only responses which were clearly observed upon visual inspection were reported as a visual response.

Axon terminals projected toward the contralateral LAL and BU, with some extensions reaching into the AOTU. By visual inspection of responses to visual stimulation, PCN11 displayed clear direction selective responses. More specifically, the neuron showed increased firing activity for the green bar moving in the right direction from -20 to 30 degrees of the visual field, in comparison to left direction. No particular response was observed for the bar moving in any vertical direction.

PCN12

In this neuron (Fig. 11), the soma was positioned posterior to PLP within the cell body rind (rPLPp). Dendritic branches exhibited sparse innervation of the LOP via the posterior optic commissure (POC). Axon terminals innervated the contralateral LAL sparsely and the contralateral PS more prominently. Clear direction selective responses were observed for both horizontal and vertical bar movement. The neuron displayed excitatory activity when the bar was moving in the rightward direction from -30 to 0 degrees (Fig. 11C), as well as for upward direction from 10 to 30 degrees (Fig. 11D), compared to when the bar was moving left or down where PCN12 displayed inhibitory responses. During the odor tests, the neuron did display an inhibitory response to air (mechanosensory input) that crossed our threshold of 10% of the stimulus duration. However, the absence of response to any of the chemical cues

indicated that this neuron is a mechanosensory rather than an olfactory one. Thus, PCN12 was classified as a visual neuron.

Figure 10

Morphological and Physiological Visualization of PCN11

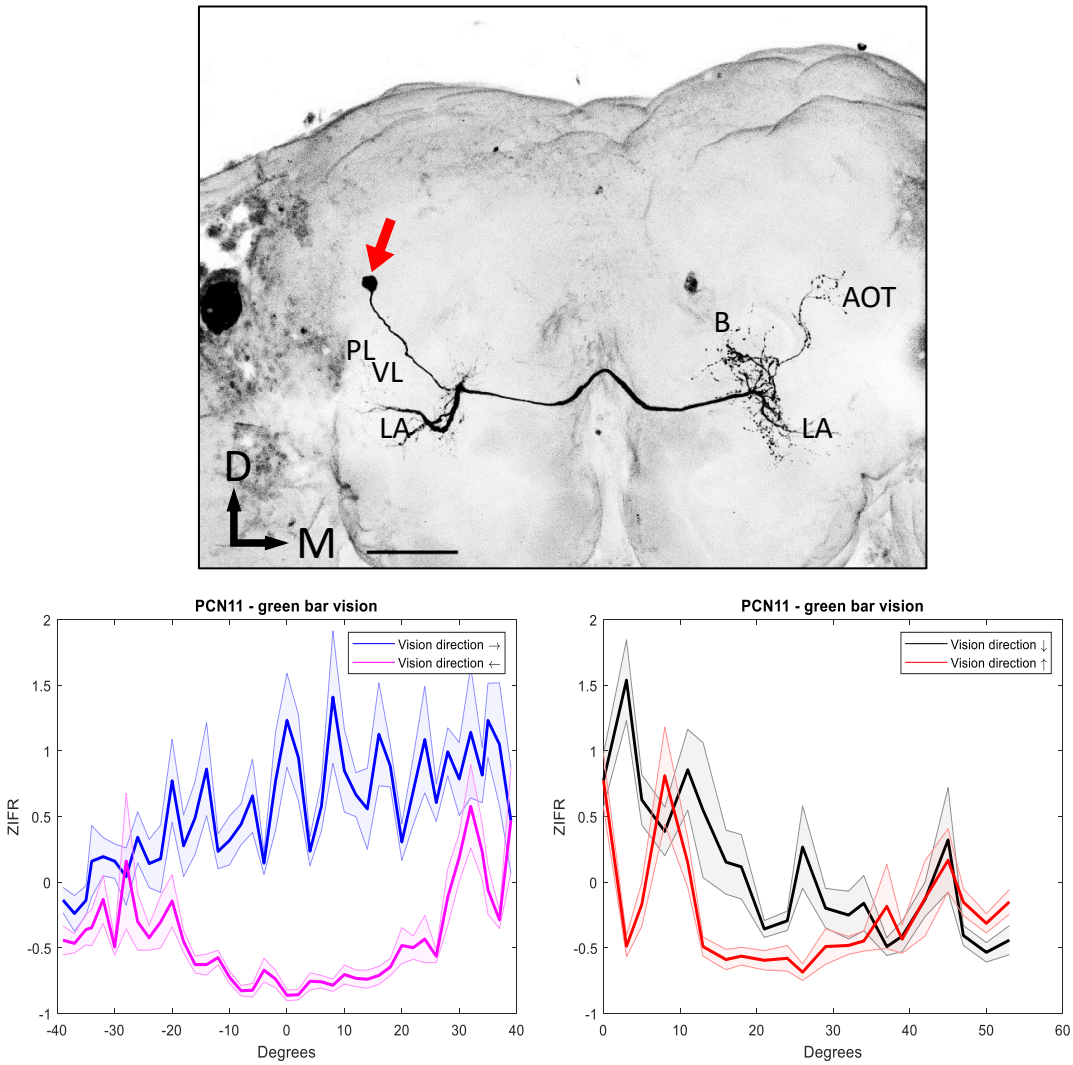

Note. Upper; confocal image of a protocerebral interneuron (ID, PCN11) in frontal view. Neuron connecting lateral protocerebrum with the contralateral anterior optic tubercle (AOTU), and lateral complex. Soma location is marked with *red* arrow. Scale bar = 100 µm. *Lower;* responses to visual stimulation (green bar). Solid line shows the mean z-scored instantaneous firing rate (ZIFR), and shadows indicate the standard error. Blue = right direction, magenta = left direction, black = downwards direction, red = upward direction. Degrees on the x-axis represent the degrees from the position of the insect, with 0 meaning right in front of it. PCN11 showed direction selective response for right direction. Bin size = 100ms. *Abbreviations*: BU, lateral complex bulb; D, dorsal; LAL, lateral accessory lobe; M, medial; PLP, posteriorlateral protocerebrum; VLP, ventrolateral protocerebrum.

Figure 11

Morphological and Physiological Visualization of PCN12

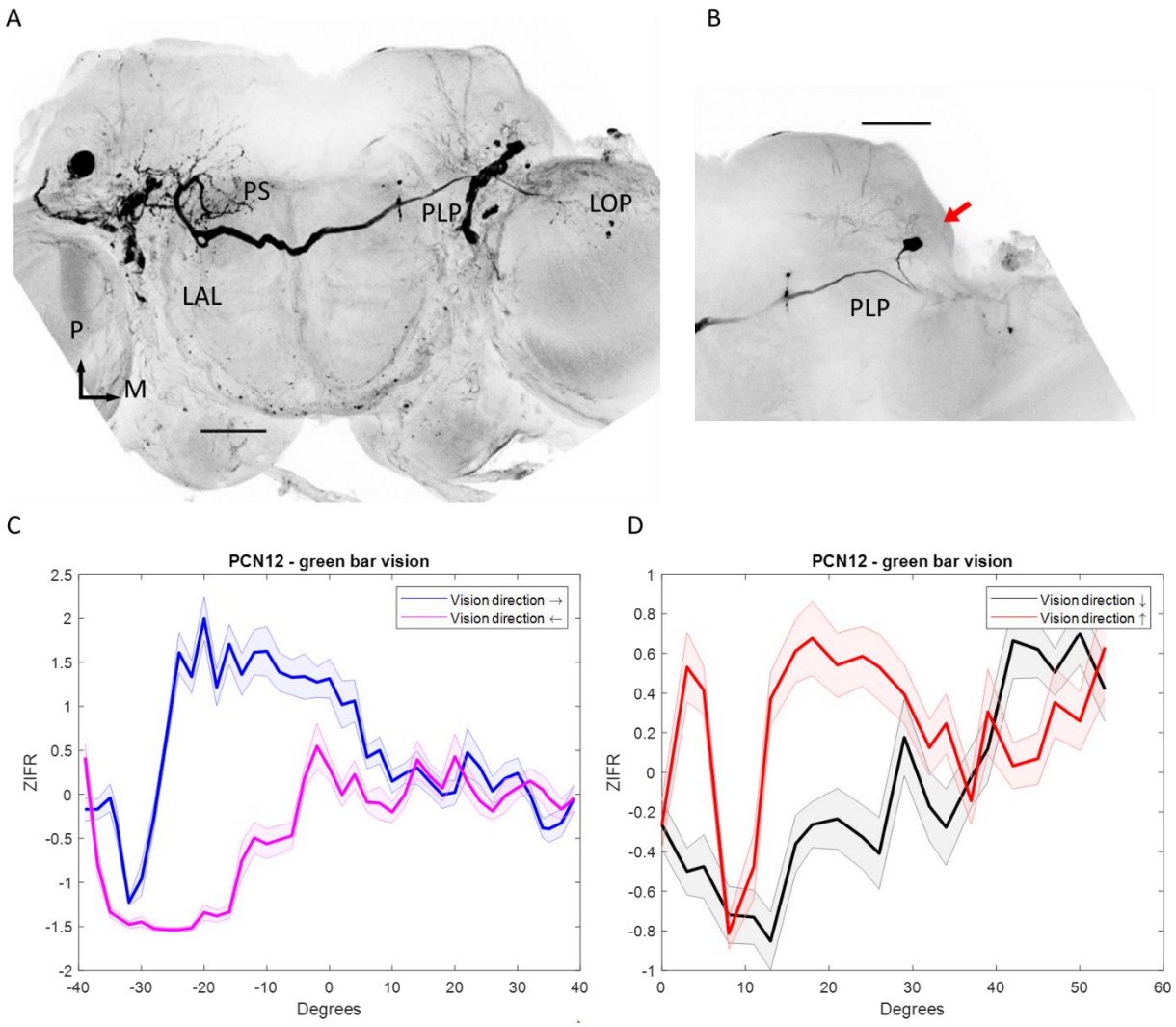

Note. Upper; confocal image of a protocerebral interneuron (ID, PCN12) in dorsal view. (**A**) Neuron connecting lateral accessory lobe (LAL) and posterior slope (PS) with the contralateral posterior lateral protocerebrum (PLP) and lobula plate (LOP). (**B**) Soma location is marked with *red* arrow. Scale bar = 100 µm. *Lower;* responses to visual stimulation (green bar) presented as described in figure 10. (**C**) PCN12 showed direction selective response for rightward and (**D**) upward direction. Bin size = 100ms. *Abbreviations*: M, medial; P, posterior; ZIFR, z-scored instantaneous firing rate.

PCN13

PCN13's soma was situated within the cell body rind posterior to PLP (rPLPp, Fig.12B). The dendrites heavily innervated the AOTU and ran through the LAL commissure (LALC). Axon terminals were projected bilaterally toward the AOTU and PS, albeit in minor amounts compared to dendritic innervations (Fig.11A). Inspection of visual stimulation responses displayed both direction selectivity and visual field responses. Concerning its direction selective nature, PCN13 displayed increased excitatory response for bar movement in the right direction (Fig 11C). However, this was represented by only a few active spikes accounted for the visual field located at -30 to -20 degrees to the left from the midline. Additionally, PCN13 showed excitatory responses for the visual field located 40 degrees to the right for the midline to bar moving both right and left. For the vertically moving bar (Fig. 11D), excitatory responses were observed around 10 to 30 degrees during upward motion. PCN13 also displayed responses within olfactory trials. However, by carefully inspecting the spike data, it is plausible that the neuron, similar to the PCN12, was primarily elicited by the first air puff in the sequence, rather than the odors. Likewise, the neuron was not classified as an odor responding neuron.

Multimodal PCNs

A total of seven neurons met the criteria for classification as multimodal PCNs. Responses to different olfactory stimuli were observed in individual multimodal PCNs across the entirety of the multimodal PCNs, indicating their collective responsiveness could reach to the full range of odors tested (totally 7 chemicals in addition to 1 mechanosensory stimuli). Three neurons displayed both excitatory and inhibitory responses to different olfactory stimulations, while one neuron displayed dual responses with both excitatory and inhibitory responses to hexane. Surprisingly, there was only one (PCN17) instance where a neuron exhibited no response to

Figure 12

Morphological and Physiological Visualization of PCN13

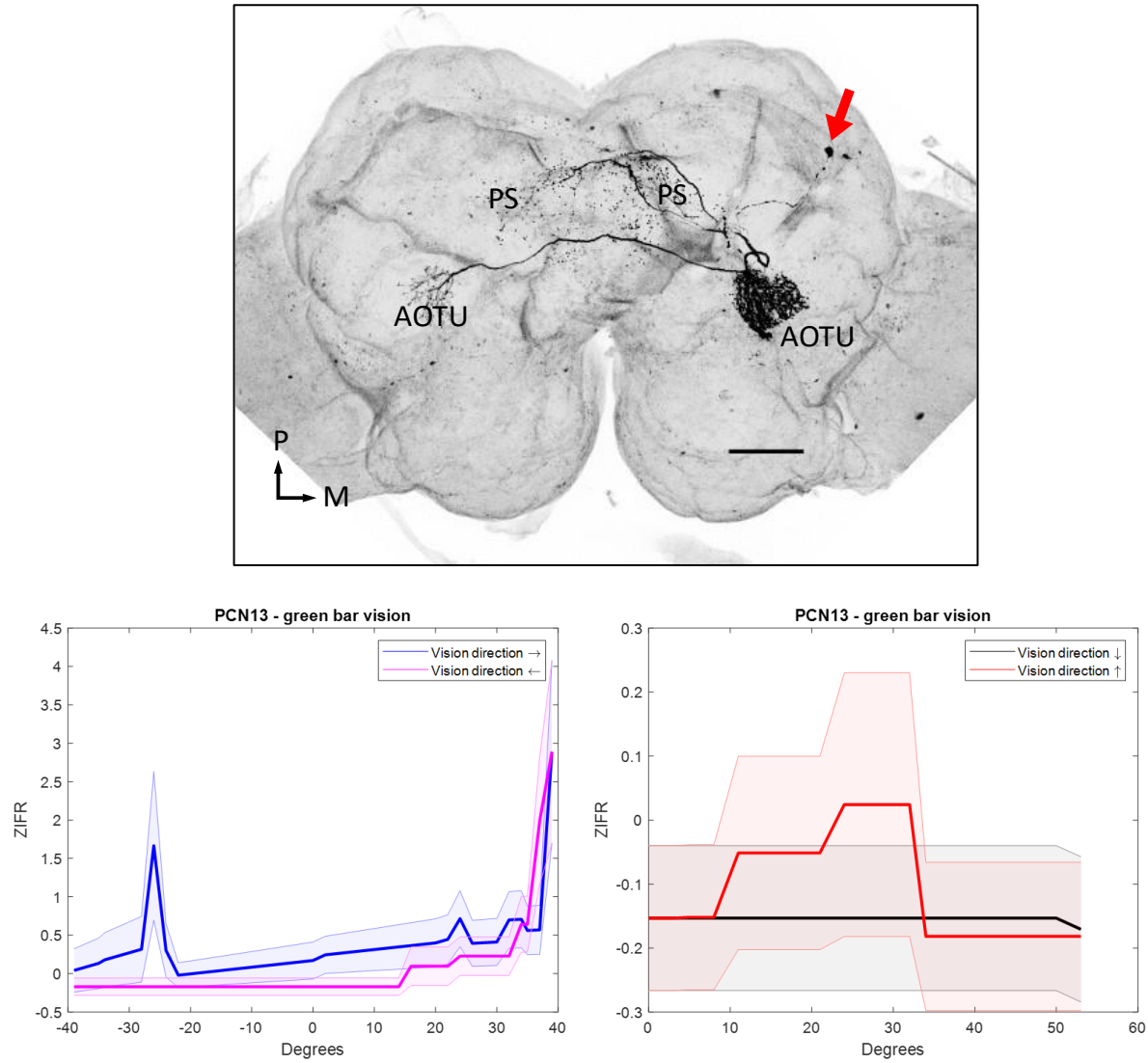

Note. Upper; confocal image of a protocerebral interneuron (ID, PCN13) in dorsal view. Neuron connecting anterior optic tubercle (AOTU) and posterior slope (PS) with the contralateral AOTU and PS. Soma location is marked with *red* arrow. Scale bar = 100 µm. *Lower;* responses to visual stimulation (green bar) presented as described in figure 10. PCN13 showed visual field responses for horizontal bar in the 40 degrees visual field, and direction selective responses for rightwards- (-30 to -20 degrees) and upwards (10-30 degrees) moving bar. Bin size = 100ms. *Abbreviations*: M, medial; P, posterior.

one specific odor (Pheromone blend), while responding to other odors (Behavioral antagonist, insect attractor component, ylang-ylang, hexane). Upon inspection of responses to visual stimulation, direction selective responses were observed for right-, down-, and upwards direction, visual field, and light ON/OFF responses. Responses to leftward motion was not observed. All responses to olfactory stimulation for multimodal PCNs have been summarized in table 3 (also see peak ZIFR in Appendix B), while visual responses have been summarized in table 4.

Table 3

Overview of Percentages of Responses During Stimulation Window for all Multimodal PCNs

ODOR / NEURON	PP	SP	BA	PB	IAC	YY	Hex	Air
PCN1	4,44 (1,86)	19,08	11,61	4,95 (2,88)	6,81 (1,04)	9,58	4,81	2,63 (5,59)
PCN2	13,24	91,01	43,23	48,80	40,85	20,03	7,07	53,59
PCN4	85,60	9,36	91,01	9,36	91,01	79,86	90,01	91,01
PCN7	14,92	3,47	2,01	15,18	9,53	4,75	6,81	5,52
PCN8	13,04	1,15	13,38	3,88	21,95	12,13	25,64 (57,71)	6,08
PCN15	3,07	4,50	6,03	17,58	9,89	5,52	6,03	2,13
PCN17	0,87	4,17	81,06	NR	26,84	91,05	39,43	NT

Note. Only odors that had a response which lasted more than 10% of the stimulation window duration are colorized in the table. Numbers signifies the proportion of the sum of response duration within the entire stimulation window of each stimulus. Green boxes indicate excitatory response, blue inhibitory, purple dual responses with both excitation and inhibition. *Abbreviations:* BA, behavioral antagonist; Hex, hexane; IAC, insect attractor component; NT, not testes; NR, no response; PB, pheromone blend; PP, primary pheromone; SP, secondary pheromone; YY, ylang-ylang.

Table 4

Overview of Visual Responses for all Categorized Multimodal PCNs

Visual Response / NEURON	Direction Selective RIGHT	Direction Selective LEFT	Direction Selective DOWN	Direction Selective UP	Visual Field	Light ON/OFF
PCN1	✓	-	-	✓	-	-
PCN2	✓	-	-	-	✓	-
PCN4	-	-	-	-	✓	-
PCN7	-	-	-	-	✓	-
PCN8	-	-	-	-	✓	-
PCN15	-	-	-	-	-	✓
PCN17	-	-	✓	-	-	-

Note. Only responses which were clearly observed upon visual inspection were reported as a visual response.

PCN1

PCN1's soma resided within the cell body rind dorsally to the LO (rLOd, Fig.13C). Dendritic extensions innervated LOP (Fig. 13B) via the posterior optic commissure (POC) and the posterior lateral fascicle (PLF). The staining of the neuron illustrated the axon terminals projecting toward the SCL and PLP were more pronounced, compared to the restricted dendritic innervations in the LOP (Fig. 13A). The neuron displayed direction selectivity for right moving bar from -10 to 0 degrees (Fig. 13D), and upward motion from 10 to 40 degrees (Fig. 13E). The neuron responded to two odors (Fig. 13F), the secondary pheromone and behavioral antagonist. The secondary pheromone induced heightened inhibitory responses in the beginning and end of the stimulation trial. Sporadic, phasic excitatory response was observed for the behavioral antagonist from throughout the stimulation window.

When exposed to multimodal stimuli (Fig. 13F) comprising both vision and olfaction elements, the neuron showed altered responses to the multimodal stimulation compared to when exposed to either odor or visual stimulus alone. More specifically, in the trail where green bar movement and secondary pheromone were presented simultaneously, the neuron displayed an inhibitory response after the first puffs. A comparable yet less pronounced

Figure 13

Overview of Morphology together with Odor, Visual, and Multimodal Responses in PCN1

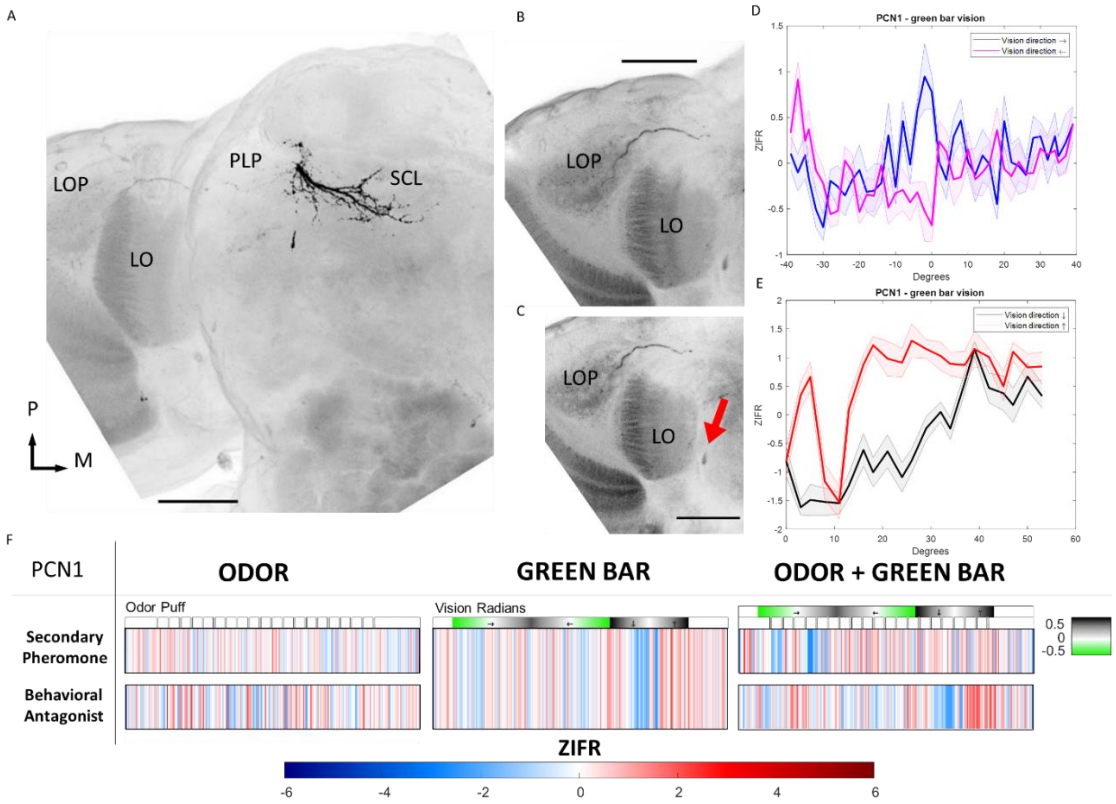

Note. (**A**) confocal image of a protocerebral interneuron (ID, PCN1) in dorsal view. Neuron connecting the posterior lateral protocerebrum (PLP), superior clamp (SCL), and (**B**) lobula plate (LOP). (**C**) Soma location is marked with *red* arrow. Scale bar = 100 µm. (**D**) Visual response to green bar moving left and right (bin size = 10ms). (**E**) Visual response to green bar moving down and up (bin size = 100ms). (**F**) Responses to odor-only (ODOR), visual-only (GREEN BAR) and multimodal (ODOR + GREEN BAR) stimulation (Bin size = 100ms). White color indicated no response, red excitatory, and blue inhibitory, and are presented as ZIFR. Only odors in which the neuron responded to are listed. The odor puffs, and visual radians is the very same as described in figure 6. PCN1 showed both olfactory and visual responses, as well as responses to combined stimuli. *Abbreviations*: M, medial; P, posterior; ZIFR, z-scored instantaneous firing rate.

inhibition was also noted in the trial where visual stimulation was presented alone. Additionally, the inhibitory response observed towards the end of the visual trial, when the green bar was moving in downwards direction from the mid half of the screen, was strongly

reduced in the multimodal trial. For the multimodal stimulus containing the behavioral antagonist, the inhibitory response observed in the vision-only trial was maintained. Here, the inhibition release in the multimodal trial was stronger than that in the vision trial.

PCN2

PCN2's soma was observed within the cell body rind positioned laterally to AVLP (rAVLPl, Fig. 14A) Dendritic neurites innervated PLP, VLP, PS, and SIP equally, primarily through the superior PLP commissure (sPLPC). Axon terminals were distributed equally across the dorsal PLP, SCL, SMP, and SIP. Upon visual inspection, a rightward direction selectivity in the visual field of -30 to 5 degrees was observed for PCN2 (Fig. 14B). Additionally, responses were observed to six odors and one mechanosensory stimulation (Fig. 14C). The neuron displayed excitatory, phasic-tonic responses to the primary- and secondary pheromone, behavioral antagonist, and insect attractor component. To ylang-ylang and air, excitatory, phasic was recorded. The onset for excitation was consistent across all odor stimulations, ranging from 157ms to 213ms, after the first puff. Inhibitory responses were measured for the pheromone blend. In this condition, the neuron had heightened activity in pre-stimulus window.

When combining the moving green bar with the mentioned olfactory stimuli, PCN2 showed altered responses, going from phasic-tonic responses in the odor-only trails, to more phasic responses for the primary- and secondary pheromone. The opposite was observed when plant odors were presented (insect attractor component and ylang-ylang), with more phasic responses in the odor-only trials, and more tonic responses to the multimodal stimulation. For the behavioral antagonist, the response to multimodal stimulation appeared to be equal to the odor-only response. The phasic response to air in the odor-only trial, was diminished in the multimodal trial. Interestingly, the response in the visual-only trial was not observable in any of the multimodal trial, suggesting suppression of visual response when combined with odors.

Figure 14

Overview of Morphology together with Odor, Visual, and Multimodal Responses in PCN2

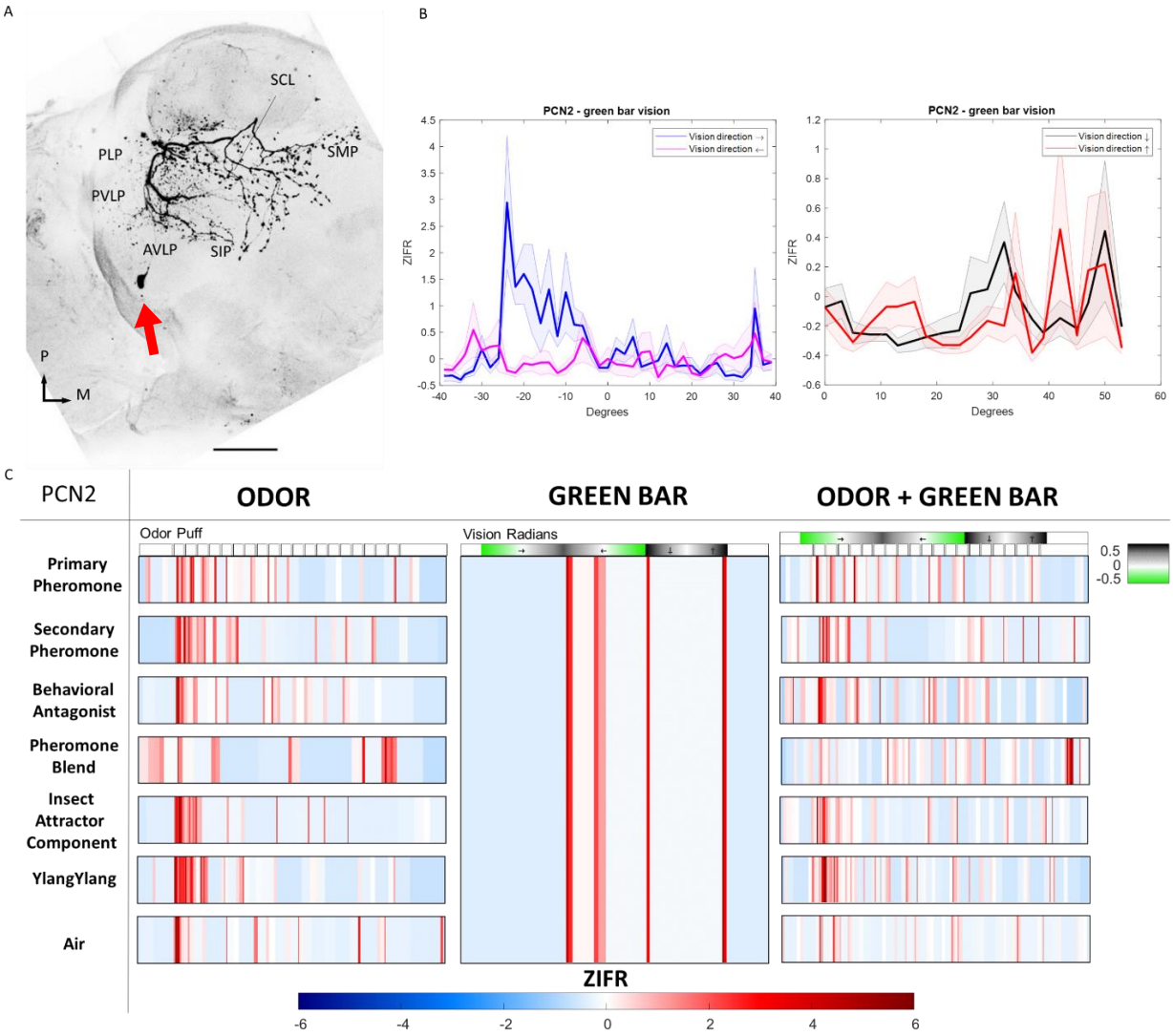

Note. (**A**) Confocal image of a protocerebral interneuron (ID, PCN2) in dorsal view. Neuron connecting posteriorlateral protocerebrum (PLP), anterior and posterior ventrolateral protocerebrum (AVLP and PVLP, respectively) with superior clamp (SCL), superior medial protocerebrum (SMP), and superior intermediate protocerebrum (SIP). Soma location is marked with *red* arrow. Scale bar = 100 µm. (B) Responses to green bar moving right to left, left to right, up to down, and down to up (Bin size = 100ms). (C) Responses to odor-only (ODOR), visual-only (GREEN BAR) and multimodal (ODOR + GREEN BAR) stimulation (bin size = 10ms). Responses presented in the same way as described in figure 6. PCN2 showed both olfactory and visual responses, as well as responses to a combined stimulation. *Abbreviations*: M, medial; P, posterior; ZIFR. Z-scored instantaneous firing rate.

PCN4

The soma of the neuron was observed within the cell body rind lateral to WED (rWEDl, Fig. 15A). Dendrite-like innervations were observed in the SIP, LH and some in SLP. The axon projected through the superior fiber system (SFS), while axon terminals heavily innervated the SLP and SMP, as well as the contralateral SLP and LH. By visual inspection, PCN4 displayed visual field responses for right and left flowing bar in the 10 to 20 degrees visual field (Fig. 15B). The neuron also displayed excitatory, phasic responses to primary pheromone and insect attractor component in the beginning and middle of the trail (Fig. 15C). Interestingly, when combining the primary pheromone with visual stimulation, the responses changed drastically showing a rhythm-like pattern following most of the air puffs (see Appendix C). Relatively weaker, excitatory responses were also observed for air-only. Similarly, excitatory responses were observed for the behavioral antagonist around in the middle of the stimulation window. Multimodal stimulation (with the behavioral antagonist) showed long-lasting excitation after the stimulation window, suggesting an inhibition release response. Hexane gave an excitatory, tonic response from the end of the first quarter of the stimulation window, followed by a phasic-tonic response in the second quarter. Sporadic, excitatory, tonic responses were observed for ylang-ylang in the first half of the stimulation. Multimodal stimulation with either insect attractor component, hexane, air, or ylang-ylang, resulted in no observed response. Thus, for the multimodal characteristics of PCN4, the neuron was selective to pheromones, rather than plant odors, or mechanosensation.

PCN7

PCN7's soma was observed in the cell body rind posterior to SLP (rSLPp, Fig.16A). From this site, dendrite-like neurites were observed extending towards LO with small branches into the PLP and SCL through the anterior optic tract (AOT). The axon projected towards the AOTU with terminals stretching into SMP. A relatively tiny axonal branch was

Figure 15

Overview of Morphology and physiological responses in PCN4

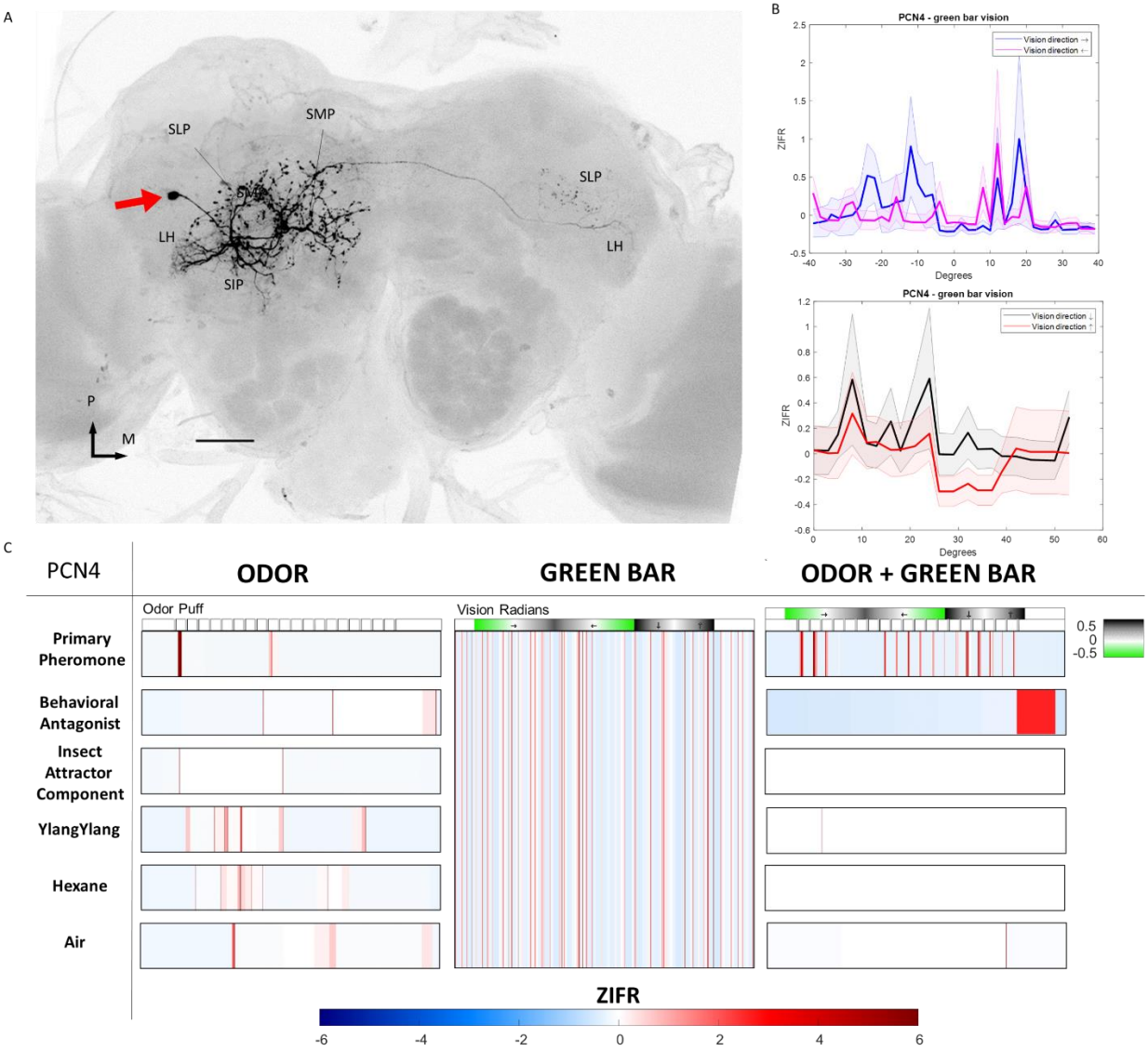

Note. (A) Confocal image of a protocerebral interneuron (ID, PCN4) in dorsal view. Neuron connecting superior lateral protocerebrum (SLP), lateral horn (LH), superior intermediate protocerebrum (SIP), superior mediate protocerebrum (SMP), and the contralateral SLP and LH. Soma location is marked with *red* arrow. Scale bar = 100 µm. (B) Responses to green bar moving right to left, left to right, up to down, and down to up (Bin size = 100ms). (C) Responses to odor-only (ODOR), visual-only (GREEN BAR) and multimodal (ODOR + GREEN BAR) stimulation (bin size = 10ms). Responses presented in the same way as described in figure 6. PCN4 showed both olfactory and visual responses, as well as responses to a combined stimulation. *Abbreviations*: M, medial; P, posterior; ZIFR, Z-scored instantaneous firing rate.

observed projecting from the main axon, into the SMP and AOTU. Inspecting the responses to visual stimulation revealed responses for rightward and leftward bar motion at -30 to 0 degrees of the visual field (Fig. 16B). In the odor-only trials, PCN7 displayed excitatory, phasic responses to the primary pheromone and pheromone blend after the first puff, with tonic responses lasting until the end of the first quarter of the stimulation trail. The excitatory response to the two pheromone stimuli occurred at approximately the same time as the visual response, leading to an enhanced response in the multimodal stimulation, with the same characteristics as observed in the odor-only trials (Fig. 16C).

PCN8

The soma of PCN8 (Fig. 17A) was found within the cell body rind posteriorly to the SLP (rSLPp). Dendritic projections heavily innervated the SCL, ICL, SLP, and SIP via the pyriform fascicle (PF), with sparse innervations in the VLP and LH (Fig. 17B). Axon terminals projected predominantly toward the SMP and PB, along with minor projections into the contralateral SMP. Through visual inspection, PCN8 displayed visual field responses for upward and downward motion in the 10 to 30 degrees visual field (Fig. 17C). The neuron displayed excitatory, long-lasting, phasic responses to the primary pheromone, and behavioral antagonist, in the first quarter, and behavioral antagonist in the second quarter. Insect attractor component induced an excitatory, phasic response in the first quarter, with tonic responses until the end of the second quarter, again occurring in the end of the stimulation window. A long-lasting, excitatory, phasic response was also observed for ylang-ylang in the middle of the stimulation, with strong inhibition release after the stimulation trial. Hexane displayed a dual response of both excitation and inhibition, with long-lasting, phasic excitation in the first quarter, and tonic responses in the end of stimulation. The inhibitory responses were observed throughout the stimulation trial, in between the first quarter and end of stimulation.

Figure 16

Overview of Morphology together with Odor, Visual, and Multimodal Responses in PCN7

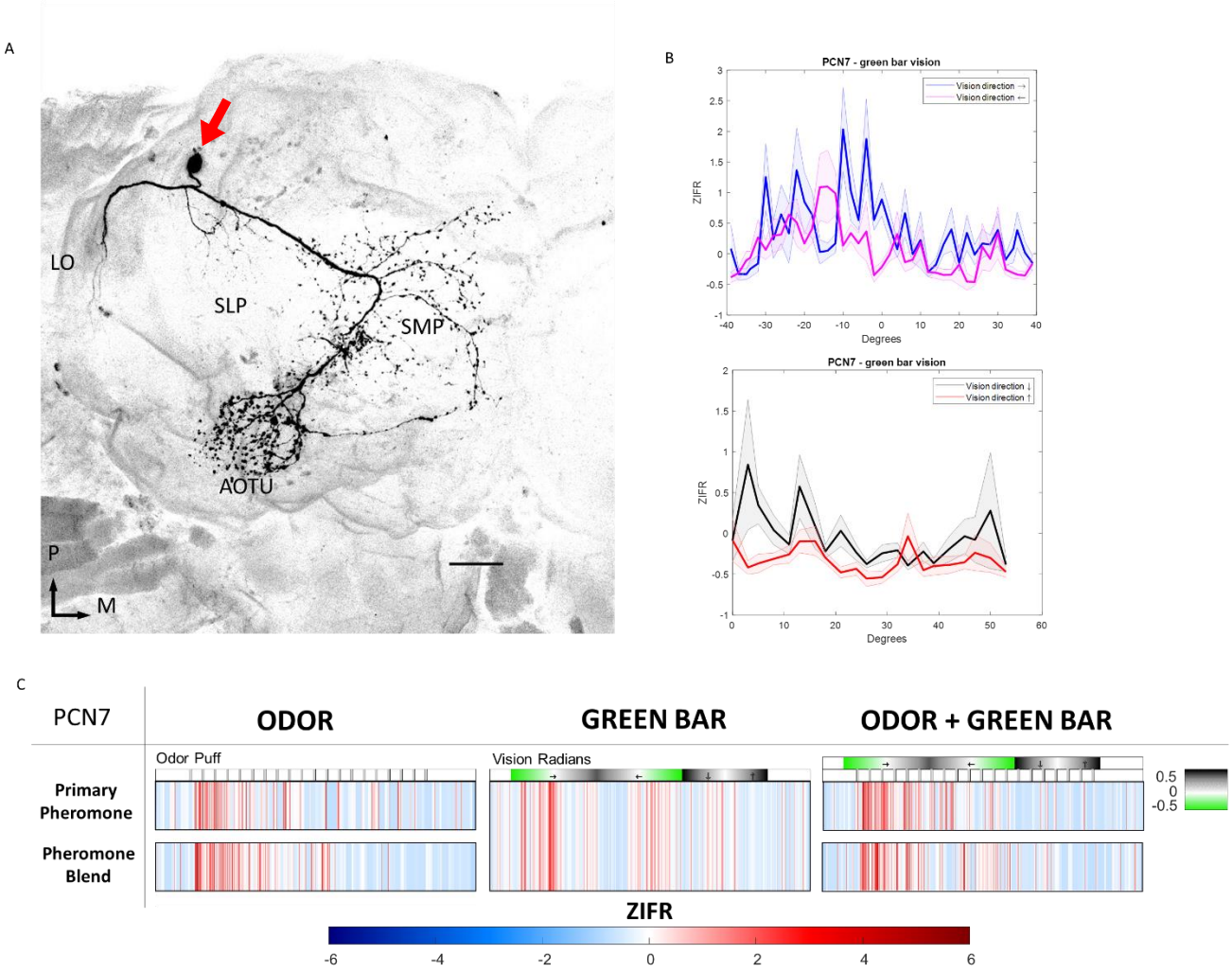

Note. (**A**) Confocal image of a protocerebral interneuron (ID, PCN7) in dorsal view. Neuron connecting lobula (LO), superior medial protocerebrum (SMP), and anterior optic tubercle (AOTU). Soma location is marked with *red* arrow. Scale bar = 100 µm. (**B**) Responses to green bar moving right to left, left to right, up to down, and down to up (Bin size = 100ms). (**C**) Responses to odor-only (ODOR), visual-only (GREEN BAR) and multimodal (ODOR + GREEN BAR) stimulation (bin size = 10ms). Responses presented in the same way as described in figure 6. PCN7 showed both olfactory and visual responses, as well as responses to a combined stimulation. *Abbreviations*: M, medial; P, posterior; SLP; superior lateral protocerebrum; ZIRF, Z-scored instantaneous firing rate.

Observations of the responses to multimodal stimulation (Fig. 17D) revealed relatively great changes from odor-only responses to multimodal stimulation. Odor-only responses were either increased (IAC), delayed (primary pheromone, behavioral antagonist), reduced (hexane), or diminished (ylang-ylang).

PCN15

PCN15's soma was located within the cell body rind laterally to VLP (rVLPl, Fig. 18A). Dendritic neurites innervated the LO via the posterior optic commissure (POC). Axon terminals were projected toward the contralateral PS. The neuron displayed equally distributed, short-lasting, phasic-tonic excitatory responses throughout the stimulation window with the pheromone blend (Fig. 18C). By visual inspection, PCN15 displayed light ON/OFF responses for right-, left-, up-, and downward flowing bar (Fig. 18B). The light ON/OFF response was observed as an excitation after the stimulation window. This response was maintained in the multimodal stimulation with pheromone blend. The multimodal response was similar to the odor-only trial, only with increased excitation at the same time as observed in the vision-only trials. In other words, the multimodal response appeared to be a combination of the odor-only and vision-only trials.

PCN17

The soma was observed laterally to the VLP within the cell body rind (rVLPl) in PCN17 (Fig. 19B). Dendritic extensions (Fig. 19C) stretched toward the VLP and LO via the anterior optic tract (AOT). Axon terminals innervated the LAL heavily (Fig. 19A). PCN17 displayed an excitatory, tonic response to the behavioral antagonist and insect attractor component (last quarter). Strong, excitatory, phasic response was observed to the first puff with ylang-ylang and inhibition was measured for hexane (pre-stimulus window contained heightened activity).

Figure 17

Overview of Morphology of PCN8

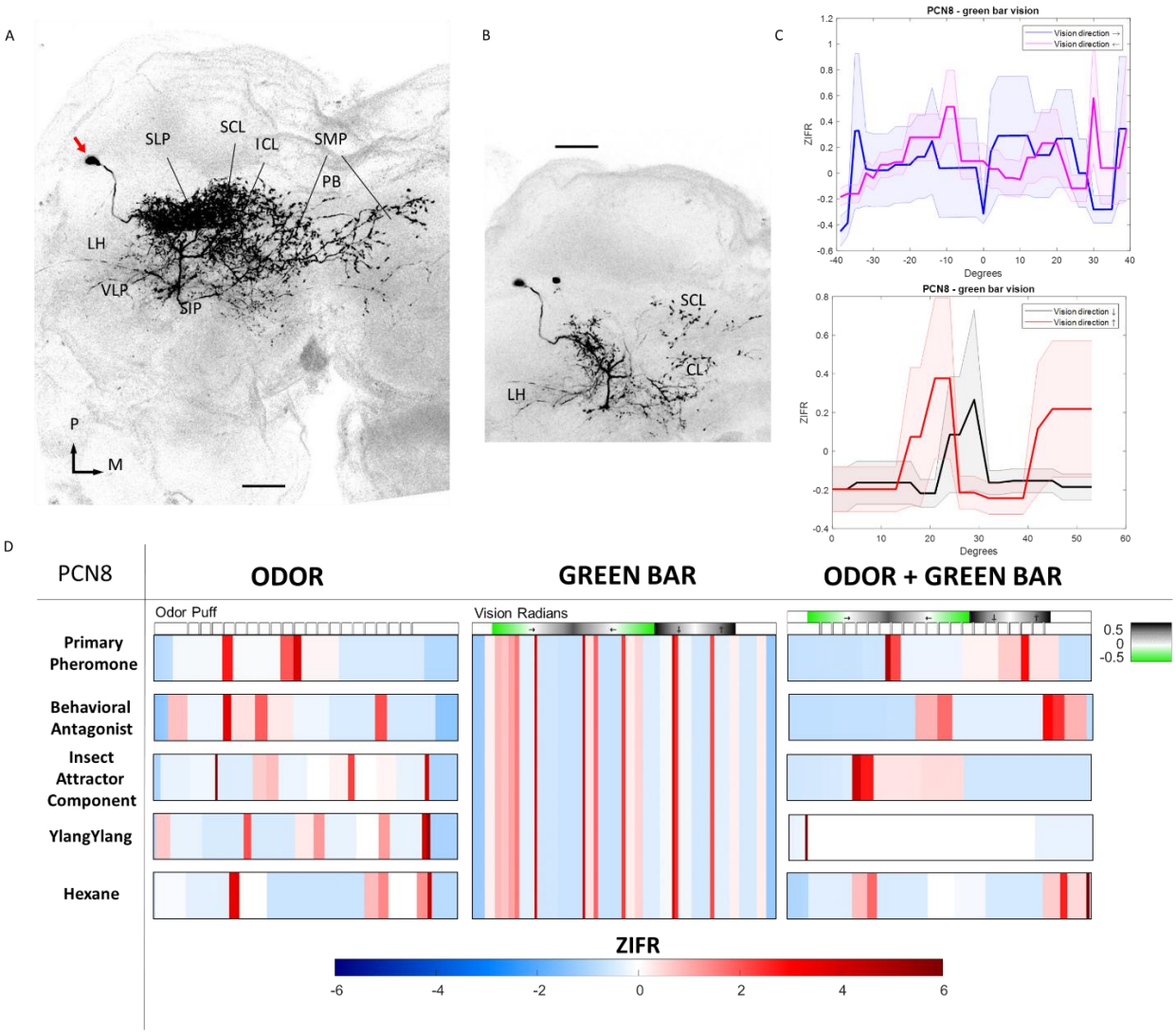

Note. (**A**) Confocal image of a protocerebral interneuron (ID, PCN8) in dorsal view. Neuron connecting the superior intermediate protocerebrum (SIP), ventrolateral protocerebrum (VLP), superior lateral protocerebrum (SLP), (**B**) superior clamp (SCL), inferior clamp (ICL), and lateral horn (LH). Soma location is marked with *red* arrow. Scale bar = 100 µm. (**C**) Responses to green bar moving right to left, left to right, up to down, and down to up (bin size = 100ms). (**D**) Responses to odor-only (ODOR), visual-only (GREEN BAR) and multimodal (ODOR + GREEN BAR) stimulation (bin size = 10ms). Responses presented in the same way as described in figure 6. PCN8 showed both olfactory and visual responses, as well as responses to a combined stimulation. *Abbreviations*: M, medial; P, posterior, ZIFR, Z-scored instantaneous firing rate.

Figure 18

Overview of Morphology together with Odor, Visual, and Multimodal Responses in PCN15

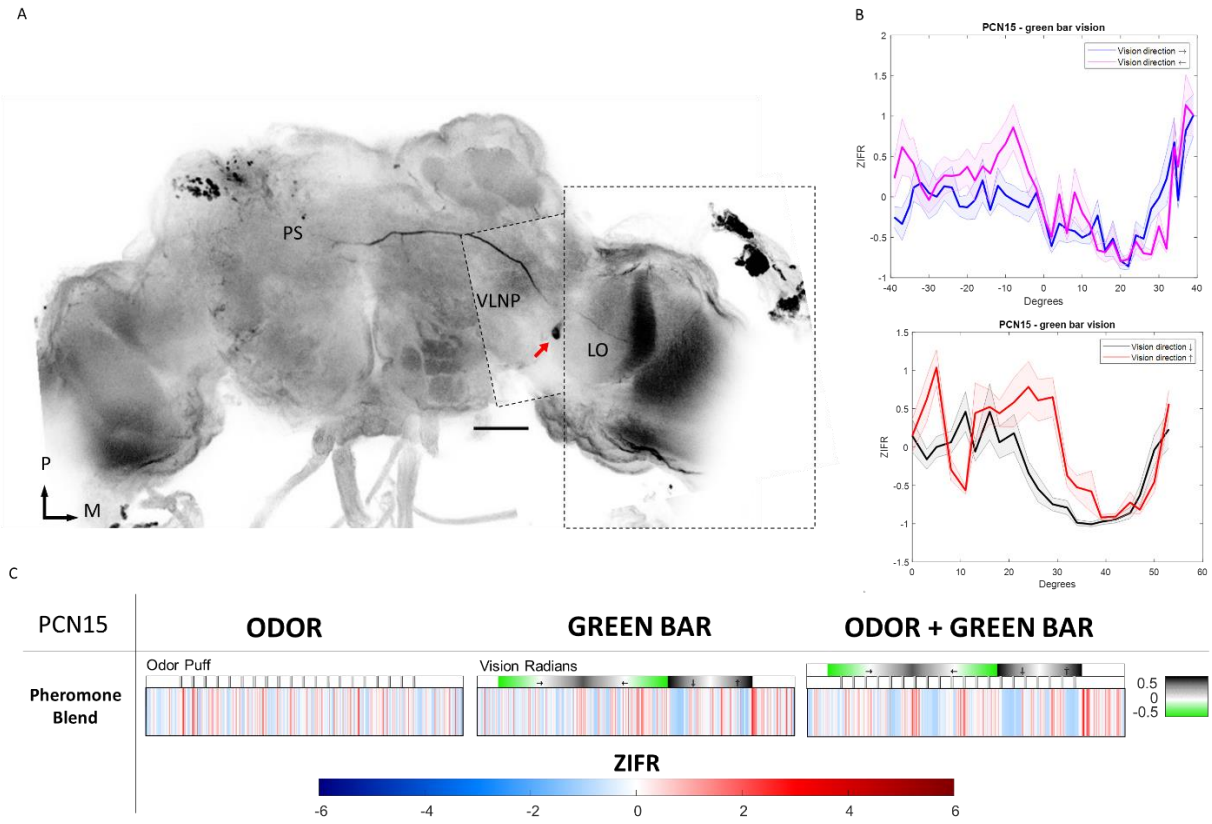

Note. (A) Confocal image of a protocerebral interneuron (ID, PCN15) in dorsal view. Neuron connecting lobula (LO), ventrolateral protocerebrum (VLP), and the contralateral posterior slope (PS). Soma location is marked with *red* arrow. Scale bar = 100 µm. (B) Responses to green bar moving right to left, left to right, up to down, and down to up (bin size = 100ms). (C) Responses to odor-only (ODOR), visual-only (GREEN BAR) and multimodal (ODOR + GREEN BAR) stimulation (bin size = 10ms). Responses presented in the same way as described in figure 6. PCN15 showed both olfactory and visual responses, as well as responses to a combined stimulation. *Abbreviations*: M, medial; P, posterior, ZIFR, Z-scored instantaneous firing rate.

Direction selective responses to downward motion from 10 to 55 degrees of the visual field was observed to the visual stimulus (Fig. 19D). By visual inspection, in the multimodal trials (Fig. 19E) several effects were shown. The neuron displayed a reduction of the excitatory response from the plant-odor trials (insect attractor component and ylang-ylang), enhancement of excitation (behavioral antagonist) and inhibition (hexane).

Figure 19

Overview of Morphology of PCN17

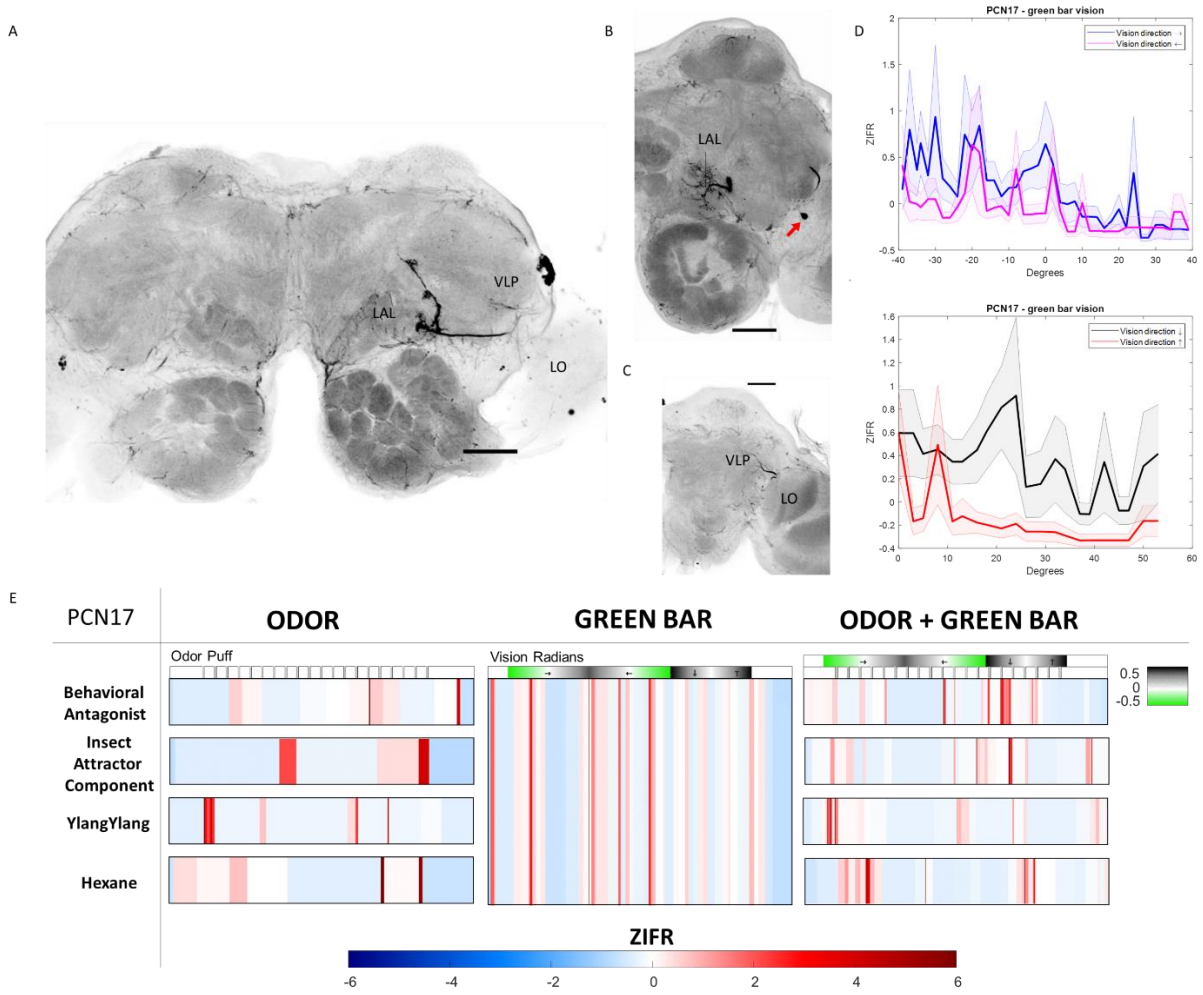

Note. (A) Confocal image of a protocerebral interneuron (ID, PCN17) in dorsal view. Neuron connecting (B) the lateral accessory lobe (LAL), (C) ventrolateral protocerebrum (VLP), and lobula (LO). Soma location is marked with *red* arrow (B). Scale bar = 100 µm. (D) Responses to green bar moving right to left, left to right, up to down, and down to up (bin size = 100ms). (E) Responses to odor-only (ODOR), visual-only (GREEN BAR) and multimodal (ODOR + GREEN BAR) stimulation (bin size = 10ms). Responses presented in the same way as described in figure 6. PCN17 showed both olfactory and visual responses, as well as responses to a combined stimulation. *Abbreviations*: M, medial; P, posterior; ZIFR, Z-scored instantaneous firing rate.

Nonresponsive PCNs

Among the 17 PCNs collected, three did not meet our set criteria for classification as olfactory, visual, or multimodal despite having innervations within protocerebral neuropils associated with visual and/or olfactory processing. The three neurons did not show any significant responses to any given olfactory stimulation that crossed our threshold of 10% of the stimulus duration. Upon visual inspection of responses to visual stimulation, no direction selective, visual field, or light on/off responses were clearly observed. Thus, the three PCNs were so far labelled as nonresponsive PCNs. The morphological characteristics can be elucidated in figure 20A (PCN5), 20B (PCN9), and 20C (PCN16) and further detailed in the accompanying legend.

Figure 20

Overview of Morphology of Nonresponsive PCN5, PCN9, and PCN16

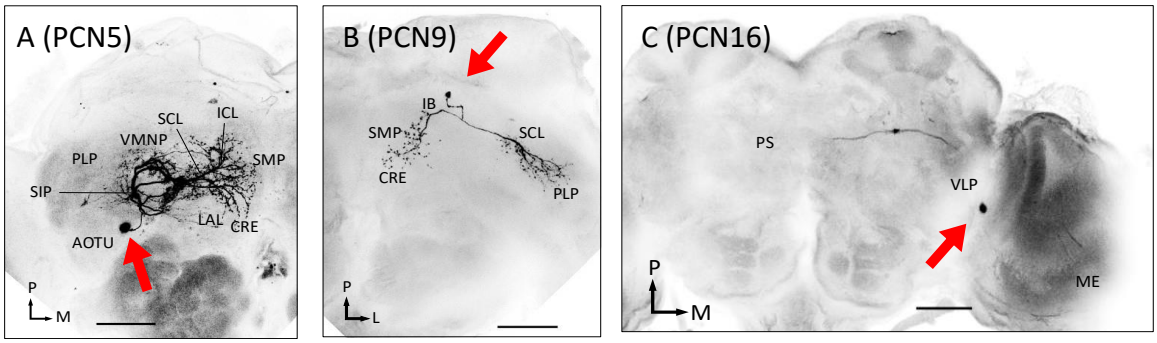

Note. (**A**) PCN5's soma was situated within the cell body rind ventral to the anterior optic tubercle (rAOTUv). Dendritic processes extended mainly toward the inferior neuropils such as ICL, SCL, and CRE, with sparse extensions into the LAL, PLP, and VMNP via the vertical VLP fascicle and superior arch commissure (ARC). Axon terminals projected largely toward SMP and relatively less toward SIP. (**B**) PCN9's soma was situated posterior to the IB in the cell body rind (rIBp). Dendrite-like neurites were observed heavily innervating the PLP, along with sparse innervation of the SCL. The axon ran through the superior PLP commissure (sPLPC). Axon terminals were observed innervating the SMP and CRE. (**C**) PCN16's soma was observed within the cell body rind laterally to the VLP (rVLPl). Through the posterior optic tract (POC), dendrite-like branches were observed innervating the ME. Contralaterally, axon terminals were observed innervating the PS. Soma location is marked with *red* arrows. Scale bars = 100 µm. Abbreviations: CRE, crepine; IB, inferior bridge; ICL, inferior clamp; LAL, lateral accessory lobe; ME, medulla; PLP, posteriorlateral protocerebrum; PS, posterior slope; SCL, superior clamp; SIP, superior intermediate protocerebrum; SMP, superior medial protocerebrum; VLP, ventrolateral protocerebrum; VMNP, ventromedial neuropils.

Discussion

Behavioral studies have illustrated that, in addition to olfaction, moths also rely heavily on the visual input when tracing an odor source (Baker & Hansson, 2016). Without the visual input, male moths will not track airborne pheromone plumes effectively (Kennedy & Marsh, 1974). Our results from the double air pressure mass staining in the visual center OL and the pheromone center MGC (Fig. 5A) showed that neurons from the OL innervated the majority of the protocerebrum, with clear projections to the AOTU (Fig. 5C), while the MGC output targeted more distinct regions. The intriguing aspect is that the SIP, the target of PNs responding to sex pheromones (Fig. 5B), is positioned adjacent to the main optic lobe output center, the AOTU (Fig. 5A). The proximity of olfactory and visual neuropils in the protocerebrum suggest the presence of putative olfactory-visual multimodal neurons within this region. Intracellular recordings from that region same revealed four classes of PCNs: olfactory, visual, multimodal, and nonresponsive. Specifically, we recorded four olfactory-, three visual-, seven multimodal-, and three nonresponsive PCNs, adding up a total number of 17 individually recorded and stained neurons.

Olfactory PCN Sensitivity to Pheromones and Plant Odors

Although the output of PNs processing pheromones and PNs processing plant odors generally has been demonstrated to be separated within higher order protocerebral neuropils (Jefferis et al., 2007; Kymre et al., 2021b; Namiki et al., 2013), there are some regions, like the VLP (Kymre et al., 2022), and SIP (Chu et al., 2020) where PN output seems to target the same region within the neuropil. This highlights the presence of protocerebral neurons processing only pheromone signals or only plant odor signals, but also single neurons processing both pheromone- and plant odor signals (e.g. Lei et al., 2001). Correspondingly, out of the four olfactory classified PCNs, one (PCN6) responded only to attraction-associated pheromones, another only to plant odor (PCN10), while two (PCN3 and PCN14) responded to both pheromones and plant odors.

PCN6 demonstrated inhibitory responses towards both the primary pheromone and the pheromone blend, traditionally regarded as attractants for the moth within its ecological context (Kehat & Dunkelblum, 1990). However, the intricate morphology of PCN6 poses challenges with respect to understanding the functional role of the regions innervated by the neuron`s dendrites. Specifically, as the dendrite-like projections span both large parts of the superior neuropils and the inferior neuropils, one cannot pinpoint the precise origin of the olfactory responses observed.

The singular olfactory classified PCN that responded only to plant odors was PCN10. This neuron responded to the plant odor named 'insect attractor component' with excitatory responses. The neuron had dendrites encompassing the SMP and SLP, with bilateral terminal projections innervating the calyces in both hemispheres. Despite its impressing, aesthetic morphology, the neuron's processing characteristics are not very surprising. The SLP is shown to be a main output region from the LH (Namiki & Kanzaki, 2019), with the latter receiving information from all AL glomeruli (Kymre et al., 2022). Additionally, CA has been described as a memory center in insects (Galizia, 2014), involved in olfactory associative learning (Hammer, 1993), which might suggest that this neuron (PCN10) is involved in coding of associative memory related to plant odors, specifically those components included in the insect attractor component. Considering its dendritic innervations into the posterior part of the SLP, its response to plant odors becomes reasonable, as this area of the SLP has been described as receiving non-pheromone input, in comparison to its more anterior parts, receiving projections from the male-specific cumulus. (Kymre et al., 2021b; Kymre et al., 2022).

In contrast to the two aforementioned neurons, one neuron (PCN14) responded to both pheromones and plant odors. This makes sense considering the morphology of the neurons having connections with the LH and VLP (representation sites for both the plant odors and

behavioral antagonist), and SLP, which in its turn receives input from the LH (Namiki & Kanzaki, 2019). Intriguingly, the neural branches of PCN14 within these regions appeared as terminals in the ipsilateral hemisphere, and as dendrites in the contralateral PLP. Thus, it may suggest that the neuron possesses complex communication properties, similar to those observed in the contra-laterally projecting serotonin-immunoreactive deutocerebral neuron (Coates et al., 2020). However, despite PCN14 having terminal-like processes in the LH, VLP, and SLP, it does not necessarily rule out the possibility that this neuron also gets input within these regions. Notably, this study included some neurons that might receive input to assumed terminals, indicated by the physiological activity of the neuron.

Visual PCNs: Indication of Convergent Inputs Across Synaptic Levels

As formerly mentioned, there is no published information on the visual neural pathways in *H. armigera*, to our knowledge. Thus, our results provide novel information about some of the connection patterns between the optic lobe and protocerebrum, as well as the processing properties of such connections in this moth species.

Among the three visual neurons identified here, PCN12 provides evidence that *H. armigera* possesses a direct pathway from the optic lobe neuropil, LOP, to the protocerebrum. The LOP is known to accommodate neurons sensitive to both horizontally and vertically moving objects in other species (Scott et al., 2002). Generally, output neurons from the LOP make connections with subsequent protocerebral neurons responsible for processing shape (VLP), velocity and approaching objects (VLP and PLP) (Egelhaaf, 2023). The integration of relevant information from the surrounding environment appears crucial for the navigating moth. It enables rapid identification of motion within the visual field and direct integration of visual cues from the optic lobes into the LAL, a premotor region (Namiki & Kanzaki, 2016). Ultimately, this integration leads to the transmission of descending signals, potentially

resulting in interactive behavioral responses corresponding to the observations made by the moth.

Intriguingly, this neuron (PCN12) with dendrites in the optic lobe neuropil LOP could be upstream of another neuron in my collection. The second neuron, i.e. PCN11, had dendrites extending into the LAL, which is the output target of PCN12. Assuming PCN11 is in fact located downstream of PCN12, it seems to highlight how visual information gets broadened after crossing a synaptic level in the visual system. That is, since PCN12 responded to movement across 30 degrees of the visual field, and PCN11 across 50 degrees, it suggests that PCN11 receives convergent information from multiple LOP neurons, broadening the receptive range further downstream in the system.

Taking into account the fact that PCN12 carried information from 30 degrees of the visual field, and that this information came from one of the compound eyes, it could lay basis for a calculation of the minimum number of neurons required to cover the whole visual field of one eye. That is, if one neuron responds to 30 degrees, and one eye covers around 168 degrees of the total visual field (e.g Merry et al., 2006), it may imply that there are at least five to six similar downstream neurons needed to process objects moving in one direction through the whole visual field of one single compound eye (168 degrees). Furthermore, based on the broadened visual field at the next synaptic level (from 30 to 50 degrees), three to four neurons from the LAL would be expected as a bare minimum to cover the whole visual field of one eye.

Considering the observation that visual information gets broader the further downstream the information is conveyed, it clearly demonstrates common properties with the olfactory system with regards to central processing. The visual and olfactory sensory systems operate with distinct inputs: vision relies on light (a dimensional input), while olfaction relies on odors (a categorical input). Additionally, the organization of peripheral receptors differs

between the two systems, with the visual system having a highly structured retinotopic organization (Barnett et al., 2007) and the olfactory system having a comparatively unstructured chemotopic organization (Vosshall & Stocker, 2007). However, when we examine the central processing properties of our olfactory and visual PCNs, it becomes apparent that despite these differences, the two modalities share similar principles of convergence. In the olfactory system, what is detected in the periphery is broken down into minor segments. Subsequently, these segments will merge into larger segments at the subsequent synaptic level, repeating this process iteratively (Fig. 21A). A notable exception to this rule can be found in labeled lines systems such as insect`s pheromone processing pathways (Galizia & Rössler, 2010). Note, however, that several of our labelled PCNs (29%) responded to both plant odors and distinct pheromones, indicative of a broadened responsivity as signals travel downstream. At the peripheral level, OSNs of heliothine moths are narrowly tuned (Røstelien et al., 2005), while PNs may represent a somewhat broader array of inputs e.g. due to local interneuron mediation or having dendrites in multiple glomeruli. In the protocerebrum, olfactory PCNs may receive inputs regarding many distinct odorants, partially due to having dendrites which in some cases span several neuropils (see Appendix A), and partially due to a convergence of inputs from separate types of AL PNs with receptivity to distinct odorants (Das Chakraborty & Sachse, 2021). Our results clearly illustrate how the visual system also seems to utilize the same principle of convergence (Fig. 21B). That is, lower order visual neurons detect minor segments of the visual field (like PCN12). These segments are subsequently converged into larger segments at later synaptic levels (like PCN11). In other words, the post-synaptic level contains a broader amount of information than the pre-synaptic level (Fig. 21C). Ultimately, a reduced number of neurons receive these converged segments (Fig.21D), enabling the decoding of the signals from the periphery. The information load across synaptic levels could be more strategically tested using an

electroantennography, calculating the time from sensory neuron activation to the measured response in these multimodal PCNs, and dividing by the estimated processing time in a single synaptic level. That way, one could obtain a rough estimate on the current synaptic level of the recorded neuron and investigate the differences in informational load at such level, by comparing the responses observed at other levels. Despite the possibility of such discoveries, our findings unequivocally illustrate that the insect brain is optimized for energy efficiency, requiring fewer neurons as the informational load converges. Therefore, the significance of a smaller brain in insects should not be underestimated.

Figure 21

Information convergence across synaptic levels for olfaction and vision

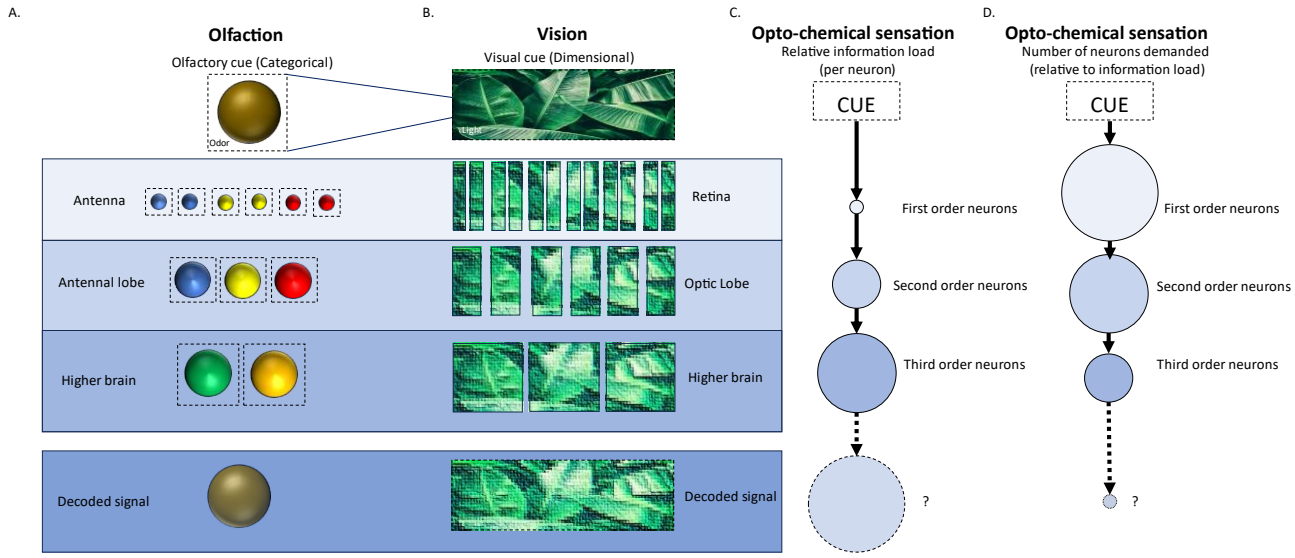

Note. Representative amount of sensory-relevant information processes in each synaptic level. Olfaction process categorical information form the environment, while vision process more continual, dimensional information. (**A**) Categorical olfactory cue gets processes by several sensory neurons in the antenna. As the information proceed up in the system, it gets converged to, finally, make a representation of perceived odor in higher order brain regions. (**B**) Dimensional information in the form of light converges for each synaptic level until the signal is decoded in higher order brain regions. (**C**) Information load for each synaptic level in both vision (optical) and olfaction (chemical) increased due to convergence. (**D**) The number of neurons demanded for each synaptic level decreases in comparison to the increasing information load at the same synaptic level.

In addition to PCN11 and PCN12., we observed a particular neuron, PCN13, exhibiting directional selectivity towards rightward and upward movements, alongside responses to visual stimuli within its receptive field. This neuron's dendrites extended into the AOTU, projecting bilaterally towards the PS, as well as the contralateral AOTU. Interestingly, PCN13's receptive field was located 40 degrees to the right of the visual midline, i.e. the end of the stimulus movement range, and responded to horizontal bar movements. These findings deviate from expectations, as the literature does not describe direct connections between the protocerebral neuropil AOTU and the optic lobe neuropil LOP, which is known for its sensitivity to horizontally moving objects (Scott et al., 2002). Instead, the AOTU typically receives information about object size from the LO (Ryu et al., 2022) and light intensity from the ME (Yukizane et al., 2002). However, it is known that the LOP projects to the PS (as previously illustrated in Fig. 2), which serves as the output region of PCN13. Considering the AOTU's input related to light intensity and object characteristics, along with the extensive dendritic branching of PCN13 within the AOTU and its bilateral projection to the PS, it is reasonable to propose that this neuron may not primarily contribute to directional selectivity or explicit visual field responses. Instead, it likely plays a role in perceived instantiated movement. The proximity of its receptive field to the extreme right of the total visual stimulation field suggests responses akin to typical light ON/OFF responses, supporting the notion that PCN13 may not specifically detect objects within that visual field but rather the appearance of objects themselves.

Multimodal PCNs Responded More Broadly than Olfactory PCNs

According to our definition, multimodal processing at the single neuron level implies the capacity of one single neuron to process information from at least two modalities. Based on their responses to olfactory stimulation, combined with observable visual-typical responses, we classified seven out of the total seventeen neurons as multimodal (41%).

The multimodal PCNs were more respondent to attraction-related female-released compounds than the olfactory PCNs. Among the seven multimodal PCNs, roughly 70% exhibited excitation in response to both the primary pheromone and pheromone blend, with approximately 14% showing inhibition solely to the pheromone blend. Conversely, none of the olfactory classified PCNs displayed excitation to these compounds (primary pheromone and pheromone blend), while only 25% showed inhibition. Responses to the secondary pheromone were observed among the multimodal PCNs, but not in the olfactory PCNs. Two of the neurons (PCN2 and PCN4) in the multimodal class also responded strongly to air, which might suggest a role within mechanosensory-visual processing. This aligns with findings from the nocturnal hawkmoth (*Daphnis nerii*), which demonstrated the importance of multimodal feedback - combining visual and antennal mechanosensory cues - for effective head stabilization in insects lacking halteres (Chatterjee et al., 2022).

The Majority of Multimodal PCNs Were More Sensitive to Pheromones than Plant Odors

Consistent with the aim of the thesis, if multimodal neurons were discovered, we wanted to describe not only the multimodal response, but also the single-modal properties including olfactory responses. Looking at these responses, out of seven multimodal PCNs, there were five of these multimodal PCNs (57%) that responded only (PCN1, PCN7, PCN15), or more strongly (PCN4) to pheromones). None of the multimodal neurons responded only to plant odors. Three of the multimodal PCNs (43%) could be described as more generalists considering their similar responses to both tested pheromones and plant odors (PCN2, PCN8, PCN17). What is interesting is that the combination of pheromones and visual stimuli increased the excitatory responses in the majority of our multimodal PCNs. Furthermore, neuron PCN17, which exhibited responses to both pheromones and plant odors, showed reduced responses to both plant odors (Insect attractor component and ylang-ylang) when combined with visual stimulation. In contrast, increased excitation was observed for

pheromones (Behavioral antagonist) under the same conditions. This aligns with the crucial role of pheromones in mating behavior (Gomez-Diaz & Benton, 2013). Taken together, our results suggest that the majority of multimodal PCNs form the recorded region are more sensitive to pheromones, as compared to plant odors.

Multimodal PCNs Innervating Optic Neuropils Responded to Plant Odors and Pheromones

Among the multimodal neurons, there were four neurons (PCN1, PCN7, PCN15, PCN17) that had their dendrites innervating the LOX of the OL. This imply that, strictly speaking, they should not be classified as multimodal PCNs, but rather as visual projection neurons (VPNs) (Wu et al., 2016). This would also make sense, as the responses among these neurons displayed clear direction selectivity, visual field, and light ON/OFF characteristics. Considering that they should have been classified as VPNs based on their dendritic innervations, it becomes rather interesting to look at their olfactory responses to both pheromones and plant odors, as it would imply that VPNs possess the ability to process olfactory information. Specifically, three (PCN1, PCN7, PCN15) out of the four VPNs, responded only to pheromones, while one (PCN17) also responded to plant odors. This highlights an observed prioritization of pheromone signals in the visual pathway, compared to plant odors, emphasizing the important role of pheromone cues in visual navigation (Baker & Hansson, 2016; Gomez-Diaz & Benton, 2013; Kennedy & Marsh, 1974). The responses to visual-only stimuli in these VPNs, were not directly recognizable in the multimodal trials. This suggests that in the visual pathway of the nocturnal moth, odor signals can partially override some of the visual signals.

The finding of odor-respondent VPNs slightly contrasted our prior belief that the multimodal processing would likely occur at higher synaptic levels in the protocerebrum. Instead, it shows that the moth is capable at such processing at least one synaptic level before our presumption. A similar concept has previously been demonstrated in the fruit fly (Ikeda et

al., 2022). However, the research demonstrated the opposite effect of what we have observed; visions ability to alter activity in olfactory projections neurons from the AL. Despite showcasing a opposite effect of vison and odor, it clearly supports that the concept of multimodal mediation affecting projection neurons from sensory centers can occur in the insect brain.

Recording from the SIP-AOTU Region.

One of the main aims of the current project was to discover processing characteristics of neurons in the male moth when stimulated with olfactory and visual- relevant cues with insertion of the recording electrode into the SIP-AOTU region. Out of a total 17 successfully labelled neurons, we discovered eight that had innervations within this region. Among these, four neurons had dendritic innervation into (among other sites) the SIP region, including one olfactory (PCN6), and three multimodal ones (PCN2, PCN4, PCN8). As mentioned earlier, the responses of PCN2 and PCN4 strongly suggest that they have a relatively higher importance in visual-mechanosensory processing, rather than vision and odor. These two neurons shared some output regions, such as SMP, and SCL, which could contribute as potential candidate centers for study of visual-mechanosensory processing in the male moth brain. PCN6, as an olfactory PCN, responded with inhibition to primary pheromone and pheromone blend. The multimodal PCN8 responded to both pheromones and plant odors, indicating that the subsequent synaptic level to SIP process both types of information, rather than solely focusing on pheromones. This aligns with our hypothesis, that the SIP is a center where multimodal processing of vision and olfaction occurs. However, considering that the SIP was not the only site for dendritic innervations, and that other multimodal neurons were observed innervating other neuropils than the SIP, our research clearly shows that such multimodal processing is not restricted to a few neuropils, rather distributed across major parts of the insect brain.

Nonresponsive PCNs

Among our data, there were three neurons (PCN5, PCN9, PCN16) that did not respond to any olfactory stimuli or displayed any visual-typical responses. The three neurons did not have similar morphological features, apart from the dendritic innervation of PCN5 and PCN9 in the SCL and PLP. The PLP has been demonstrated to receive input from the antennal lobe, yet studies have highlighted how the majority of this input comes from PNs with dendrites in the more ventroposterior glomeruli. As formerly described, these glomeruli might be associated with temperature and humidity (Kymre et al., 2022), thus suggesting why no response to our olfactory stimuli was observed. Note, however, that the PLP is also reported to be an output area of visual projection neurons (Otsuna et al., 2014), processing visual information with regards to looming (Egelhaaf, 2023), not tested in this project.

The last nonresponsive neurons, PCN16, had dendrites in the optic neuropil ME, which aligns with the absence of visual response observations. As earlier described, the ME processes information regarding light intensity (Yukizane et al., 2002) which was not tested in this project. This highlights an important part of the current project concerning our experimental approach, the limitations of our stimulation protocol, and how this research may inform future research.

Methodological Considerations

Classification of Labelled Neurons

Our data was classified into four categories (olfactory-, visual-, multimodal-, and nonresponsive PCNs) based on their response patterns. Based on our understanding of multimodal processing, mentioned in the introduction, our comprehension entailed that for a neuron to possess multimodal characteristics, it should also be able to process each modality separately. Using this as basis for classification, what was considered multimodal PCNs were those neurons that responded to both odors and showed typical visual responses (separately).

Thus, our classification did not encompass those neurons that might not have responded to each modality separately but would have shown excitation or inhibition when stimulated only with the multimodal stimuli. An example of such an instance is PCN6. This cell was classified as an olfactory PCN, because it did not display any direction selective-, visual field-, or light on/off responses. For instance, consistent with our classification one could see (Table 1) that PCN6 did not show responses to e.g. ylang-ylang. However, the neuron seems to express excitatory responses when the green bar is combined with ylang-ylang (Fig. 7). Therefore, if we had changed our classification criteria, this neuron would have been classified as multimodal. This highlights the importance of the classification criteria, showing how using small differences in criteria could give different results. Nevertheless, expanding our criteria would have resulted in losing information about the extent to which a neuron, such as PCN6, selectively responds to odors compared to visual input. Additionally, we would have missed obtaining details on how physiological properties change when two modalities are combined.

Using the pre-set criteria of 10% of the stimulation window for determination for odor-evoked responses could lack sensitivity, potentially overlooking subtle but biologically relevant responses. Solely relying on a fixed threshold may introduce bias, in which neurons are being classified differently, despite having similar function, because of one neuron's response time being 9,9% of the simulation window, and the other 10%. Yet, this threshold provided a standardized criterion for all neurons within one class, facilitating consistency in our data, while offering a decent estimation of functionality.

Sampling Strategies

In total, we were three people gathering data for this project. In our small model organism, the SIP lack clear, visually perceivable boundaries (Ito et al., 2014), which may be part of the explanation to the morphological diversity of the collected neurons. More specifically, the different contributors might have separate techniques for attempting to locate

the region of interest before insertion of the electrode, this could have led to recordings from slightly different regions.

The sample size is also quite low, considering the scope of the aim. A small sample size could drastically change the conclusions from the data, through committing type I or type II errors (e.g. Knudson & Lindsey, 2014). With 17 neurons in four categories, and highly heterogeneous morphological features, there is less that could be said about the bigger perspective of specific multimodal pathways in the *H. armigera.* The sample size was also heavily affected by the number of successful stainings. A lot of recordings were obtained but excluded due to the lack of clean labelling, i.e. either weak staining or multiple neurons being stained. More recently, we have observed how, despite similar staining techniques, the age of the dye is extremely important. Older dyes have given incomplete staining, and new dyes successful staining, when using the same protocol. Thus, having changed the dye more often throughout the project, might have increased the sample size.

Stimulation Protocol

Our protocol, consisting of stimulation with odor-only, visual-only, and combined odor and visual, demonstrates notable advantages, yet it is also subject to limitations. The most rapid experiments lasted 13 minutes (with an estimated mean of 30 minutes), which is a long time to keep constant contact with a single neuron. This especially applies because our registrations were conducted from neurites, rather than cell bodies, as typical for whole cell patch clamp recordings which allow for maintaining highly durable contacts with the neuron. In an attempt to limit plant odors down to a bare minimum, we used two components consisting of various plant odor molecules. Despite this, we had to stimulate with each odor, testing four visual directions, and combination of such, which unfortunately led us to loosing contact with several interesting neurons throughout data collection.

Experimental Technique

By using sharp intracellular recording, we were able to obtain direct contact with neurons, recording their neurophysiological characteristics. The iontophoretic staining allowed us to assess the neurons morphological properties by using confocal laser scanning microscopy. The combination of these two techniques served our aim in discovering olfactory, visual, and multimodal processing in higher order brain regions. Yet, the technique has also brought some challenges. One of the main challenges has been that by using intracellular recordings, one can only rely on experience and familiarity with the insect brain anatomy. Not knowing the precise location of the neurons that were being recorded before confocal scanning, made it challenging to locate the specific neurons of interest. In addition to this, recording from the protocerebrum increased the ratio of target neurons to non-target neurons due to the high diversity of neurons involved in computations outside of vision and olfaction. In comparison, recording from the AL would, in most cases, result in recordings of either olfactory OSNs, LNs, PNs, or CNs, while recordings from the protocerebrum can result in recording of such types of neurons from all modalities, in addition to neurons processing other types of information.

Nevertheless, in our perspective, intracellular recording was the best choice in comparison with other techniques, like for instance patch-clamp recordings or calcium imaging. Patch-clamp recordings would imply dissecting the brain, maintaining the antennae and the eyes, to align with the aim of this thesis. Also, the soma location of the multimodal neurons innervating the SIP was not known, which is necessary knowledge in order to perform the classic whole-cell patch-clamp recording, as performed e.g. in the AL of other insect species (Gouwens & Wilson, 2009; Lavialle-Defaix et al., 2015; Tabuchi et al., 2015; Warren & Kloppenburg, 2014).

Two photon calcium imaging would not have been a better choice either, in comparison to intracellular recordings. Injection of dye into target neurons, before conducting calcium imaging, would require injection using the very same method as the one used in the iontophoretic staining. Also, calcium imaging with bath application would not outperform intracellular recording with respect to our aim of characterizing multimodal neurons. With bath application, the dye would be distributed throughout the neural tissue, challenging the obtainment of information from individual neurons. Additionally, results from for example Kuebler et al. (2012) showed that bath application of the AL mainly stained the OSNs, not penetrating deeper. Thus, the working distance would be too superficial considering the diversity in morphological characteristics of neurons innervating the SIP and their projections to deeper neuropils. Additionally, since the SIP does not have clear boundaries, and considering that with bath application all neurons could be stained, it would be close to impossible to assess neurons limited to the SIP region.

It is also essential to acknowledge that, unlike the fruit fly and other species, *H. armigera* lacks genetic expression tools of comparable depth and breadth. Consequently, genetically targeting neurons in this context would not be feasible. Moreover, given that the objective of the thesis is to explore the olfactory, visual, and multimodal properties of neurons by inserting recording electrodes into the target region, the limited prior understanding of neurons in this area suggests that genetically targeting specific neurons would pose significant challenges.

Morphological Analyses

Assessing the anatomical border of distinct neuropils within the protocerebrum could in most cases be more challenging than other non-protocerebral regions. For instance, the neuropils in the OL are clearly separated and easy to recognize in a confocal image. In comparison, the SIP has no clear borders, and can only be identified by examining closely

located landmarks with clear boundaries (Ito et al., 2014). So far, both synapsin labeling and fluorescent staining have failed to label a clear boundary of the SIP (Chu et al., 2020). This complicated the assessment of whether neurons innervate the target regions or not. Yet, despite the SIP having its own term, it does not necessarily imply that the neuropil should have clear boundaries. Rather, this terminology is created on the basis of developmental processes in *D. melanogaster* (Ito et al., 2014), which does indicate that this region is not truly overlapping with adjacent regions despite the lack of clear boundaries. Considering the results of this investigation, the SIP clearly has input regarding at least two sensory modalities. In addition, the SIP is a higher order brain region, most probably receiving input from other higher-order regions processing a wide diversity of information. Consequently, higher-order regions inherently exhibit less distinct boundaries to accommodate their role in processing additional complexities.

Conclusion

Our study delved into the olfactory-visual multimodal processing characteristics of neurons in the male moth brain. Two experiments utilizing our novel air pressure mass staining technique revealed links between the pheromone processing region in the antennal lobe (MGC), and the optic lobe in the higher order protocerebral region encompassing SIP and AOTU, corresponding to suggestions from prior findings. This region was used to pinpoint the site of electrode insertion for intracellular recordings. Our results displayed that such recorded neurons displayed olfactory, visual, and multimodal to our stimulations. Based on these results, five major concepts were described:

I. Visual projection neurons responded not only to visual stimulation, but also appeared to be affected by olfactory stimulation, including both plant odors and pheromones.
II. The majority of the olfactory protocerebral interneurons, which display excitation to odors, showed even stronger excitation in the presence of visual stimuli.
III. Olfaction and vision in the nocturnal insect demonstrate similar convergence principles across synaptic levels.
IV. Multimodal higher order processing is highly distributed and occur in several brain regions which often have unclear boundaries.
V. The insect brain is optimized for energy efficiency, and the small brain should not be underestimated.

References

Andrews, E. F., Pascalau, R., Horowitz, A., Lawrence, G. M., & Johnson, P. J. (2022). Extensive Connections of the Canine Olfactory Pathway Revealed by Tractography and Dissection. *The Journal of Neuroscience*, *42*(33), 6392-6407. https://doi.org/10.1523/jneurosci.2355-21.2022

Baker, T., & Hansson, B. (2019). 10. Moth Sex Pheromone Olfaction: Flux and Flexibility in the Coordinated Confluences of Visual and Olfactory Pathways. In (pp. 139-172). https://doi.org/10.1525/9780520964433-011

Baker, T. C., & Hansson, B. S. (2016). Moth sex pheromone olfaction flux and flexibility in the coordinated confluences of visual and olfactory pathways. In *Pheromone communication in moths: Evolution, behavior, and application* (pp. 139-171). University of California press.

Barnett, P. D., Nordström, K., & O'carroll, D. C. (2007). Retinotopic organization of small-field-target-detecting neurons in the insect visual system. *Current Biology*, *17*(7), 569-578.

Borst, A. (2009). Drosophila's View on Insect Vision.

Buck, L., & Axel, R. (1991). A novel multigene family may encode odorant receptors: a molecular basis for odor recognition. *Cell*, *65*(1), 175-187.

Budick, S. A., Reiser, M. B., & Dickinson, M. H. (2007). The role of visual and mechanosensory cues in structuring forward flight in Drosophila melanogaster. *J Exp Biol*, *210*(Pt 23), 4092-4103. https://doi.org/10.1242/jeb.006502

Buehlmann, W., Goulard; Webb, Graham, Niven. (2020). Mushroom bodies are required for accurate visual navigation in ants

Cardona, A., Saalfeld, S., Preibisch, S., Schmid, B., Cheng, A., Pulokas, J., Tomancak, P., & Hartenstein, V. (2010). An Integrated Micro- and Macroarchitectural Analysis of the Drosophila Brain by Computer-Assisted Serial Section Electron Microscopy. *PLOS Biology*, *8*(10), e1000502. https://doi.org/10.1371/journal.pbio.1000502

Catania, K. (2019). Mole senses. *Current Biology*, *29*(17), R825-R828. https://doi.org/https://doi.org/10.1016/j.cub.2019.07.065

Chatterjee, P., Prusty, A. D., Mohan, U., & Sane, S. P. (2022). Integration of visual and antennal mechanosensory feedback during head stabilization in hawkmoths. *eLife*, *11*, e78410. https://doi.org/10.7554/eLife.78410

Chow, D. M., & Frye, M. A. (2008). Context-dependent olfactory enhancement of optomotor flight control in Drosophila. *J Exp Biol*, *211*(Pt 15), 2478-2485. https://doi.org/10.1242/jeb.018879

Chu, X., Heinze, S., Ian, E., & Berg, B. G. (2020). A Novel Major Output Target for Pheromone-Sensitive Projection Neurons in Male Moths [Original Research]. *Frontiers in Cellular Neuroscience*, *14*. https://doi.org/10.3389/fncel.2020.00147

Coates, K. E., Calle-Schuler, S. A., Helmick, L. M., Knotts, V. L., Martik, B. N., Salman, F., Warner, L. T., Valla, S. V., Bock, D. D., & Dacks, A. M. (2020). The Wiring Logic of an Identified Serotonergic Neuron That Spans Sensory Networks. *The Journal of Neuroscience*, *40*(33), 6309-6327. https://doi.org/10.1523/jneurosci.0552-20.2020

Collett, T. (1972). Visual neurones in the anterior optic tract of the privet hawk moth. *Journal of comparative physiology*, *78*(4), 396-433. https://doi.org/10.1007/BF01417943

Das Chakraborty, S., & Sachse, S. (2021). Olfactory processing in the lateral horn of Drosophila. Cell and Tissue Research, 383, 113-123.

Egelhaaf, M. (2023). Optic flow based spatial vision in insects.

el Jundi, B., Pfeiffer, K., Heinze, S., & Homberg, U. (2014). Integration of polarization and chromatic cues in the insect sky compass. *J Comp Physiol A Neuroethol Sens Neural Behav Physiol*, *200*(6), 575-589. https://doi.org/10.1007/s00359-014-0890-6

el Jundi, B., Pfeiffer, K., & Homberg, U. (2011). A Distinct Layer of the Medulla Integrates Sky Compass Signals in the Brain of an Insect. *PLOS ONE*, *6*(11), e27855. https://doi.org/10.1371/journal.pone.0027855

Emanuel, S., Kaiser, M., Pflueger, H. J., & Libersat, F. (2020). On the Role of the Head Ganglia in Posture and Walking in Insects. *Front Physiol*, *11*, 135. https://doi.org/10.3389/fphys.2020.00135

Eriksson, M., Nylin, S., & Carlsson, M. A. (2019). Insect brain plasticity: effects of olfactory input on neuropil size. *Royal Society Open Science*, *6*(8), 190875. https://doi.org/doi:10.1098/rsos.190875

Fadamiro, H. Y., Wyatt, T. D., & Birch, M. C. (1998). Flying beetles respond as moths predict: optomotor anemotaxis to pheromone plumes at different heights. *Journal of Insect Behavior*, *11*, 549-557.

Fleischer, J., Pregitzer, P., Breer, H., & Krieger, J. (2018). Access to the odor world: olfactory receptors and their role for signal transduction in insects. *Cell Mol Life Sci*, *75*(3), 485-508. https://doi.org/10.1007/s00018-017-2627-5

Frye, M. A., Tarsitano, M., & Dickinson, M. H. (2003). Odor localization requires visual feedback during free flight in Drosophila melanogaster. *J Exp Biol*, *206*(Pt 5), 843-855. https://doi.org/10.1242/jeb.00175

Fusca, D., & Kloppenburg, P. (2021). Task-specific roles of local interneurons for inter- and intraglomerular signaling in the insect antennal lobe. *eLife*, *10*, e65217. https://doi.org/10.7554/eLife.65217

Galizia, C. G. (2014). Olfactory coding in the insect brain: data and conjectures. *European Journal of Neuroscience*, *39*(11), 1784-1795. https://doi.org/https://doi.org/10.1111/ejn.12558

Galizia, C. G., & Rössler, W. (2010). Parallel olfactory systems in insects: anatomy and function. *Annu Rev Entomol*, *55*, 399-420. https://doi.org/10.1146/annurev-ento-112408-085442

Gallio, M., Ofstad, T. A., Macpherson, L. J., Wang, J. W., & Zuker, C. S. (2011). The coding of temperature in the Drosophila brain. *Cell*, *144*(4), 614-624. https://doi.org/10.1016/j.cell.2011.01.028

Gomez-Diaz, C., & Benton, R. (2013). The joy of sex pheromones. *EMBO Rep*, *14*(10), 874-883. https://doi.org/10.1038/embor.2013.140

Goodale, M. A., & Milner, A. D. (1992). Separate visual pathways for perception and action. *Trends in neurosciences*, *15*(1), 20-25.

Gouwens, N. W., & Wilson, R. I. (2009). Signal propagation in Drosophila central neurons. *J Neurosci*, *29*(19), 6239-6249. https://doi.org/10.1523/jneurosci.0764-09.2009

Goyret, J., Markwell, P. M., & Raguso, R. A. (2007). The effect of decoupling olfactory and visual stimuli on the foraging behavior of Manduca sexta. *J Exp Biol*, *210*(Pt 8), 1398-1405. https://doi.org/10.1242/jeb.02752

Gravina, S. A., Yep, G. L., & Khan, M. (2013). Human biology of taste. *Ann Saudi Med*, *33*(3), 217-222. https://doi.org/10.5144/0256-4947.2013.217

Guo, J., & Guo, A. (2005). Crossmodal interactions between olfactory and visual learning in Drosophila. *Science*, *309*(5732), 307-310. https://doi.org/10.1126/science.1111280

Guo, M., Du, L., Chen, Q., Feng, Y., Zhang, J., Zhang, X., Tian, K., Cao, S., Huang, T., Jacquin-Joly, E., Wang, G., & Liu, Y. (2021). Odorant Receptors for Detecting Flowering Plant Cues Are Functionally Conserved across Moths and Butterflies. *Mol Biol Evol*, *38*(4), 1413-1427. https://doi.org/10.1093/molbev/msaa300

Hammer, M. (1993). An identified neuron mediates the unconditioned stimulus in associative olfactory learning in honeybees. *Nature*, *366*(6450), 59-63. https://doi.org/10.1038/366059a0

Hausen, K. (1984). The Lobula-Complex of the Fly: Structure, Function and Significance in Visual Behaviour.

Heinze, S., & Homberg, U. (2007). Maplike representation of celestial E-vector orientations in the brain of an insect. *Science*, *315*(5814), 995-997. https://doi.org/10.1126/science.1135531

Homberg, U. (1994). Flight-correlated activity changes in neurons of the lateral accessory lobes in the brain of the locust Schistocerca gregaria.

Homberg, U. (2004). In search of the sky compass in the insect brain. *Naturwissenschaften*, *91*, 199-208.

Homberg, U. (2020). Visual circuits in arthropod brains. *Journal of Comparative Physiology A*, *206*(2), 105-107. https://doi.org/10.1007/s00359-020-01407-9

Homberg, U., Christensen, T. A., & Hildebrand, J. G. (1989). Structure and function of the deutocerebrum in insects. *Annu Rev Entomol*, *34*, 477-501. https://doi.org/10.1146/annurev.en.34.010189.002401

Homberg, U., Heinze, S., Pfeiffer, K., Kinoshita, M., & el Jundi, B. (2011). Central neural coding of sky polarization in insects. *Philosophical Transactions of the Royal Society B: Biological Sciences*, *366*(1565), 680-687. https://doi.org/doi:10.1098/rstb.2010.0199

Homberg, U., Montague, R. A., & Hildebrand, J. G. (1988). Anatomy of antenno-cerebral pathways in the brain of the sphinx moth Manduca sexta. *Cell and Tissue Research*, *254*(2), 255-281. https://doi.org/10.1007/BF00225800

Honkanen, A., Immonen, E. V., Salmela, I., Heimonen, K., & Weckström, M. (2017). Insect photoreceptor adaptations to night vision. *Philos Trans R Soc Lond B Biol Sci*, *372*(1717). https://doi.org/10.1098/rstb.2016.0077

Honkanen, A., Saari, P., Takalo, J., Heimonen, K., & Weckström, M. (2018). The role of ocelli in cockroach optomotor performance. *J Comp Physiol A Neuroethol Sens Neural Behav Physiol*, *204*(2), 231-243. https://doi.org/10.1007/s00359-017-1235-z

Horne, J. A., Langille, C., McLin, S., Wiederman, M., Lu, Z., Xu, C. S., Plaza, S. M., Scheffer, L. K., Hess, H. F., & Meinertzhagen, I. A. (2018). A resource for the Drosophila antennal lobe provided by the connectome of glomerulus VA1v. *eLife*, *7*. https://doi.org/10.7554/eLife.37550

Ian, E., Kirkerud, N. H., Galizia, C. G., & Berg, B. G. (2017). Coincidence of pheromone and plant odor leads to sensory plasticity in the heliothine olfactory system. *PLOS ONE*, *12*(5), e0175513. https://doi.org/10.1371/journal.pone.0175513

Ian, E., Zhao, X. C., Lande, A., & Berg, B. G. (2016). Individual Neurons Confined to Distinct Antennal-Lobe Tracts in the Heliothine Moth: Morphological Characteristics and Global Projection Patterns [Original Research]. *Frontiers in Neuroanatomy*, *10*. https://doi.org/10.3389/fnana.2016.00101

Ikeda, K., Kataoka, M., & Tanaka, N. K. (2022). Nonsynaptic transmission mediates light context-dependent odor responses in drosophila melanogaster. *Journal of Neuroscience*, *42*(46), 8621-8628.

Ito, K., Shinomiya, K., Ito, M., Armstrong, J. D., Boyan, G., Hartenstein, V., Harzsch, S., Heisenberg, M., Homberg, U., Jenett, A., Keshishian, H., Restifo, L. L., Rössler, W., Simpson, J. H., Strausfeld, N. J., Strauss, R., & Vosshall, L. B. (2014). A systematic nomenclature for the insect brain. *Neuron*, *81*(4), 755-765. https://doi.org/10.1016/j.neuron.2013.12.017

Jefferis, G. S., Potter, C. J., Chan, A. M., Marin, E. C., Rohlfing, T., Maurer, C. R., & Luo, L. (2007). Comprehensive maps of Drosophila higher olfactory centers: spatially segregated fruit and pheromone representation. *Cell*, *128*(6), 1187-1203.

Järvilehto, M., & Zettler, F. (1971). Localized intracellular potentials from pre-and postsynaptic components in the external plexiform layer of an insect retina. *Zeitschrift für vergleichende Physiologie*, *75*(4), 422-440.

KC, P., Chu, X., Kvello, P., Zhao, X.-C., Wang, G.-R., & Berg, B. G. (2020). Revisiting the Labial Pit Organ Pathway in the Noctuid Moth, Helicoverpa armigera [Original Research]. *Frontiers in Physiology*, *11*. https://doi.org/10.3389/fphys.2020.00202

Kehat, M., & Dunkelblum, E. (1990). Behavioral responses of maleHeliothis armigera (Lepidoptera: Noctuidae) moths in a flight tunnel to combinations of components identified from female sex pheromone glands. *Journal of Insect Behavior*, *3*(1), 75-83. https://doi.org/10.1007/BF01049196

Kennedy, J. S., & Marsh, D. (1974). Pheromone-regulated anemotaxis in flying moths. *Science*, *184*(4140), 999-1001. https://doi.org/10.1126/science.184.4140.999

Kent, K. S., Harrow, I. D., Quartararo, P., & Hildebrand, J. G. (1986). An accessory olfactory pathway in Lepidoptera: the labial pit organ and its central projections in Manduca sexta and certain other sphinx moths and silk moths. *Cell and Tissue Research*, *245*(2), 237-245. https://doi.org/10.1007/BF00213927

Klapoetke, N. C., Nern, A., Rogers, E. M., Rubin, G. M., Reiser, M. B., & Card, G. M. (2022). A functionally ordered visual feature map in the Drosophila brain. *Neuron*, *110*(10), 1700-1711 e1706. https://doi.org/10.1016/j.neuron.2022.02.013

Knudson, D. V., & Lindsey, C. (2014). Type I and Type II Errors in Correlations of Various Sample Sizes. *Comprehensive Psychology*, *3*, 03.CP.03.01. https://doi.org/10.2466/03.CP.3.1

Kuebler, L. S., Schubert, M., Kárpáti, Z., Hansson, B. S., & Olsson, S. B. (2012). Antennal Lobe Processing Correlates to Moth Olfactory Behavior. *The Journal of Neuroscience*, *32*(17), 5772-5782. https://doi.org/10.1523/jneurosci.6225-11.2012

Kvello, P., Løfaldli, B., Rybak, J., Menzel, R., & Mustaparta, H. (2009). Digital, three-dimensional average shaped atlas of the heliothis virescens brain with integrated gustatory and olfactory neurons [Original Research]. *Frontiers in Systems Neuroscience*, *3*. https://doi.org/10.3389/neuro.06.014.2009

Kymre, Liu, X., Ian, E., Berge, C. N., Wang, G., Berg, B. G., Zhao, X., & Chu, X. (2021b). Distinct protocerebral neuropils associated with attractive and aversive female-produced odorants in the male moth brain. *eLife*, *10*, e65683. https://doi.org/10.7554/eLife.65683

Kymre, J. H., Berge, C. N., Chu, X., Ian, E., & Berg, B. G. (2021a). Antennal-lobe neurons in the moth Helicoverpa armigera: Morphological features of projection neurons, local interneurons, and centrifugal neurons. *J Comp Neurol*, *529*(7), 1516-1540. https://doi.org/10.1002/cne.25034

Kymre, J. H., Chu, X., Ian, E., & Berg, B. G. (2022). Organization of the parallel antennal-lobe tracts in the moth. *Journal of Comparative Physiology A*, *208*(5), 707-721. https://doi.org/10.1007/s00359-022-01566-x

Lavialle-Defaix, C., Jacob, V., Monsempès, C., Anton, S., Rospars, J. P., Martinez, D., & Lucas, P. (2015). Firing and intrinsic properties of antennal lobe neurons in the Noctuid moth Agrotis ipsilon. *Biosystems*, *136*, 46-58. https://doi.org/10.1016/j.biosystems.2015.06.005

Lee, S. G., Celestino, C. F., Stagg, J., Kleineidam, C., & Vickers, N. J. (2019). Moth pheromone-selective projection neurons with cell bodies in the antennal lobe lateral cluster exhibit diverse morphological and neurophysiological characteristics. *J Comp Neurol*, *527*(9), 1443-1460. https://doi.org/10.1002/cne.24611

Lei, H., Anton, S., & Hansson, B. S. (2001). Olfactory protocerebral pathways processing sex pheromone and plant odor information in the male moth Agrotis segetum. *J Comp Neurol*, *432*(3), 356-370. https://doi.org/10.1002/cne.1108

Lei, H., Chiu, H. Y., & Hildebrand, J. G. (2013). Responses of protocerebral neurons in Manduca sexta to sex-pheromone mixtures. *J Comp Physiol A Neuroethol Sens Neural Behav Physiol*, *199*(11), 997-1014. https://doi.org/10.1007/s00359-013-0844-4

Lin, T.-Y., Luo, J., Shinomiya, K., Ting, C.-Y., Lu, Z., Meinertzhagen, I. A., & Lee, C.-H. (2016). Mapping chromatic pathways in the Drosophila visual system. *Journal of Comparative Neurology*, *524*(2), 213-227. https://doi.org/https://doi.org/10.1002/cne.23857

Liu, G., Seiler, H., Wen, A., Zars, T., Ito, K., Wolf, R., Heisenberg, M., & Liu, L. (2006). Distinct memory traces for two visual features in the Drosophila brain. *Nature*, *439*(7076), 551-556. https://doi.org/10.1038/nature04381

Liu, Y., Liu, C., Lin, K., & Wang, G. (2013). Functional specificity of sex pheromone receptors in the cotton bollworm Helicoverpa armigera. *PLOS ONE*, *8*(4), e62094. https://doi.org/10.1371/journal.pone.0062094

Løfaldli, B., Kvello, P., Kirkerud, N., & Mustaparta, H. (2012). Activity in Neurons of a Putative Protocerebral Circuit Representing Information about a 10 Component Plant Odor Blend in Heliothis virescens [Original Research]. *Frontiers in Systems Neuroscience*, *6*. https://doi.org/10.3389/fnsys.2012.00064

Maselli, V., Al-Soudy, A. S., Buglione, M., Aria, M., Polese, G., & Di Cosmo, A. (2020). Sensorial Hierarchy in Octopus vulgaris's Food Choice: Chemical vs. Visual. *Animals (Basel)*, *10*(3). https://doi.org/10.3390/ani10030457

Merry, J. W., Morehouse, N. I., Yturralde, K., & Rutowski, R. L. (2006). The eyes of a patrolling butterfly: Visual field and eye structure in the Orange Sulphur, Colias eurytheme (Lepidoptera, Pieridae). *Journal of Insect Physiology*, *52*(3), 240-248. https://doi.org/https://doi.org/10.1016/j.jinsphys.2005.11.002

Namiki, I., Kono, Kanzaki (2014). Information flow through neural circuits for pheromone orientation.

Namiki, S., Iwabuchi, S., Pansopha Kono, P., & Kanzaki, R. (2014). Information flow through neural circuits for pheromone orientation. *Nature communications*, *5*(1), 5919.

Namiki, S., & Kanzaki, R. (2016). Comparative Neuroanatomy of the Lateral Accessory Lobe in the Insect Brain. *Front Physiol*, *7*, 244. https://doi.org/10.3389/fphys.2016.00244

Namiki, S., & Kanzaki, R. (2019). Morphology and physiology of olfactory neurons in the lateral protocerebrum of the silkmoth Bombyx mori. *Sci Rep*, *9*(1), 16604. https://doi.org/10.1038/s41598-019-53318-8

Namiki, S., Takaguchi, M., Seki, Y., Kazawa, T., Fukushima, R., Iwatsuki, C., & Kanzaki, R. (2013). Concentric zones for pheromone components in the mushroom body calyx of the moth brain. *The Journal of comparative neurology*, *521*. https://doi.org/10.1002/cne.23219

Namiki, S., Wada, S., & Kanzaki, R. (2018). Descending neurons from the lateral accessory lobe and posterior slope in the brain of the silkmoth Bombyx mori. *Scientific Reports*, *8*(1), 9663. https://doi.org/10.1038/s41598-018-27954-5

Neuser, K., Triphan, T., Mronz, M., Poeck, B., & Strauss, R. (2008). Analysis of a spatial orientation memory in Drosophila. *Nature*, *453*(7199), 1244-1247. https://doi.org/10.1038/nature07003

Nishino, H., Nishikawa, M., Mizunami, M., & Yokohari, F. (2009). Functional and topographic segregation of glomeruli revealed by local staining of antennal sensory neurons in the honeybee Apis mellifera. *J Comp Neurol*, *515*(2), 161-180. https://doi.org/10.1002/cne.22064

Otsuna, H., Shinomiya, K., & Ito, K. (2014). Parallel neural pathways in higher visual centers of the Drosophila brain that mediate wavelength-specific behavior [Original Research]. *Frontiers in Neural Circuits*, *8*. https://doi.org/10.3389/fncir.2014.00008

Reinhard, J., Srinivasan, M. V., & Zhang, S. (2006). Complex memories in honeybees: can there be more than two? *Journal of Comparative Physiology A*, *192*, 409-416.

Ritzmann, R. E., Ridgel, A. L., & Pollack, A. J. (2008). Multi-unit recording of antennal mechano-sensitive units in the central complex of the cockroach, Blaberus discoidalis. *J Comp Physiol A Neuroethol Sens Neural Behav Physiol*, *194*(4), 341-360. https://doi.org/10.1007/s00359-007-0310-2

Rowe, C. (2002). Sound improves visual discrimination learning in avian predators. *Proceedings of the Royal Society of London. Series B: Biological Sciences*, *269*(1498), 1353-1357.

Ryu, L., Kim, S. Y., & Kim, A. J. (2022). From Photons to Behaviors: Neural Implementations of Visual Behaviors in Drosophila. *Front Neurosci*, *16*, 883640. https://doi.org/10.3389/fnins.2022.883640

RØ, H., Müller, D., & Mustaparta, H. (2007). Anatomical organization of antennal lobe projection neurons in the moth Heliothis virescens. *Journal of Comparative Neurology*, *500*(4), 658-675. https://doi.org/https://doi.org/10.1002/cne.21194

Røstelien, T. (2019). Recognition of Plant Odor Information in Moths. In J.-F. Picimbon (Ed.), *Olfactory Concepts of Insect Control - Alternative to insecticides: Volume 2* (pp. 49-91). Springer International Publishing. https://doi.org/10.1007/978-3-030-05165-5_3

Røstelien, T., Stranden, M., Borg-Karlson, A. K., & Mustaparta, H. (2005). Olfactory receptor neurons in two heliothine moth species responding selectively to aliphatic green leaf volatiles, aromatic compounds, monoterpenes and sesquiterpenes of plant origin. Chemical senses, 30(5), 443-461.

Scott, E. K., Raabe, T., & Luo, L. (2002). Structure of the vertical and horizontal system neurons of the lobula plate in Drosophila. *J Comp Neurol*, *454*(4), 470-481. https://doi.org/10.1002/cne.10467

Seki, Y., Aonuma, H., & Kanzaki, R. (2005). Pheromone processing center in the protocerebrum of Bombyx mori revealed by nitric oxide-induced anti-cGMP immunocytochemistry. *Journal of Comparative Neurology*, *481*(4), 340-351. https://doi.org/https://doi.org/10.1002/cne.20392

Sharma, A., Kumar, R., Aier, I., Semwal, R., Tyagi, P., & Varadwaj, P. (2019). Sense of Smell: Structural, Functional, Mechanistic Advancements and Challenges in Human Olfactory Research. *Curr Neuropharmacol*, *17*(9), 891-911. https://doi.org/10.2174/1570159x17666181206095626

Shimojo, S., & Shams, L. (2001). Sensory modalities are not separate modalities: plasticity and interactions. *Current Opinion in Neurobiology*, *11*(4), 505-509. https://doi.org/https://doi.org/10.1016/S0959-4388(00)00241-5

Song, B.-M., & Lee, C.-H. (2018). Toward a Mechanistic Understanding of Color Vision in Insects [Review]. *Frontiers in Neural Circuits*, *12*. https://doi.org/10.3389/fncir.2018.00016

Strausfeld, N. J., & Li, Y. (1999). Organization of olfactory and multimodal afferent neurons supplying the calyx and pedunculus of the cockroach mushroom bodies. *J Comp Neurol*, *409*(4), 603-625.

Strauss, R. (2002). The central complex and the genetic dissection of locomotor behaviour. *Curr Opin Neurobiol*, *12*(6), 633-638. https://doi.org/10.1016/s0959-4388(02)00385-9

Strube-Bloss, M. F., & Rössler, W. (2018). Multimodal integration and stimulus categorization in putative mushroom body output neurons of the honeybee. *Royal Society Open Science*, *5*(2), 171785. https://doi.org/doi:10.1098/rsos.171785

Tabuchi, M., Dong, L., Inoue, S., Namiki, S., Sakurai, T., Nakatani, K., & Kanzaki, R. (2015). Two types of local interneurons are distinguished by morphology, intrinsic membrane properties, and functional connectivity in the moth antennal lobe. *J Neurophysiol*, *114*(5), 3002-3013. https://doi.org/10.1152/jn.00050.2015

Taisz, I., Donà, E., Münch, D., Bailey, S. N., Morris, B. J., Meechan, K. I., Stevens, K. M., Varela-Martínez, I., Gkantia, M., Schlegel, P., Ribeiro, C., Jefferis, G., & Galili, D. S. (2023). Generating parallel representations of position and identity in the olfactory system. *Cell*, *186*(12), 2556-2573.e2522. https://doi.org/10.1016/j.cell.2023.04.038

Thiagarajan, D., & Sachse, S. (2022). Multimodal Information Processing and Associative Learning in the Insect Brain. *Insects*, *13*(4), 332. https://www.mdpi.com/2075-4450/13/4/332

Triphan, T., Poeck, B., Neuser, K., & Strauss, R. (2010). Visual targeting of motor actions in climbing Drosophila. *Curr Biol*, *20*(7), 663-668. https://doi.org/10.1016/j.cub.2010.02.055

van der Kooi, C. J., Stavenga, D. G., Arikawa, K., Belušič, G., & Kelber, A. (2021). Evolution of Insect Color Vision: From Spectral Sensitivity to Visual Ecology. *Annual Review of Entomology*, *66*(Volume 66, 2021), 435-461. https://doi.org/https://doi.org/10.1146/annurev-ento-061720-071644

van Swinderen, B., & Greenspan, R. J. (2003). Salience modulates 20-30 Hz brain activity in Drosophila. *Nat Neurosci*, *6*(6), 579-586. https://doi.org/10.1038/nn1054

Verspui, R., & Gray, J. R. (2009). Visual stimuli induced by self-motion and object-motion modify odour-guided flight of male moths (Manduca sexta L.). *Journal of Experimental Biology*, *212*(20), 3272-3282. https://doi.org/10.1242/jeb.031591

Vosshall, L. B., Amrein, H., Morozov, P. S., Rzhetsky, A., & Axel, R. (1999). A spatial map of olfactory receptor expression in the Drosophila antenna. *Cell*, *96*(5), 725-736. https://doi.org/10.1016/s0092-8674(00)80582-6

Vosshall, L. B., & Stocker, R. F. (2007). Molecular architecture of smell and taste in Drosophila. *Annu Rev Neurosci*, *30*, 505-533. https://doi.org/10.1146/annurev.neuro.30.051606.094306

Warren, B., & Kloppenburg, P. (2014). Rapid and slow chemical synaptic interactions of cholinergic projection neurons and GABAergic local interneurons in the insect antennal lobe. *J Neurosci*, *34*(39), 13039-13046. https://doi.org/10.1523/jneurosci.0765-14.2014

Wicklein, M., & Strausfeld, N. J. (2000). Organization and significance of neurons that detect change of visual depth in the hawk moth Manduca sexta. *J Comp Neurol*, *424*(2), 356-376.

Wu, H., Xu, M., Hou, C., Huang, L. Q., Dong, J. F., & Wang, C. Z. (2015). Specific olfactory neurons and glomeruli are associated to differences in behavioral responses to pheromone components between two Helicoverpa species. *Front Behav Neurosci*, *9*, 206. https://doi.org/10.3389/fnbeh.2015.00206

Wu, M., Nern, A., Williamson, W. R., Morimoto, M. M., Reiser, M. B., Card, G. M., & Rubin, G. M. (2016). Visual projection neurons in the Drosophila lobula link feature detection to distinct behavioral programs. *eLife*, *5*. https://doi.org/10.7554/eLife.21022

Xu, M., Guo, H., Hou, C., Wu, H., Huang, L.-Q., & Wang, C.-Z. (2016). Olfactory perception and behavioral effects of sex pheromone gland components in Helicoverpa armigera and Helicoverpa assulta. *Scientific Reports*, *6*(1), 22998. https://doi.org/10.1038/srep22998

Yagi, R., Mabuchi, Y., Mizunami, M., & Tanaka, N. K. (2016). Convergence of multimodal sensory pathways to the mushroom body calyx in Drosophila melanogaster. *Scientific Reports*, *6*(1), 29481. https://doi.org/10.1038/srep29481

Yukizane, M., Kaneko, A., & Tomioka, K. (2002). Electrophysiological and morphological characterization of the medulla bilateral neurons that connect bilateral optic lobes in the cricket, Gryllus bimaculatus. *Journal of Insect Physiology*, *48*(6), 631-641. https://doi.org/https://doi.org/10.1016/S0022-1910(02)00091-4

Zhao, X.-C., Chen, Q.-Y., Guo, P., Xie, G.-Y., Tang, Q.-B., Guo, X.-R., & Berg, B. G. (2016). Glomerular identification in the antennal lobe of the male moth Helicoverpa armigera. *Journal of Comparative Neurology*, *524*(15), 2993-3013. https://doi.org/https://doi.org/10.1002/cne.24003

Zhao, X.-C., Kvello, P., Løfaldli, B. B., Lillevoll, S. C., Mustaparta, H., & Berg, B. G. (2014). Representation of pheromones, interspecific signals, and plant odors in higher olfactory centers; mapping physiologically identified antennal-lobe projection neurons in the male heliothine moth [Original Research]. *Frontiers in Systems Neuroscience*, *8*. https://doi.org/10.3389/fnsys.2014.00186

Zhao, X. C., Tang, Q. B., Berg, B. G., Liu, Y., Wang, Y. R., Yan, F. M., & Wang, G. R. (2013). Fine structure and primary sensory projections of sensilla located in the labial-palp pit organ of Helicoverpa armigera (Insecta). *Cell Tissue Res*, *353*(3), 399-408. https://doi.org/10.1007/s00441-013-1657-z

Appendix A

Class	ID	Dendrites	Terminals	Soma
Olfactory PCNs	PCN3	SEZ	LO, [PLP]	rALl
	PCN6	SNPs	PB, SMP	rSMPd
	PCN10	SMP, SLP, c.l. SMP	b.l. CA	rSIPd
	PCN14	cl. PLP	SLP, VLP, LH, [PLP, ACA]	rSMPmp
Visual PCNs	PCN11	LAL, [PLP, VLP]	c.l. LAL, c.l. BU, [AOTU]	rPLPp
	PCN12	LOP	c.l. PS, [LAL]	rPLPp
	PCN13	AOTU	PS, c.l. PS, c.l. AOTU	rPLPp
Multimodal PCNs	PCN1	LOP	SCL, PLP	rLOd
	PCN2	PLP, VLP, PS, SIP	dPLP, SCL, SMP, SIP	rAVLPl
	PCN4	SIP, LH, [SLP]	SLP, SMP, c.l. SLP, c.l. LH	rWEDl
	PCN7	Lo, PLP, SCL	AOTU, SMP	rSLPp
	PCN8	SCL, ICL, SLP, SIP, [VLP, LH]	SMP, PB, [c.l. SMP]	rSLPp
	PCN15	LO	c.l. PS	rVLPl
	PCN17	VLP, LO	LAL	rVLPl
Nonresponsive PCNS	PCN5	ICL, SCL, CRE, [LAL, PLP, VMNP]	SMP, [SIP]	rAOTUv
	PCN9	PLP, [SCL]	SMP, CRE	rIBp
	PCN16	ME	c.l. PS	rVLPl

Note. Table of all protocerebral interneurons included in this thesis, their IDs and corresponding dendrite-like innervation site, terminals projection, and soma location. Minor innervations are marked in [*brackets*]. Contralateral is marked “c.l.” and bilateral “b.l.” and are to be understood as relative to location of soma. For soma location the first letter “r” refers to the location being in a cell body rind relative to the neuropil mentioned subsequently. The last letter refers to the anatomical position of the cell body ring. E.g. rSMPd, refer to the cell body rind located dorsally to the SMP.

Appendix B

ODOR / NEURON	PP	SP	BA	PB	IAC	YY	Hex	Air
PCN3	17.42	NR	5.77	7.54	7.75	20.47	14.61	NR
PCN6	[-1.75]	NR	5.01	[-1.71]	9.17	5.51 [-2.11]	4.53	NR
PCN10	5.66	NR	4.04	6.58	5.69	6.86	5.37	NR
PCN14	10.01	NR	13.07	10.96	14.46	7.26	8.93	NR
PCN1	3.66 [-2.04]	[-1.96]	3.50	2.72 [-2.67]	3.23 [-1.76]	2.64	3.49	3.87 [-2.01]
PCN2	21.61	13.00	19.21	[-0.55]	12.60	13.29	13.04	14.12
PCN4	19.77	7.51	18.87	39.11	16.24	20.28	27.07	17.28
PCN7	8.28	10.49	5.16	8.57	10.58	12.95	9.37	13.25
PCN8	3.85	4.78	3.56	6.40	7.67	2.0]	3.53 [-0.57]	3.70
PCN15	5.21	14.46	22.89	9.83	10.60	4.60	5.08	7.10
PCN17	10.79	25.49	13.59	NR	4.01	11.91	[-0.62]	NT

Note. Peak z-scored instantaneous firing rate olfactory responses to all tested olfactory stimuli and controls among olfactory and multimodal PCNs. Only odors that had a response which lasted more than 10% of the stimulation window duration are colorized in the table. Green boxes indicate excitatory response, blue inhibitory, purple dual responses with both excitation and inhibition. Inhibition is marked in "[Brackets]". Olfactory PCNs are marked in *light yellow*, and multimodal PCNs in *light blue*. Abbreviations: BA, behavioral antagonist; Hex, hexane; IAC, insect attractor component; NT, not testes; NR, no response; PB, pheromone blend; PP, primary pheromone; SP, secondary pheromone; YY, ylang-ylang.

Appendix C

Example of responses to visual, odor, and multimodal stimulation compared to control

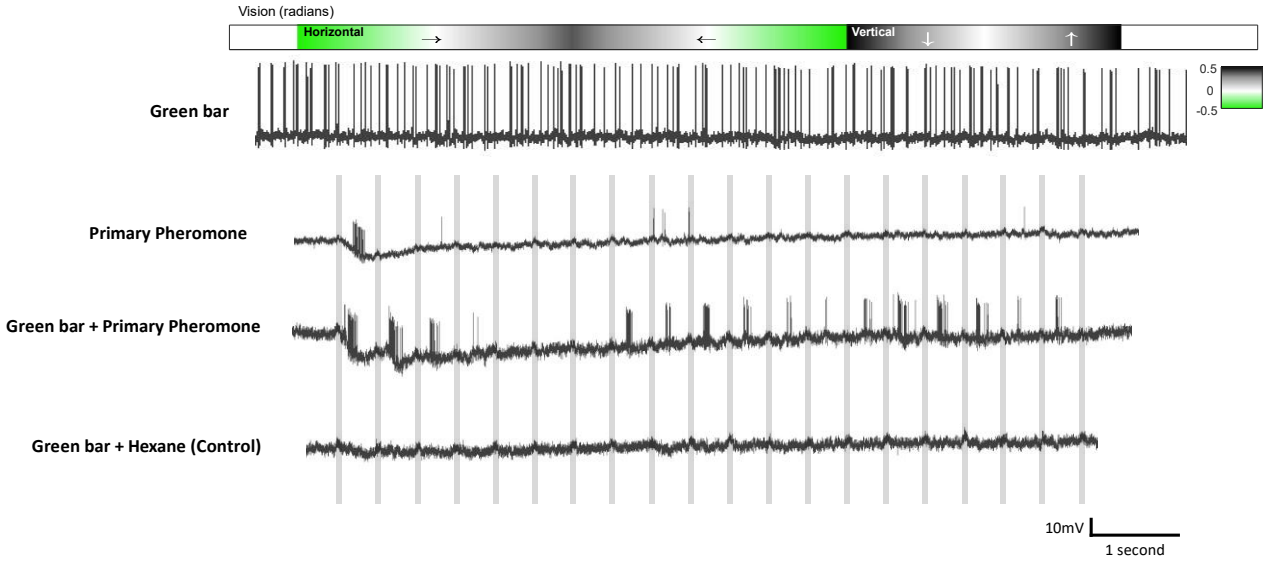

Note. The 15 seconds stimulation window is being displayed. Location and motion of bar for visual stimulation (green bar) is represented on the top (Horizontal: *green* = left, *white* = middle; *grey* = right; Vertical: *black* = top, *white* = middle) with time of 20 odor puffs presented under as gray bars (80ms puff, 520ms inter-pulse interval). The neuron displayed response to the primary pheromone, and when combined with green bar (multimodal stimulation) the neuron showed a rhythm-like pattern following most of the air puffs.

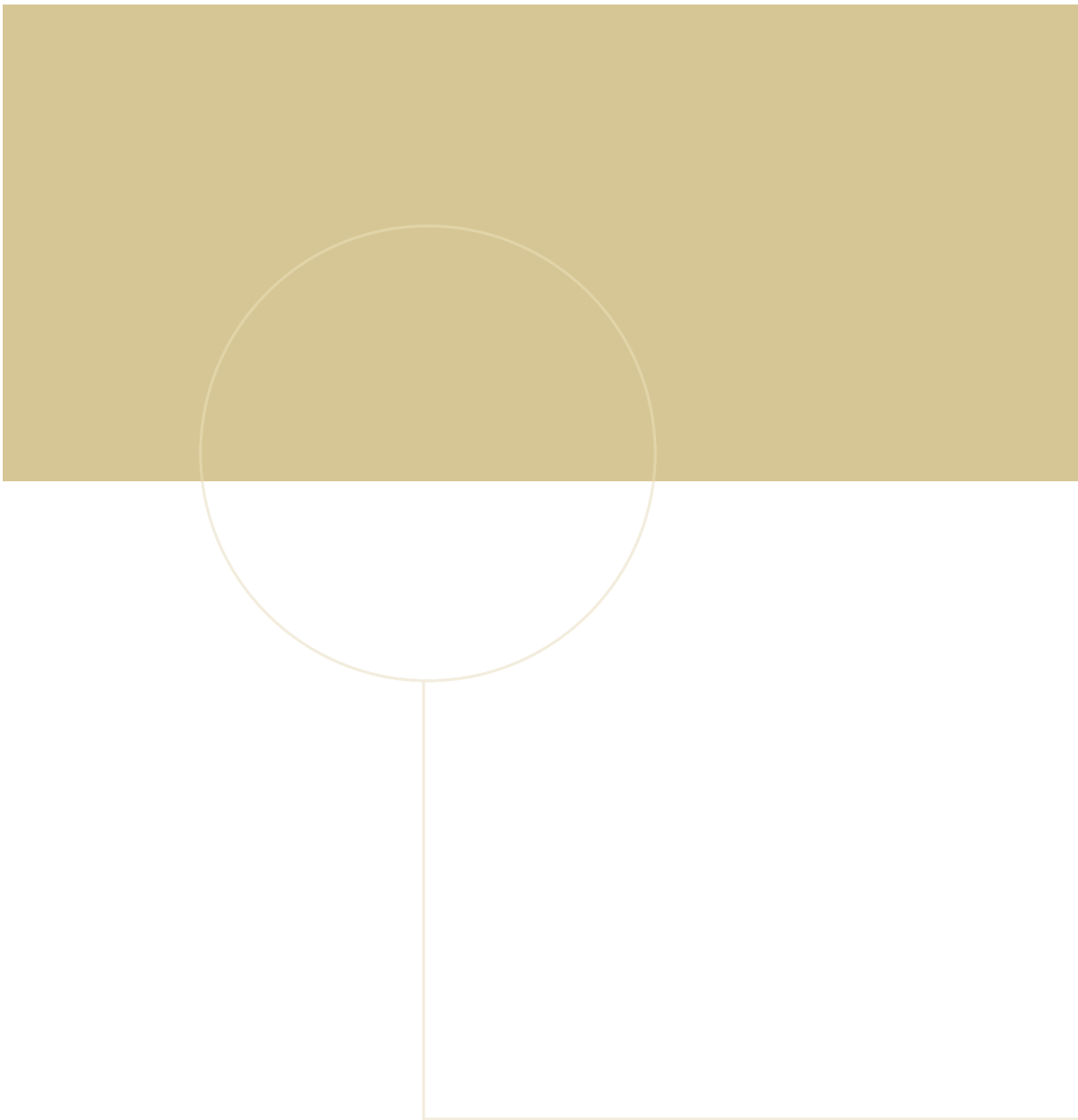

NTNU

Norwegian University of
Science and Technology